**UNIVERSITY OF ALBERTA**

*Examination of the Reproducibility of Inverse Gas Chromatography Data for HDPE/LLDPE Blends*

By

*Glenn Innes*

A thesis submitted to the Faculty of Graduate Studies and Research in partial fulfillment of the requirements for the degree of *Master of Science*

*Department of Chemical and Materials Engineering*

Edmonton, Alberta

Fall, 2002

National Library of Canada
Acquisitions and Bibliographic Services
395 Wellington Street
Ottawa ON K1A 0N4
Canada

Bibliothèque nationale du Canada
Acquisitions et services bibliographiques
395, rue Wellington
Ottawa ON K1A 0N4
Canada

Your file Votre référence

Our file Notre référence

The author has granted a non-exclusive licence allowing the National Library of Canada to reproduce, loan, distribute or sell copies of this thesis in microform, paper or electronic formats.

L'auteur a accordé une licence non exclusive permettant à la Bibliothèque nationale du Canada de reproduire, prêter, distribuer ou vendre des copies de cette thèse sous la forme de microfiche/film, de reproduction sur papier ou sur format électronique.

The author retains ownership of the copyright in this thesis. Neither the thesis nor substantial extracts from it may be printed or otherwise reproduced without the author's permission.

L'auteur conserve la propriété du droit d'auteur qui protège cette thèse. Ni la thèse ni des extraits substantiels de celle-ci ne doivent être imprimés ou autrement reproduits sans son autorisation.

0-612-82379-2

Canada

University of Alberta

Library Release Form

Name of Author: *Glenn Innes*

Title of Thesis: *Examination of the Reproducibility of Inverse Gas Chromatography Data of HDPE/LLDPE Blends*

Degree: *Master of Science*

Year this Degree Granted: *2002*

Permission is hereby granted to the University of Alberta Library to reproduce single copies of this thesis and to lend or sell such copies for private, scholarly or scientific research purposes only.

The author reserves all other publication and other rights in association with the copyright in the thesis, and except as herein before provided, neither the thesis nor any substantial portion thereof may be printed or otherwise reproduced in any material form whatever without the author's prior written permission.

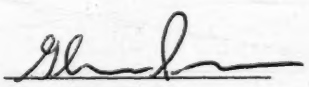

Glenn Innes
#38, 52225 Range Road 232
Sherwood Park, AB
T8B 1L5

August 19, 2002

"*Welcome to the Jungle*"

William A. Rose

University of Alberta

Faculty of Graduate Studies and Research

The undersigned certify that they have read, and recommend the Faculty of Graduate Studies and Research for acceptance, a thesis entitled *An Examination of the Reproducibility of Inverse Gas Chromatography Data for HDPE/LLDPE Blends* submitted by *Glenn Innes* in partial fulfillment of the requirements for the degree of *Master of Science*.

Dr. Phillip (Yip-Kam) Choi

Dr. Hasan Uludag

Dr. Thomas [redacted] Forest

Date: August 12, 2002

Dedicated to the memory of Dave "The Iron Horse" Hunter RIP October 31, 2001.

## ABSTRACT

A new data analysis method suggested by Zhao and Choi (2001) for Inverse Gas Chromatography (IGC) measurements was used in order to obtain solvent independent polymer-polymer interaction parameters ($\chi_{23}$) for high-density polyethylene (HDPE) / linear low-density polyethylene (LLDPE) blends. The calculated $\chi_{23}$ values were much larger than those obtained by other methods and the associated error values were fairly large. Therefore, measures were taken to improve the accuracy of the method. With the improvements, the HDPE/LLDPE blends were observed to be more immiscible as the branch content of LLDPE increased, with the critical branch content occurring ~90 branches per 1,000 backbone carbons. However, the blends did not exhibit a clear temperature trend, indicating that the effect of temperature on the miscibility is secondary to the branch content. Additionally, no clear molecular weight dependence was observed. The calculated $\chi_{23}$ values and the associated error values are still noted to be large; further improvements should be made.

**ACKNOWLEDGEMENTS**

I would like to thank the following for their assistance in completing this project:

Dr. Phillip Choi for his assistance with this project and guidance for my future endeavors.

NOVA Chemicals and NSERC for the financial assistance, which made it possible to do this project.

Metal Sludge for high quality entertainment whilst performing my IGC experiments.

My Mom and Dad for always being supportive of what I do and for providing valuable guidance. I can hardly believe I made a statement like that…but it's true!

Jojo Belladona for spiritual guidance and for consistently livening things up when I was frustrated.

And finally, thanks to Laura-lee Brown. It was a pleasure to share the lab with her and without her in the lab, I am not sure that I would have retained my sanity. I appreciate all the input that she provided me with regarding my work and my future plans; the motivation to get my work done; and all the other discussions about life in general. She is truly one of the best friends a guy like me could ever ask for and deserves a lot of the credit for the completion of this degree. Thanks for helping me make it through this!

## TABLE OF CONTENTS


| | Page |
|---|---|
| CHAPTER 1 – Introduction | |
| 1.1 Introduction | 1 |
| 1.2 Quantifying Miscibility | 4 |
| 1.3 Purpose | 6 |
| 1.4 References | 6 |
| CHAPTER 2 – Inverse Gas Chromatography (IGC) | |
| 2.1 Introduction | 9 |
| 2.2 The Flory-Huggins Lattice Theory | 15 |
| 2.3 Phase Equilibria | 21 |
| 2.4 Inverse Gas Chromatography Thermodynamics | 28 |
| 2.5 Solvent Dependency Problem | 32 |
| 2.6 A Modified Flory-Huggins Lattice Theory for IGC Measurements | 35 |
| 2.7 Experimental Methods | 39 |
| 2.7.1 Materials | 39 |
| 2.7.2 Column Preparation | 41 |
| 2.7.3 Mass Determination | 42 |
| 2.7.4 Equipment | 43 |
| 2.8 References | 44 |
| CHAPTER 3 – Miscibility of High-density Polyethylene (HDPE) / Low-density Polyethylene (LLDPE) Blends Review | |
| 3.1 Introduction | 48 |

3.2 Literature Review 49

3.2.1 Solid State Miscibility 49

3.2.2 Indirect Measurement of Melt Miscibility 52

3.2.3 Simulations of Melt State Miscibility 60

3.2.4 Direct Measurement of Melt State Miscibility 60

3.2.5 Summary 63

3.3 References 64

CHAPTER 4 – Miscibility of HDPE/LLDPE Blends

4.1 Background 70

4.2 Experimental Methods 72

4.2.1 Materials 72

4.2.2 Sample Preparation 73

4.2.3 Operating Conditions 73

4.3 Results 74

4.3.1 Retention Time and Specific Retention Volume Measurements 74

4.3.2 Interaction Parameters ($\chi_{23}$) 74

4.3.3 Temperature Dependence of $\chi_{23}$ 75

4.3.4 Effect of Branch Content of LLDPE on $\chi_{23}$ of HDPE/LLDPE Blends 78

4.3.5 Effect of Molecular Weight of HDPE on $\chi_{23}$ of HDPE/LLDPE Blends 78

4.4 Summary 81

4.5 References 82

CHAPTER 5 – Error Analysis

5.1 Error Reduction Methods Implemented and Justifications of Changes 84

5.2 Effect of Using Different Column Lengths For the Calculation of $\chi_{12}$ Values 90

5.3 Results for Pure HDPE Samples Using Different Column Loadings 95

5.4 HDPE/LLDPE Blend Results Using 3m Columns 98

5.4.1 HDPE-2/LLDPE Blends 99

5.4.2 HDPE-1/LLDPE Blends 101

5.4.3 Molecular Weight Effect of HDPE on HDPE/LLDPE Blends 105

5.5 References 105

CHAPTER 6 – Conclusions and Future Work

6.1 Conclusions and Future Work 108

6.2 References 112

APPENDIX A – Sample Calculations of Flory-Huggins Interaction Parameters

A.1 Sample Calculation of $\chi_{12}$, $\chi_{13}$, and $\chi_{1(23)}$ 114

A.2 Sample Calculation of $\chi_{23}$ 116

APPENDIX B – Error Analysis of IGC Data

B.1 Experimental Errors 118

B.2 Error Propagation 119

B.3 The Standard Deviation of $\chi_{23}$ 121

## LIST OF TABLES


| | | Page |
|---|---|---|
| Table 2.1 | Polyethylene Samples Studied | 40 |
| Table 5.1 | $\chi_{12}$ Values For HDPE-2 Using Different Column Lengths | 91 |
| Table 5.2 | $\chi_{12}$ For HDPE-2 Samples Using Different Column Lengths and Polymer Loading | 95 |

## LIST OF FIGURES


| | | Page |
|---|---|---|
| Figure 2.1 | Inverse Gas Chromatography Equipment | 11 |
| Figure 2.2 | Schematic Diagram of a GC Column | 13 |
| Figure 2.3 | Schematic Representation of a Two-Dimensional Lattice Model Containing Low Molecular Weight Solvent and Low Molecular Weight Solute Molecules | 16 |
| Figure 2.4 | Schematic Representation of a Two-Dimensional Flory-Huggins Lattice Containing a Polymer Chain in Solution | 19 |
| Figure 2.5 | Gibbs Free Energy of Mixing of a Immiscible Binary Mixture on Composition at Constant Pressure and Temperature | 22 |
| Figure 2.6 | Gibbs Free Energy of Mixing of a Miscible Binary Mixture on Composition at Constant Pressure and Temperature | 23 |
| Figure 2.7 | Gibbs Free Energy of Mixing of a Partially Miscible Binary Polymer Mixture on Composition at Constant Pressure and Temperature | 24 |
| Figure 2.8 | Representative Phase Diagrams for a Polymer Solution Displaying an Upper Critical Solution Temperature | 27 |
| Figure 4.1 | $\chi_{23}$ Versus Temperature For HDPE-1/LLDPE Blends | 76 |
| Figure 4.2 | $\chi_{23}$ Versus Temperature For HDPE-2/LLDPE Blends | 77 |
| Figure 4.3 | $\chi_{23}$ Versus Branch Content of LLDPE for HDPE-1/LLDPE Blends | 79 |
| Figure 4.4 | $\chi_{23}$ Versus Branch Content of LLDPE for HDPE-2/LLDPE Blends | 80 |

Blends

Figure 5.1 $\chi_{12}$ Versus Polymer Mass (a) T = 170°C, (b) T = 190°C, (c) T = 210°C, (d) T = 230°C 93

Figure 5.2 Temperature Dependence of $\chi_{23}$ for HDPE-2/LLDPE Blends 100

Figure 5.3 Branch Content Dependence of $\chi_{23}$ for HDPE-2/LLDPE Blends 102

Figure 5.4 Temperature Dependence of $\chi_{23}$ for HDPE-1/LLDPE Blends 103

Figure 5.5 Branch Content Dependence of $\chi_{23}$ for HDPE-1/LLDPE Blends 104

## NOMENCLATURE

| | |
|---|---|
| $a_1$ | Degree of polymerization of component 1 |
| $a_2$ | Degree of polymerization of component 2 |
| $B_{11}$ | Second viral coefficient |
| C | Quaternary carbons |
| CH | Methane |
| $CH_2$ | Methylene |
| $CH_3$ | Methyl |
| $C_1^g$ | Concentration of the solvent in the gas phase |
| $C_1^l$ | Concentration of the solvent in the liquid phase |
| D | Deuterated state |
| DHDPE | Deuterated high-density polyethylene |
| DMA | Dynamic mechanical analysis |
| DSC | Differential scanning calorimetry |
| F | Carrier gas flowrate |
| FID | Flame ionization detector |
| FTIR | Fourier transform infrared spectroscopy |
| GC | Gas chromatography |
| GLC | Gas-liquid chromatography |
| GSC | Gas-solid chromatography |
| H | Hydrogeneous state |
| $H_2$ | Hydrogen |
| HDPE | High-density polyethylene |

| | |
|---|---|
| i-PP | Isotactic polypropylene |
| IGC | Inverse gas chromatography |
| J | James-Martin correction factor |
| $k$ | Boltzman constant |
| $L$ | Avogadro's number |
| LAM | Raman longitudinal-acoustic-mode spectroscopy |
| LCST | Lower critical solution temperature |
| LDPE | Low-density polyethylene |
| LLDPE | Linear low-density polyethylene |
| LLPS | Liquid-liquid phase separation |
| LS | Light scattering |
| MD | Molecular dynamics |
| $M_n$ | Number average molecular weight |
| $M_w$ | Weight average molecular weight |
| $M_2$ | Molecular weight of the polymer |
| N | Total number of solvent and solute molecules |
| $n_1$ | Number of solvent molecules |
| $n_2$ | Number of solute molecules |
| PDI | Polydispersity index |
| PE | Polyethylene |
| PS | Polystyrene |
| $P_i$ | Inlet pressure |
| $P_o$ | Outlet pressure |

| | |
|---|---|
| $P_1^0$ | Saturated vapor pressure of the solute |
| R | Gas constant |
| $R^2$ | Coefficient of determination |
| r | Ratio of the polymer volume to the solvent volume |
| SANS | Small angle neutron scattering |
| SAXS | Small angle X-ray scattering |
| T | Temperature |
| TC | Thermal conductivity |
| TEM | Transmission electron microscopy |
| $T_g$ | Glass transition temperature |
| $t_m$ | Retention time of the marker |
| $t_n$ | Net retention time |
| $t_p$ | Retention time of the solute |
| UCST | Upper critical solution temperature |
| USANS | Ultra-small angle neutron scattering |
| WAXD | Wide angle X-ray diffraction |
| $w_2$ | Weight fraction of polymer 2 |
| $w_3$ | Weight fraction of polymer 3 |
| XD | X-ray diffraction |
| $x_1$ | Mole fraction of solvent |
| $x_2$ | Mole fraction of solute |
| $V_0$ | Reference volume |
| $V_1$ | Molar volume of component 1 |

| | |
|---|---|
| $V_2$ | Molar volume of component 2 |
| $V_g^0$ | Specific retention volume |
| $V_1^0$ | Molar volume of the solvent |
| z | Coordination number |
| $\Delta G_m$ | Gibbs free energy change of mixing |
| $\Delta H_m$ | Enthalpy change of mixing |
| $\Delta S_m$ | Entropy change of mixing |
| $\Delta\mu_1^l$ | Difference in the chemical potentials of the solute in the mixture and pure liquid phases |
| $\Delta\mu_1^g$ | Difference in the chemical potentials of the solute in the mixture and pure gas phases |
| $\delta$ | Hildebrand solubility parameter |
| $\Omega$ | Number of ways of arranging the molecules |
| $\chi$ | Flory-Huggins interaction parameter |
| $\chi_{12}$ | Solvent (1)-polymer (2) Flory-Huggins interaction parameter |
| $\chi_{13}$ | Solvent (1)-polymer (3) Flory-Huggins interaction parameter |
| $\chi_{1(23)}$ | Solvent (1)-polymer blend (23) Flory-Huggins interaction parameter |
| $\chi_{23}$ | Polymer (2)-Polymer (3) Flory-Huggins interaction parameter |
| $\chi'_{23}$ | Apparent polymer (2)-polymer (3) Flory-Huggins interaction parameter |
| $(\chi_{12})_{crit}$ | Critical Flory-Huggins interaction parameter |
| $\rho_2$ | Density of the polymer in the amorphous state |
| $\phi_1$ | Lattice volume fraction of the solvent |

| | |
|---|---|
| $\phi_2$ | Lattice volume fraction of the polymer |
| $\mu_2^A$ | Chemical potential of polymer 2 in phase A |
| $\mu_2^B$ | Chemical potential of polymer 2 in phase B |
| $\mu_3^A$ | Chemical potential of polymer 3 in phase A |
| $\mu_3^B$ | Chemical potential of polymer 3 in phase B |
| $\nu$ | Specific volume |
| $\nu_2$ | Specific volume of the polymer 2 |
| $\nu_3$ | Specific volume of the polymer 3 |
| $\psi$ | Interaction energy |
| $\psi_{11}$ | Interaction energy of the 1-1 molecular interactions |
| $\psi_{12}$ | Interaction energy of the 1-2 molecular interactions |
| $\psi_{22}$ | Interaction energy of the 2-2 molecular interactions |

# Chapter 1

# Introduction

## 1.1 Introduction

Polyethylene (PE), which is a specific type of polyolefin, is one of the most widely produced polymers in the world. Polyolefins have an overall chemical composition of $CH_2$. The relative number and placements of methyl ($-CH_3$), methylene ($-CH_2$), methane (-CH), and quaternary carbons (-C) vary from polymer to polymer (Crist and Hill, 1997). Polyolefins are the largest class of synthetic polymers produced, with roughly 50 million metric tons produced annually (Paul and Bucknall, 2000). There is a large demand for polyethylene (and polyolefins in general) since they have several useful properties such as light weight, low cost, high strength, high chemical resistance, excellent process-ability, and so on.

Polyethylene was first produced by Imperial Chemicals Limited in 1933 by polymerizing ethylene under very high pressures (at least 120 MPa). With the discovery of an organo-metallic type catalyst by Ziegler and Natta in the 1950's, the commercial production of polyethylene was made feasible since it could be produced at much lower pressures and temperatures. For example, linear polyethylene can be produced at atmospheric pressure and room temperature with the use of this type of catalyst. Due to recent advances in polymerization technology, polyethylene can be produced in a variety of molecular architectures, which exhibit different processing and performance properties, through the use of Ziegler-Natta and metallocene catalysts. Each different form of polyethylene has different properties that result from variations in its structure (Agamalian, 2000). The three major molecular architectures of polyethylene that are

commercially produced are high-density polyethylene (HDPE), low-density polyethylene (LDPE), and linear low-density polyethylene (LLDPE). HDPE is the most crystalline form because the chains contain very little branching. Typical LDPE contains both short chain branches (1-3 per 100 backbone carbon atoms) as well as long chain branches (0.1-0.3 per 100 backbone carbon atoms). LLDPE contains only short chain branches, but can have a wide range of branch contents depending on the catalyst and concentration of comonomer added. Both HDPE and LDPE are homopolymers that are made by polymerizing ethylene monomers, while LLDPE is a co-polymer formed by co-polymerizing ethylene and α-olefin monomers. The type of α-olefin that is used determines the branch length on the LLDPE that is produced. Common α-olefins used in the production of LLDPEs are 1-butene, 1-hexene, and 1-octene.

It has been found that by blending HDPE, LDPE, and LLDPE, specific properties that differ from the neat polymers can be obtained. The concept of blending two or more polymers to obtain new polymer systems is attracting widespread interest for commercial utilization. Blending provides a simpler and more economical alternative for obtaining polymeric systems with desired properties, as compared to the synthesis of new homopolymers (Al-Saigh and Chen, 1991). For example, LDPE is a polymer with both long and short chain branches and it is often blended with LLDPE to improve the melt properties of LLDPE films. Long chain branching is an important structural parameter in the processing of polymers. Therefore, it is believed that the long chain branches present in LDPE give better melt strength to these films by increasing the extensional strain characteristics of the melt. It has been shown that the processing behaviour of blown LLDPE films can be significantly improved by the addition of up to 30% (by mass)

LDPE. LLDPE provides superior mechanical and thermal properties for these films. In addition, the blending of LDPE into LLDPE is found to improve the optimal properties of the LLDPE films (Chen et al., 2001).

The growing demand for polymer blends has consequently resulted in a need for a better understanding of their miscibility, which in turn has generated tremendous interest in techniques that can be used to characterize the blends. In order to optimize the design of such blends to achieve the desired physical and mechanical properties, a great deal of attention has been focused on improving our understanding of the phase behaviour as well as on developing techniques for characterizing and predicting the miscibility between the components of the blend (Olabisi et al., 1979).

For polyolefin blends, which represent perhaps 30% of all polyolefin products, the state of the miscibility is critically important to their use (Paul and Bucknall, 2000). Miscibility occurs when specific interaction forces develop between the backbones of the two polymers. Specific interactions may be in the form of hydrogen bonding, charge transfer complexes, acid-base type interactions, dipole moments, electron donor-acceptor complexes, etc. (Al-Saigh and Chen, 1991). These specific interactions are of a highly directional nature and are present in addition to the dispersive forces. Thus, the interaction between unlike polymers is "repulsive" for the majority of orientations that bring into proximity the interacting groups. Since all polyolefins are saturated hydrocarbons substances (empirical formula $CH_2$) and therefore, chemically similar, it could be hypothesized that all polyolefins would be miscible with one another. Yet, the lack of any polarity or other functionality means that there are no specific attractions between such high molecular weight saturated hydrocarbons, which could lead to the

hypothesis that they are never miscible. Consequently, numerous experimental and computational techniques have been developed to study the phase behaviour of these blends, which has led to a certain level of understanding of their phase behaviour.

## 1.2 Quantifying Miscibility

Whether or not a polymer and solvent or a polymer and a polymer are mutually soluble (miscible) is governed by the Gibbs free energy change of mixing ($\Delta G_m$) as well as the second derivative of the Gibbs free energy change of mixing with respect to the volume fraction of component 1 or 2 (for a binary mixture). According to the Flory-Huggins theory, the combinatorial entropy portion of the Gibbs free energy change of mixing is small for polymer blends. Consequently, the enthalpy term determines miscibility. This term depends on a dimensionless parameter, the so-called Flory-Huggins interaction parameter ($\chi$) that corresponds to the interaction energy between two components. A more detailed explanation of determining the miscibility of blends using the Flory-Huggins theory is supplied in Chapter 2 of this thesis.

There are several different methods that can be used to determine $\chi$ values for polymer solutions and polymer blends. Traditionally, most methods that have been used to study polymer miscibility are expensive, time consuming, and in many cases cannot be used to study the blend in the melt state. It is believed that melt miscibility can significantly influence the solid-state morphology and mechanical properties of the polymer blend. Therefore, it is desirable to develop a reliable and inexpensive method that can be used to study polymer blends in their melt state.

Among the experimental techniques commonly used for the measurement of $\chi$, inverse gas chromatography (IGC) is the least expensive method. In 1969, Smidsrod and Guillet proposed that IGC could be used to determine polymer-solvent interaction parameters. Deshpande et al. (1974) then suggested that IGC could be used to characterize the miscibility of polymer blends. Traditionally, a weakness of using IGC for the determination of Flory-Huggins interaction parameters has been that the measured values are dependent on the probe that is used in the characterization of the polymer blends. This so-called "probe dependence" problem has severely limited the widespread use of IGC. Zhao and Choi (2001) have developed a novel method for the determination of probe independent polymer-polymer interaction parameters by IGC. Further discussion regarding the process of using IGC to characterize polymer blends is presented in Chapter 2 of this thesis.

Zhao and Choi (2001) obtained promising results for a variety of polyolefin blends, including HDPE/isotactic polypropylene (i-PP), HDPE/polystyrene (PS), HDPE/LDPE, HDPE/LLDPE and LDPE/LLDPE blend systems. For these different blend systems, they obtained solvent independent polymer-polymer interaction parameters. However, in most cases the calculated $\chi$ values were at least one order of magnitude larger than values reported in the literature that were obtained using other methods such as Small Angle Neutron Scattering (SANS) or Molecular Dynamics (MD) simulations.
In the case of the HDPE/LLDPE blends, a low molecular weight HDPE was blended with five LLDPEs of differing branch contents. The HDPE/LLDPE blends were studied at three different compositions (30/70, 50/50 and 70/30 wt%) over a temperature range (170, 190, 210, and 230°C). Solvent independent $\chi$ values were obtained and blend

immiscibility occurred when the branch content of the LLDPE was roughly above 50 branches per 1,000 backbone carbons. The miscibility trend observed is in agreement with results obtained from other methods such as Differential Scanning Calorimetry (DSC) and Fourier transform infrared spectroscopy (FTIR) (Tashiro et al. 1992 and 1994), Transmission Electron Microscopy (TEM) (Hill and Barham, 1992), and Small Angle Neutron Scattering (SANS) (Alamo et al., 1997). Surprisingly, even though a trend consistent with the literature is observed, the magnitude of the $\chi$ measured by the authors is typically two to three orders of magnitude larger than those obtained by other methods. Additionally, the associated errors of $\chi$ are very large as well.

## 1.3 Purpose

For this thesis, HDPE/LLDPE blends were studied in the melt state using the method proposed by Zhao and Choi (2001). The same LLDPE samples used by the authors were used, while two different HDPE samples were used. One was the same low molecular weight HDPE that was used in the previous studies, while the other was a high molecular weight HDPE. The purpose of this research was to investigate the effect of the molecular weight of HDPE on the miscibility of the HDPE/LLDPE blends. Also the sources of error were evaluated critically in an attempt to reduce the associated uncertainties.

## 1.4 References

Alamo, R.G., Graessely, W.W., Krishnamoorti, R., Lohse, D.J., Londono, J.D., Mandelkern, L., Stehling, F.C., and Wignall, G.D. (1997) Small Angle Neutron

Scattering Investigations of Melt Miscibility and Phase Segregation in Blends of Linear and Branched Polyethylenes as a Function of the Branch Content, Macromolecules, 30, 561-566.

Agamalian, M.M., Alamo, R.G., Londono, J.D., Mandelkern L and Wignall G.D. (2000) Phase Behaviour of Blends on Linear and Branched Polyethylenes on Micron Length Scales Via Ultra-Small Angle Neutron Scattering (USANS), Journal of Applied Crystallography, 33, 843-846.

Al-Saigh, Z.Y. and Chen, P. (1991) Characterization of Semicrystalline Polymers by Inverse Gas Chromatography. 2. A Blend of Poly(vinylidene fluoride) and Poly(ethyl methacrylate), Macromolecules, 24, 3788-3795.

Chen, F., Shanks, R., and Amarsinghe, G. (2001) Miscibility Behaviour of Metallocene Polyethylene Blends, Journal of Applied Polymer Science, 81, 2227-2236.

Crist B. and Hill, M.J. (1997) Recent Developments in Phase Separation of Polyolefin Melt Blends, Journal of Polymer Science: Part B: Polymer Physics, 35, 2329-2353.

Deshpande, D.D., Patterson, D., Schreiber, H.P. and Su, C.S. (1974) Thermodynamic Interactions in Polymer Systems by Gas-Liquid Chromatography. IV. Interactions Between Components in a Mixed Stationary Phase, Macromolecules, 7,4,530-535.

DiPaola-Barany, G. (1989) Thermodynamics of Polymer Blends by Inverse Gas Chromatography, ACS Symposium Series, 391, 108-120.

Hill, M.J., Barham, P.J., and Keller, A. (1992) Phase Segregation in Blends of Linear with Branched Polyethylene: the Effect of Varying the Molecular Weight of the Linear Polymer, Polymer, 33, 12, 2530-2541.

Olabisi, O.L., Robeson, M. and Shaw, M.T., (1979) Polymer-Polymer Miscibility, Academic Press, New York, NY.

Paul, D.R. and Bucknall, C.B. (2000) Polymer Blends, 1, John Wiley and Sons, New York, NY.

Smidsrod, O. and Guillet, J.E. (1969) Study of Polymer-Solute Interactions by Gas Chromatography, Macromolecules, 2, 3, 272-277.

Tashiro, K., Stein, R.S., and Hsu, S.L. (1992) Cocrystallization and Phase Segregation of Polyethylene Blends. 1. Thermal and Vibrational Spectroscopic Study by Utilizing the Deuteration Technique, Macromolecules, 25, 1801-1808.

Tashiro, K., Izuchi, M., Kabayashi, M., and Stein, R.S. (1994) Cocrystallization and Phase Segregation of Polyethylene Blends Between the D and H Species. 3. Blend Content Dependence of the Crystallization Behaviour, Macromolecules, 27, 1221-1227.

Zhao, L. and Choi, P. (2001) Determination of Solvent-Independent Polymer-Polymer Interaction Parameters by an Improved Gas Chromatographic Approach, Polymer, 42, 1075-1081.

# Chapter 2

# Inverse Gas Chromatography

## 2.1 Introduction

There are two types of gas chromatography analysis: gas-solid chromatography (GSC) and gas-liquid chromatography (GLC). This review will focus on GLC since this was used in the present work. Here GLC will be referred to as GC throughout the rest of this review.

The analytical uses of GC have become very common and widely accepted as a method of analysis. For example, GC has become a widely accepted method to analyze an unknown sample (of low molecular weight) to determine its composition. However, the development of GC as a method of obtaining physico-chemical information has been relatively slow. One of the researchers recognizing the potential of GC for measurement of physico-chemical properties was Martin (1956), one of the inventors of GC. He commented that the method provides a simple means of studying the thermodynamics of the interaction of a volatile solute with a non-volatile solvent. Although this was identified almost 50 years ago, the GC method has still not been exploited to its fullest potential.

GC can provide accurate thermodynamic data on binary solutions where the components differ considerably in volatility or molecular weight (Patterson et al., 1971). The substance of lower molecular weight is injected into the mobile gas phase and dissolves at essentially infinite dilution into the high molecular weight stationary phase. The convenience of this method is that the activity coefficient data for hundreds of systems has already been accumulated, thus enabling the accurate and rapid analysis of

unknown gases. However, activity coefficient data for polymer systems is much less available.

Smidrod and Guillet first applied GC to polymer systems in 1969. They were primarily interested in demonstrating the versatility of the technique in determining first and second-order phase transitions, degrees of crystallinity, and other physical characteristics of polymers. Since then, the method has been used fairly extensively to determine thermodynamic quantities of polymers and polymer blends with limited success.

Owing to the fact that polymers cannot be vaporized, they are employed exclusively as the stationary phase in GC analysis. Traditionally, polymer-solute interactions were characterized by static equilibrium methods, which are very time consuming. Thus, GC is a desirable method since it allows for rapid analysis (Smidrod and Guillet, 1969). Another advantage of GC analysis is that it is applicable over a wide range of temperatures, making it possible to analyze materials of a wide range of volatilities, and perhaps more importantly for polymers, at their processing temperatures.

A typical GC apparatus is shown in Figure 2.1. It consists of a carrier gas cylinder, combustion gas cylinders ($H_2$ and air), a column packed with a stationary phase in an oven, an inlet injector, and a tail gas detector. An advantage to this experimental set-up is that the equipment is relatively inexpensive, widely available, and the general operation is simple and quick.

The general principle of GC is based on the distribution of a compound between two phases, which are the mobile gaseous phase and the stationary liquid phase. Unlike traditional GC, for Inverse Gas Chromatography (IGC), the species of interest is the

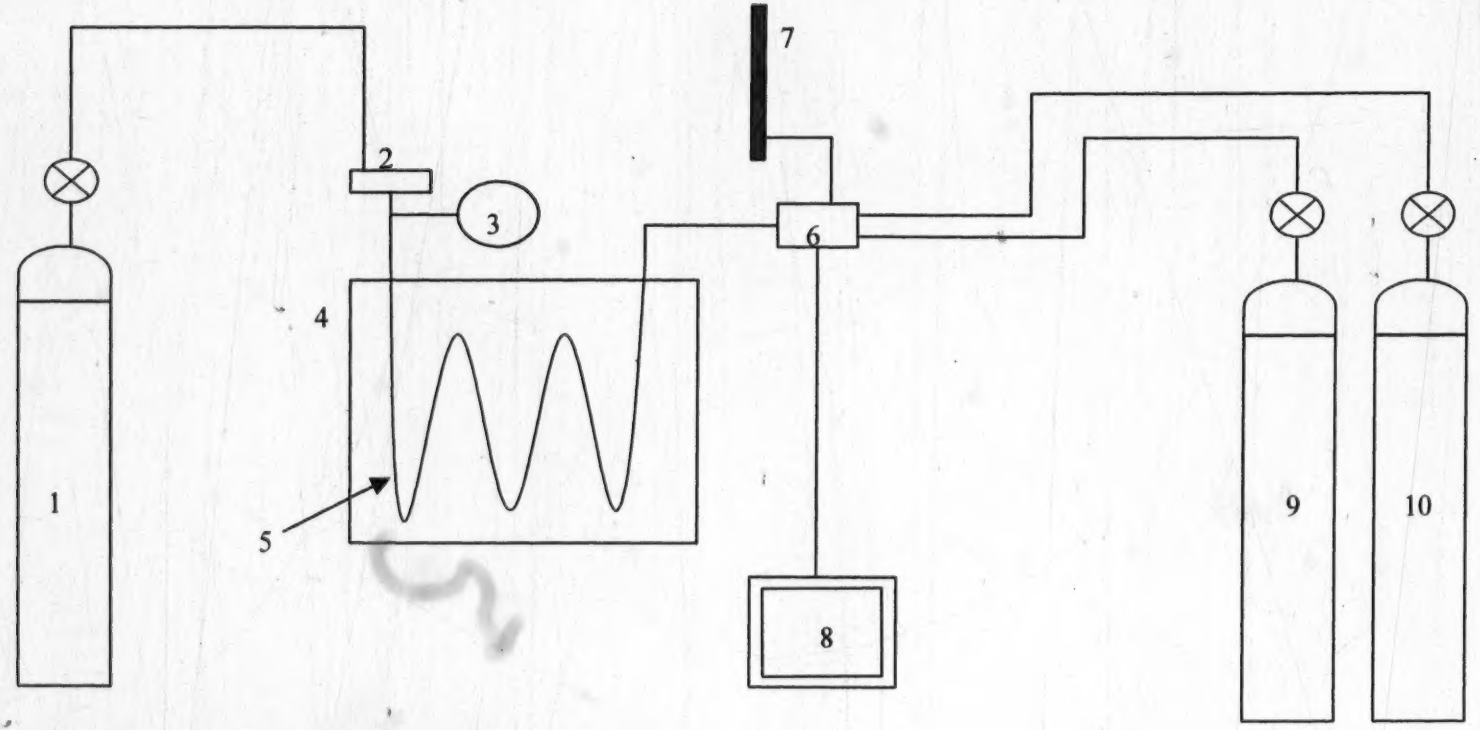


**Figure 2.1 Inverse Gas Chromatography Equipment**

(1) Helium Gas Cylinder (carrier gas); (2) Injection Point; (3) Pressure Gauge; (4) Oven; (5) Column; (6) Flame Ionization Detector; (7) Bubble Flowmeter; (8) Computer Interface; (9) Hydrogen Gas Cylinder; (10) Air Cylinder.

stationary phase rather than the gaseous phase. Thus, for analysis of the stationary phase, it is required that the mobile gas phase has accurately known physico-chemical properties. In IGC the stationary phase typically consists of a polymer-coated support. A gaseous sample (probe) is injected into the column containing the stationary phase, which undergoes a continuous sorption-desorption process as the probe is swept through the system by an inert carrier gas. This process occurs repeatedly as the sample moves towards the end of the column as depicted in Figure 2.2. This is in contrast to conventional analytical GC where the stationary phase is of interest only as far as its ability to separate the injected compounds (Etxeberria et al., 1992). Also, in IGC, typically only one pure compound is injected at a time. Usually compounds with different distribution characteristics are used. These different distribution characteristics are vital to the application of IGC since the size and retention times of the eluted peaks can be used to calculate relevant thermodynamic characteristics of the solution process, namely the partition coefficient, the activity coefficient, and the change in the excess partial molar thermodynamic functions of the solute in the stationary phase. Also, IGC has received recognition as a simple method for the rapid measurement of polymer's solubility parameters. In essence, the thermo-physical properties of the polymer are inferred from the interactions between the solvent and the polymer. Since the technique was introduced, it has been used to accurately investigate physical properties of polymer systems such as, glass transition temperature, diffusion coefficients, crystallinity, solubility parameters, adsorption isotherms, heats of adsorption, surface area, interfacial phenomena, and diffusion coefficients.

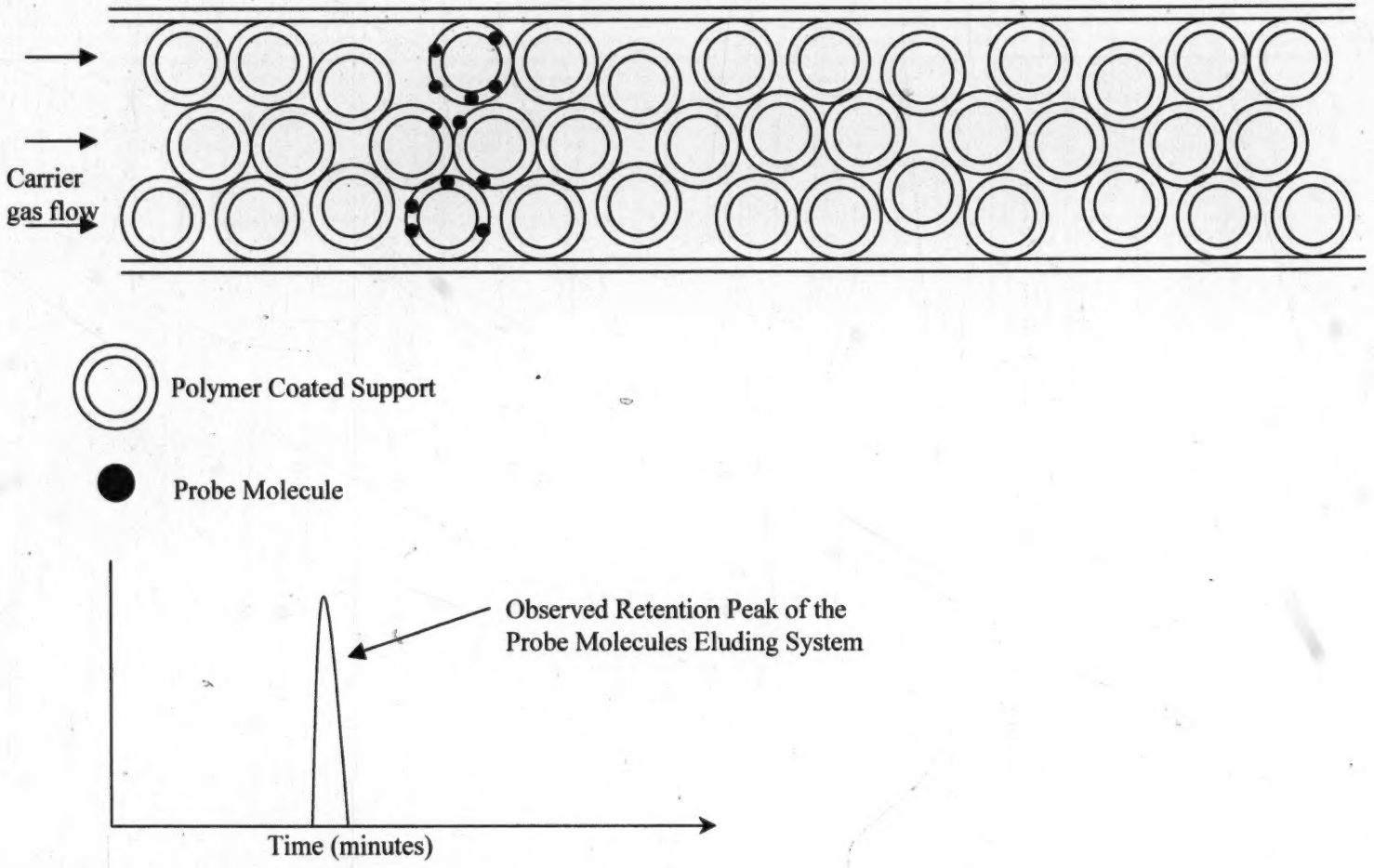


**Figure 2.2 Schematic illustration of a GC Column**

IGC has been known as a method to analyze homopolymers since Guillet's work in 1969. However, it wasn't until 1974 that Deshpande et al. suggested that IGC could be used to characterize the miscibility of polymer blends. Based on the ternary version of the Flory-Huggins expression for the Gibbs' free energy change of mixing, $\Delta G_m$, they proposed a method of analysis for IGC data on polymer blends that would yield the Flory-Huggins polymer-polymer interaction parameter, $\chi_{23}$, a measure of the polymer blend miscibility. Olabisi (1975) also independently suggested a similar technique in which three IGC columns (two from homopolymers and a third from the blend) are used to calculate $\chi_{23}$. In this case, $\chi_{23}$ was also derived using the classical Flory-Huggins expression for the Gibbs' free energy change of mixing. The thermodynamic interactions in a ternary system are expressed as a combination of the pair interaction parameters, which have been implicitly assumed to be independent of the combination of the stationary phase (Tyagi et al., 1987).

There are two methods by which the Flory-Huggins interaction parameter can be determined when using IGC. In one method, the Hildebrand solubility parameters of the components comprising the blend are measured and such parameters are used to calculate $\chi$. The other method is to measure the interaction parameter of the blend directly. The first approach requires positive $\chi_{12}$ (solvent-polymer interaction) to obtain the Hildebrand solubility parameter, $\delta$. A drawback of the method is that the composition dependence (of the blend) on $\chi_{23}$ cannot be obtained. This is problematic since it is well known that $\chi_{23}$ is composition dependent. Owing to these shortcomings the second approach was used in the present work.

## 2.2 The Flory-Huggins Lattice Theory

For polymer solutions, non-ideal thermodynamic behaviour has been observed even though the polymer and the solvent exhibit comparable intermolecular interaction (i.e., nearly zero $\Delta H_m$). Therefore, the deviations from ideality for long chain molecules mixed with small molecules must be due to non-ideal entropy. The first attempts to calculate the non-ideal entropy were investigated in the early 1940's by Paul Flory (1941) and Maurice Huggins (1941). Each, working independently, developed a theory based on a simple lattice model that could be used to understand the non-ideal nature of polymer solutions. In the Flory-Huggins theory, both the size difference between the solvent and polymer molecules, as well as the intermolecular interactions are considered, it is assumed that each polymer molecule is composed of a series of segments. Typically, each lattice site is defined as the size of a solvent molecule, or a polymer segment with the same volume as a solvent molecule. Therefore, each polymer segment will take one lattice site. The Flory-Huggins model is used to calculate the total number of ways that the lattice sites can be occupied by the solvent molecules and by the connected polymer segments.

A simple example of the lattice theory is illustrated in Figure 2.3, where a low molecular weight solvent (component 1) is mixed with a low molecular weight solute (component 2). It is assumed that the solute molecules have the same size as the solvent molecules. For the simple lattice model, the increase in entropy due to the mixing process, $\Delta S_m$, is obtained using the Boltzman relation:

$$\Delta S_m = k \ln \Omega \qquad (1)$$

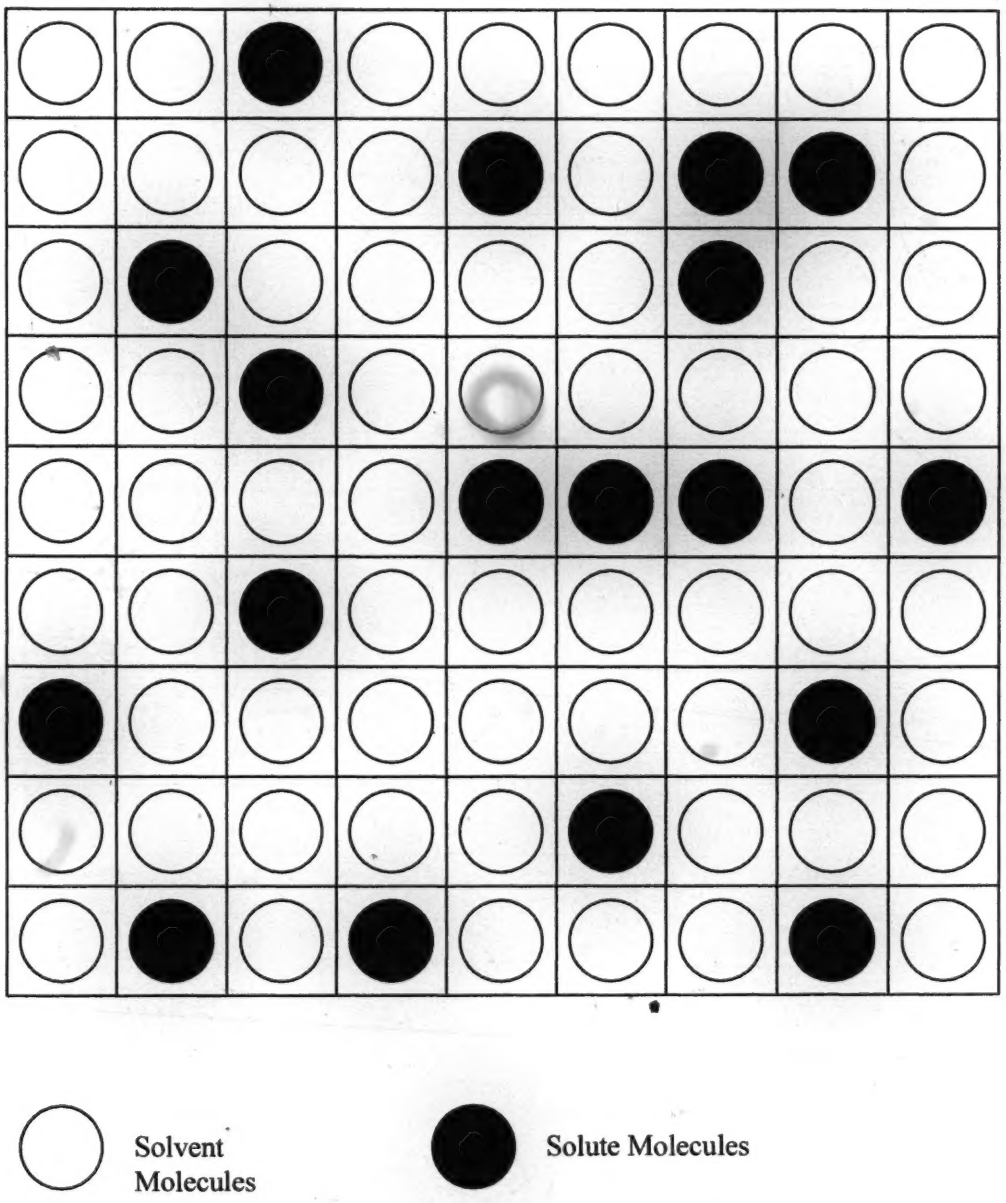


**Figure 2.3** **Schematic Representation of a Two-Dimensional Lattice Model Containing Low Molecular Weight Solvent and Low Molecular Weight Solute Molecules**

where $k$ is the Boltzman constant and $\Omega$ corresponds to the number of ways of arranging the molecules in space and is calculated as follows:

$$\Omega = \frac{N!}{n_1! n_2!} \tag{2}$$

where $n_1$ is the number of solvent molecules, $n_2$ is the number of solute molecules and $N = n_1 + n_2$. To simplify the above expression, Stirling's approximation (Equation 3),

$$\ln n! = n \ln n - n \tag{3}$$

is then used to determine the expression for the entropy change of mixing as:

$$\Delta S_m = -k(n_1 \ln x_1 + n_2 \ln x_2) \tag{4}$$

or

$$\Delta S_m = -R(x_1 \ln x_1 + x_2 \ln x_2) \tag{5}$$

where $R$ is the gas constant; $x_1$ and $x_2$ are the mole fractions of the solvent and solute, which are calculated as follows:

$$x_1 = \frac{n_1}{n_1 + n_2} \tag{6-a}$$

$$x_2 = \frac{n_2}{n_1 + n_2} \tag{6-b}$$

For a solution of a low molecular weight solvent with a high molecular weight polymer, $\Delta S_m$ is smaller than what is calculated by either Equation 4 or 5. This reduction in the entropy is due to the loss in conformational entropy due to the connectivity of polymer segments (Fried, 1995).

In this case, the lattice is established by dividing the polymer chain into $r$ segments each having the size of the solvent with which it is in contact. The term, $r$, is the ratio of the polymer volume to the solvent volume:

$$r = \frac{M_2}{\rho_2 V_1^o} \tag{7}$$

where $M_2$ is the molecular weight of the polymer; $\rho_2$ is density of the polymer in the amorphous state at solution temperature and $V_1^o$ is the molar volume of the solvent.

The Flory-Huggins lattice model is illustrated in Figure 2.4. It is noticeably different than the original lattice theory illustrated in Figure 2.3.

According to the Flory-Huggins theory, the entropy change on mixing is calculated as:

$$\Delta S_m = -R(n_1 \ln \phi_1 + n_2 \ln \phi_2) \tag{8}$$

where $R$ is the gas constant; $n_i$ is the number of moles of the $i$th component; $\phi_i$ is the lattice volume fraction of the $i$th component, which is calculated as follows:

$$\phi_1 = \frac{n_1}{n_1 + rn_2} \tag{9}$$

$$\phi_2 = \frac{rn_2}{n_1 + rn_2} \tag{10}$$

Equation 8 is similar to Equation 5 except that the volume fractions have replaced mole fractions. The difference in the two equations is a reflection of the fact that the entropy of mixing of polymers is small compared to a low molecular weight solvent / low molecular weight solute system since there are fewer possible arrangements of solvent molecules and polymer segments than there would be if the segments were not connected to each other (Rudin, 1998).

Equation 8 provides the entropy term in the Gibbs free energy change of mixing,

$$\Delta G_m = \Delta H_m - T\Delta S_m \tag{11}$$

where $T$ is the temperature and $\Delta H_m$ is the enthalpy change of mixing.

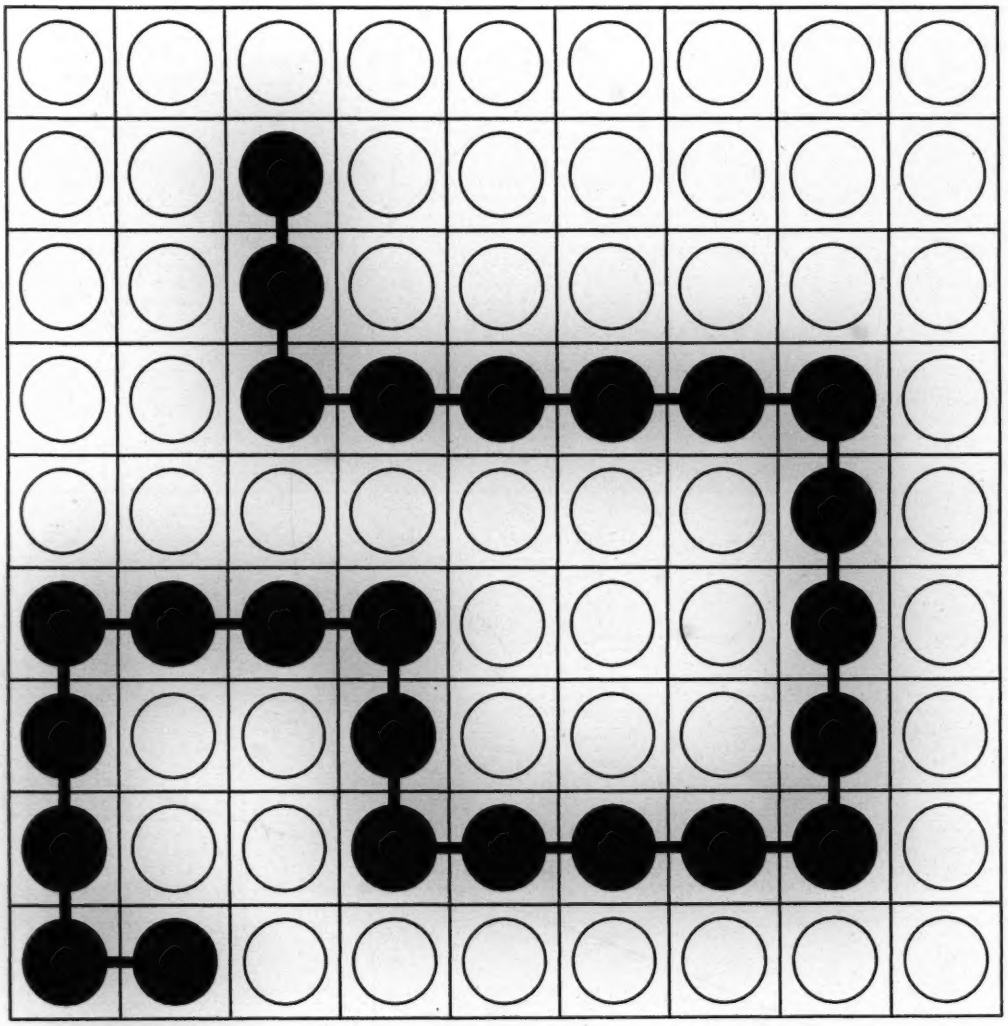


**Figure 2.4** **Schematic Representation of a Two-Dimensional Flory-Huggins Lattice Containing a Polymer Chain in Solution**

For ideal or athermal solutions, $\Delta H_m = 0$, but in the case of real polymer mixtures, $\Delta H_m \neq 0$. Flory and Huggins defined the enthalpy change of mixing as:

$$\Delta H_m = z\Psi(n_1 + rn_2)\phi_1\phi_2 L \tag{12}$$

where $z$ is the coordination number or numbers of cells that are first neighbours to a given cell, $r$ is the number of polymer segments, $L$ is Avogadro's number, $\Psi$ is the interaction energy:

$$\Psi = \Psi_{12} - \frac{1}{2}(\Psi_{11} + \Psi_{22}) \tag{13}$$

where $\psi_{ij}$ is the energy of the *i-j* contacts. It can be seen from Equations 12 and 13 that for an ideal solution ($\Delta H_m = 0$) that the interaction energy of the 1-2 molecular interactions are equal to the arithmetic average of those of 1-1 and 2-2.

The Flory-Huggins interaction parameter, $\chi_{12}$, is a dimensionless quantity that is defined as:

$$\chi_{12} = \frac{z\Psi L}{RT} \tag{14}$$

As can be observed from Equation 14, $\chi_{12}$ is defined as being inversely dependent on temperature and independent of concentration.

The enthalpy change of forming a mixture with volume fraction $\phi_2$ of polymer in $n_1$ moles of solvent is then obtained by combining Equations 12 and 14:

$$\Delta H_m = RT\chi_{12} n_1 \phi_2 \tag{15}$$

Combining Equations 8 and 15 the Flory-Huggins expression for the Gibbs free energy of mixing is shown as follows:

$$\Delta G_m = RT(n_1 \ln\phi_1 + n_2 \ln\phi_2 + \chi_{12} n_1 \phi_2) \tag{16}$$

Similarly, for a ternary system,

$$\Delta G_m = RT(n_1 \ln \phi_1 + n_2 \ln \phi_2 + n_3 \ln \phi_3 + n_1\phi_2\chi_{12} + n_1\phi_3\chi_{13} + n_2\phi_3\chi_{23}) \quad (17)$$

## 2.3 Phase Equilibria

For a polymer-solvent or polymer-polymer solution to be mutually soluble, or miscible, the Gibbs free energy of mixing (Equation 11) must be negative. Even though positive contributions of the combinatorial entropy favours mixing, as the size of the components increase, the effect of the entropy becomes negligible. Therefore, negative enthalpy change of mixing is needed for such molecules to be miscible. This, in turn, requires that the interaction parameter, $\chi_{12}$, is negative (i.e., exothermic heats of mixing).

However, $\Delta G_m < 0$ is not a sufficient condition solely. In order to satisfy stability considerations for a binary system, the following is also required (Fried, 1995):

$$\left(\frac{\partial^2 \Delta G_m}{\partial \phi_2^2}\right) > 0 \quad (18)$$

Three different composition dependencies of $\Delta G_m$ are typically observed at constant temperature and pressure. Figure 2.5 illustrates an immiscible system where $\Delta G_m$ is positive over the entire composition range. Therefore, the two components will exist as two distinct phases. Two other possibilities exist, total miscibility and partial miscibility as illustrated in Figures 2.6 and 2.7 respectively. In Figure 2.6 both miscibility conditions are satisfied; however, in Figure 2.7, two minima in $\Delta G_m$ are observed. This indicates that the criterion expressed by Equation 18 is not satisfied at certain

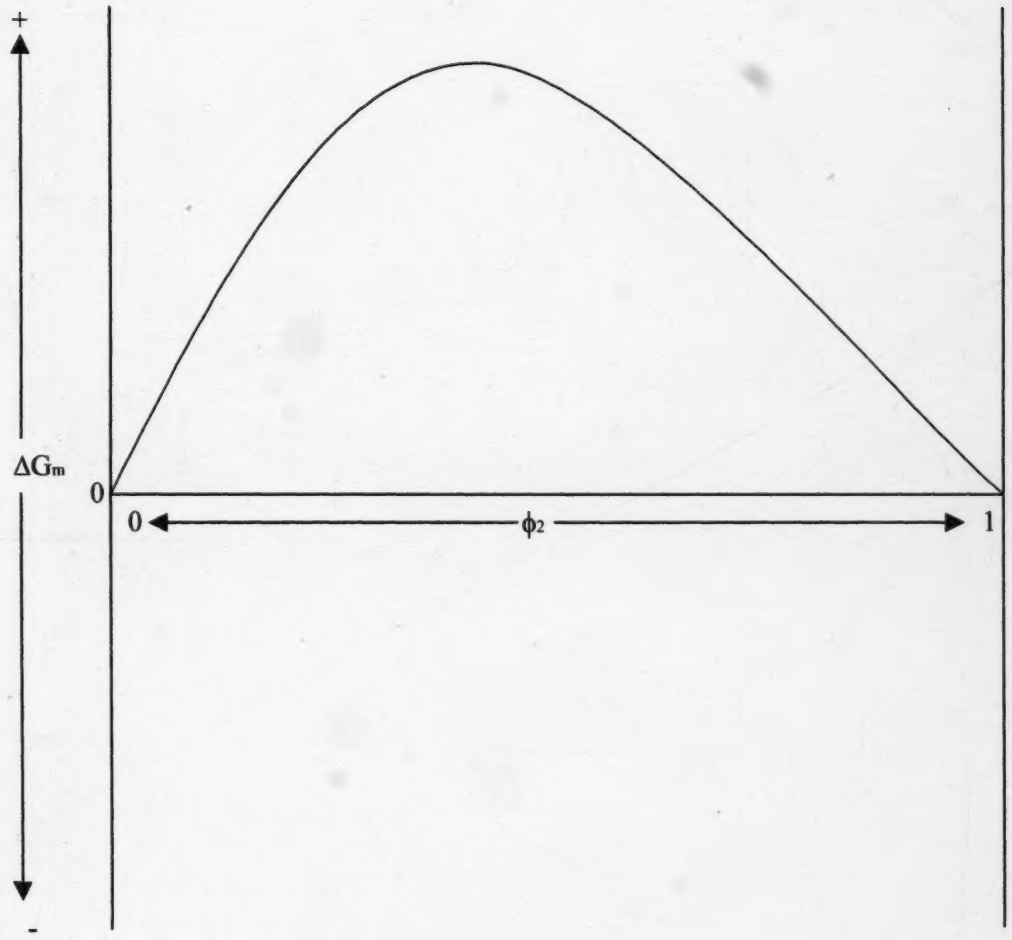


**Figure 2.5** **Gibbs Free Energy of Mixing of a Immiscible Binary Mixture on Composition at Constant Pressure and Temperature**

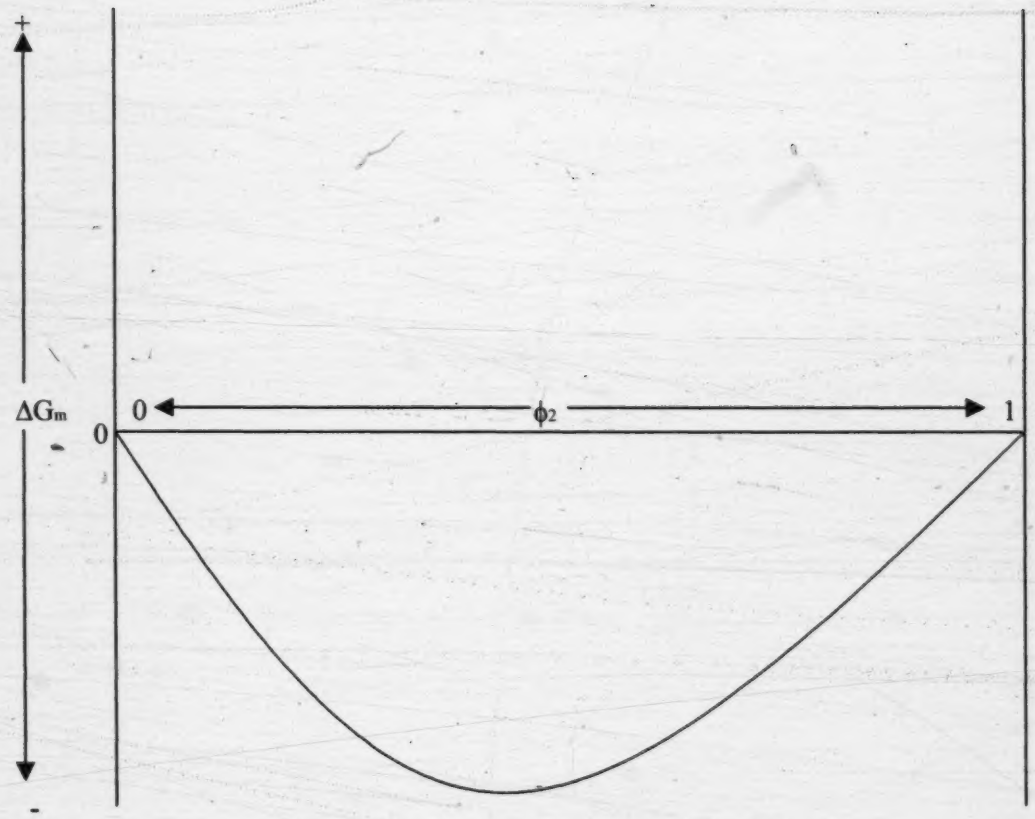


**Figure 2.6** **Gibbs Free Energy of Mixing of a Miscible Binary Mixture on Composition at Constant Pressure and Temperature**

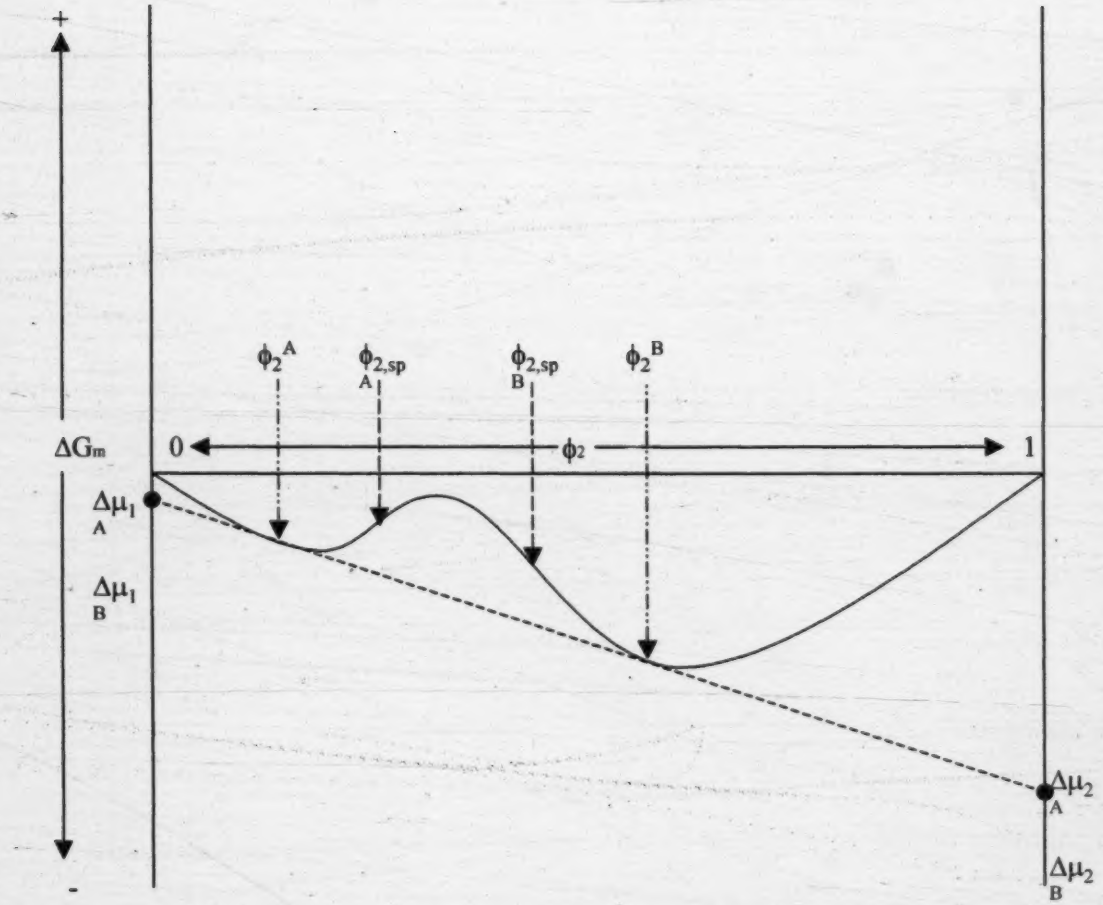


**Figure 2.7** **Gibbs Free Energy of Mixing of a Partially Miscible Binary Polymer Mixture on Composition at Constant Pressure and Temperature**

compositions. For a partially miscible solution phase separation at equilibrium will occur resulting in the formation of two phases each containing different compositions of both components.

The points of common tangent as illustrated in Figure 2.7 give the compositions of the two separate phases. It is well known that the phase equilibrium is strongly affected by the solution temperature. By changing the temperature of a given system any of the three phase behaviours may result.

For solutions of low molecular weight compounds, it has traditionally been observed that the solubility increases with an increase in temperature and it has also been observed for polymer blends. This situation is illustrated in Figure 2.8. At temperatures above the upper critical solution temperature (UCST) the solution is totally miscible. When the temperature is below the UCST phase separation may occur depending upon the overall composition of the mixture. At temperatures below the UCST with compositions outside of the curves, the system is thermodynamically unstable and phase separation will occur at equilibrium. The compositions of the two phases are given by points lying along the curve called the binodal. The binodal is defined as occurring when the conditions for thermodynamic equilibrium for a polymer solution are satisfied as follows:

$$\mu_2^A = \mu_2^B \qquad (19\text{-A})$$

$$\mu_3^A = \mu_3^B \qquad (19\text{-B})$$

where A and B are the phases of differing composition and 2 and 3 are the components of the polymer blend. The difference in the chemical potentials of solvent in the solution

and pure component states are found graphically from the intercepts of the common tangent as drawn in Figure 2.7.

The metastable region, as illustrated in Figure 2.8, is between the binodal and the unstable region. It is bound by the spinodal. It is possible for the system to resist small concentration fluctuations in the metastable region, but the system will equilibrate to the stable two-phase state given by the binodal. The time frame of this occurring could be instantaneous to very long depending on how far from the binodal the system is at. Points that lie along the spinodal correspond to the points of inflection that are observed in Figure 2.7 which satisfy the relationship given in Equation 18. As illustrated in Figure 2.8 the binodal and spinodal coincided at the critical point, which satisfies the relation:

$$\left(\frac{\partial^3 \Delta G_m}{\partial \phi_2^3}\right) = 0 \tag{20}$$

Although, the UCST behaviour is observed in many dilute polymer solutions, Freeman and Rowlinson (1961) observed that phase separation of polymer solutions could occur with an increase in temperature. For this case, the binodal and spinodal curves coincide at a temperature called the lower critical solution temperature (LCST). It has since been observed that a system may exhibit both a UCST and LCST. A serious problem with the Flory-Huggins theory is that it cannot predict a LCST (Fried, 1995).

By taking the second and third derivatives of Equation 16 (defined in terms of the degree of polymerization) with respect to the volume fraction and setting them to zero and then equating the results, after some manipulation the following criterion for the miscibility is obtained:

$$(\chi_{12})_{crit} = \frac{1}{2}\left(\frac{1}{\sqrt{a_1}} + \frac{1}{\sqrt{a_2}}\right)^2 \tag{21}$$

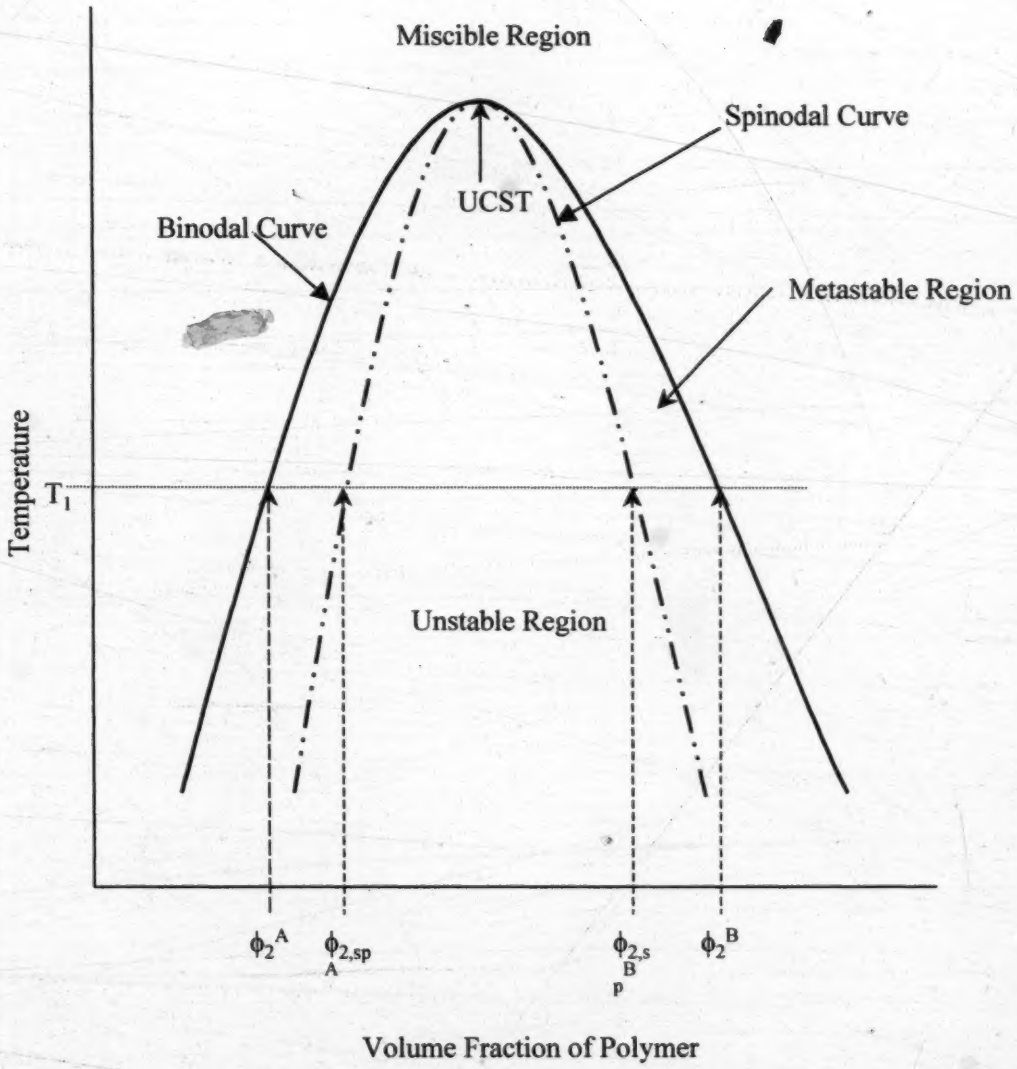


**Figure 2.8 Representative Phase Diagrams for a Polymer Solution Displaying an Upper Critical Solution Temperature**

For small molecule solutions, $a_1 \approx a_2 \approx 1$ and therefore the critical value of the interaction parameter for miscible solutions is obtained as $(\chi_{12})_{crit} = 2$. In the case of a polymer-solvent solution $a_1 \approx 1$, $a_2 \approx \infty$ and the result is that $(\chi_{12})_{crit} = 0.5$. For a polymer blend, $a_1 \approx a_2 \approx \infty$ and therefore, $(\chi_{12})_{crit} = 0$. Therefore, for a polymer blend, it is expected that a negative or small positive $\chi$ is required for miscibility.

## 2.4 Inverse Gas Chromatography Thermodynamics

For inverse gas chromatography, the term that describes the elution behaviour of the injected volatile solute from the chromatographic column is the specific retention volume, $V_g^\circ$. It is defined as follows:

$$V_g^\circ = \frac{273.15 t_n F J}{wT} \tag{22}$$

Here $t_n$ is the net retention time; $F$ is the flow rate of the carrier gas measured at the experimental temperature $T$; $w$ is the mass of the polymer in the chromatographic column; $J$ is the James-Martin correction factor that is used to correct for the pressure gradient across the column.

The net retention time is defined as the difference between the retention times of the solute ($t_p$) and of the unretained solute marker ($t_m$):

$$t_n = t_p - t_m \tag{23}$$

The James-Martin correction factor, $J$, is defined as:

$$J = \frac{3}{2}\left[\frac{\left(\frac{P_i}{P_o}\right)^2 - 1}{\left(\frac{P_i}{P_o}\right)^3 - 1}\right] \tag{24}$$

where $P_i$ and $P_o$ are the inlet and outlet pressures of the column.

The specific retention volume, $V_g^\circ$, is also related to the partition coefficient of the solvent, which is defined as the ratio of the concentration of the solvent in the liquid phase, $C_1^l$, to that in the gaseous phase, $C_1^g$. For a column containing a single polymer:

$$V_g^\circ = \left(\frac{C_1^l}{C_1^g}\right) v_2 \left(\frac{273.15}{T}\right) \tag{25}$$

Here $v_2$ is the specific volume of the polymer in the liquid phase at the column temperature.

For the case of a chromatographic column containing a binary polymer blend:

$$V_g^\circ = \left(\frac{C_1^l}{C_1^g}\right)\left(w_2 v_2 + w_3 v_3\right)\left(\frac{273.15}{T}\right) \tag{26}$$

where $v_i$ and $w_i$ are the specific volume and weight fraction of the polymer $i$ in the liquid phase.

All types of polyethylene (HDPE, LDPE, or LLDPE) exhibit the same specific volume in the melt state. To calculate the specific volume of a polyethylene in the melt state, the following equation is used for temperatures ranging from 150 to 260 °C (Rudin et al., 1970):

$$v = 1.282 + 9.0 * 10^{-4}(T - 150) \tag{27}$$

In this equation $T$ is in °C and $v$ is in $cm^3/g$.

Fast equilibrium is usually established between the stationary and mobile phases in a chromatographic column. Therefore, $V_g^\circ$ measured by IGC is amenable to thermodynamic interpretation. However, if the column temperature is not at least 50 °C above the $T_g$, then this assumption is not valid due to surface adsorption and kinetic effects (Al-Saigh, 1997).

The differences of the chemical potential of the solute in the gaseous phase and liquid phase from a chosen reference state are equal to one another:

$$\Delta\mu_1^l = \Delta\mu_1^g \tag{28}$$

Assuming that both $C_1^l$ and $C_1^g$ are very small (infinite dilution) throughout the chromatographic column, then the chemical potential of the solute in the gas phase at equilibrium is given by:

$$\Delta\mu_1^g = RT \ln \frac{RTC_1^g}{M_1 P_1^\circ} - B_{11} P_1^\circ \tag{29}$$

where $M_1$ is the molecular weight of the solute; $R$ is the gas constant; $P_1^\circ$ is the saturated vapour pressure of the solute; and $B_{11}$ is the second viral coefficient of the solute in the gaseous phase. The last term in Equation 29 represents the correction for non-ideality of the solute in the gas phase. Higher viral terms are typically neglected (Al-Saigh, 1997).

The chemical potential of the solute in the liquid phase is given by:

$$\Delta\mu_1^l = -V_1 P_1^\circ + \left( \frac{\partial \Delta G_m}{\partial n_1} \right) \tag{30}$$

where $n_1$ is the number of moles of component 1 in a mixture and $V_1$ is its molar volume.

The derivative in Equation 30 is determined from Equation 16 as:

$$\left(\frac{\partial \Delta G_m}{\partial n_1}\right) = RT\left[\ln\phi_1 + 1 - \frac{V_1}{V_2} + \chi_{12}\right] \tag{31}$$

When a system is at equilibrium, the chemical potentials are equal (as defined by Equation 28). By combining Equations 25, 28-31 for a single polymer system, the following is obtained to solve for the solvent-polymer interaction parameter:

$$\chi_{12} = \ln\frac{273.15Rv_2}{V_g^{\circ}V_1P_1^{\circ}} - 1 + \frac{V_1}{M_2v_2} - \frac{B_{11} - V_1}{RT}P_1^{\circ} \tag{32}$$

which is the equation traditionally used for the calculation of the solvent-polymer interaction parameter.

For a polymer blend, the Gibbs free energy change of mixing of a ternary system must be used (Equation 17). Its derivative is:

$$\left(\frac{\partial \Delta G_m}{\partial n_1}\right) = RT\left[\ln\phi_1 + 1 - \frac{V_1}{V_2}\phi_2 - \frac{V_1}{V_2}\phi_3 + \phi_2\chi_{12} + \phi_3\chi_{13} - \frac{V_1}{V_2}\phi_2\phi_3\chi_{23}\right] \tag{33}$$

Using Equations 28-32 and Equation 33 the following is obtained:

$$\ln\frac{273.15R(w_2v_2 + w_3v_3)}{V_g^{\circ}V_1P_1^{\circ}} - 1 - \frac{B_{11} - V_1}{RT}P_1^{\circ} = \phi_2\left[\chi_{12} - \frac{V_1}{M_2v_2}\right] + \phi_3\left[\chi_{13} - \frac{V_1}{M_3v_3}\right] - \frac{V_1}{V_2}\phi_2\phi_3\chi_{23} \tag{34}$$

In order to solve for $\chi_{23}$, it is therefore required that $\chi_{12}$ and $\chi_{13}$ be known. Thus, it is required that three columns be prepared; two from homopolymers and a third from the blend. Typically Equation 34 is simplified by defining:

$$\chi'_{23} = \frac{V_1}{V_2}\chi_{23} \tag{35}$$

and noting that,

$$\frac{V_1}{M_2 v_2} \approx \frac{V_1}{M_3 v_3} \approx 0 \tag{36}$$

when $M_2$ and $M_3$ are large (i.e. polymers). Therefore, Equation 34 can be simplified to:

$$\ln \frac{273.15R(w_2 v_2 + w_3 v_3)}{V_g^{\circ} V_1 P_1^{\circ}} - 1 - \frac{B_{11} - V_1}{RT} P_1^{\circ} = \phi_2 \chi_{12} + \phi_3 \chi_{13} - \phi_2 \phi_3 \chi_{23}' \tag{37}$$

For simplicity, the following is defined:

$$\chi_{1(23)} = \phi_2 \chi_{12} + \phi_3 \chi_{13} - \phi_2 \phi_3 \chi_{23}' \tag{38}$$

where $\chi_{1(23)}$ is the solvent-polymer blend interaction parameter. It is obtained in the same manner as the pure component solvent-polymer interaction parameters (i.e. Equation 32). Therefore, once $\chi_{12}$, $\chi_{13}$ and $\chi_{1(23)}$ are obtained, the polymer-polymer interaction parameter can be obtained simply from Equation 38.

## 2.5 Solvent Dependency Problem

As mentioned, Deshpande et al. (1974) were the first to use IGC for the determination of polymer blend miscibility. They suggested that the method is useful for characterizing a mixture of two low molecular weight polymers. However, they discovered that the calculated polymer-polymer interaction parameters ($\chi_{23}$) are dependent on the chemical nature of the probe used to characterize the stationary phase. This is a severe drawback to the method, which has continued to make the use of IGC for the determination of polymer blend miscibility questionable. Olabisi et al. (1975) confirmed Deshpande's findings that the probe dependency problem is real. They attributed the solvent dependency to the inability of the Flory-Huggins lattice theory to account for all of the polymer-solvent interactions.

Al-Saigh and Munk (1984) suggested that the observed probe dependence is due to uncontrolled experimental artefacts and errors. However, upon further study, they found that they were able to minimize solvent dependency by meticulously controlling experimental variables, but they were not able to totally eliminate solvent dependency.

Al-Saigh and Chen (1991) found that the calculated $\chi_{23}$ might contain other solvent-dependent contributions to the Gibbs free energy change of mixing that are not properly accounted for by the polymer solution thermodynamic theories. Voelkel (1991) suggested that the observed probe dependence is due to an inadequacy of the Flory-Huggins model for the polymer-polymer probe ternary system as a result of preferential interactions involving solubility with one of the components of the blend. This is suggested based on the idea that probes with different chemical structures should behave differently in a mixture of polymers of very different polarity.

Dipaola-Baranyi (1981) proposed that non-random partitioning of probe molecules could affect the forces acting between molecules of the mixed and stationary phases. Su and Patterson (1977) suggested that the non-random partitioning of the probe with the two components of the stationary phase appeared in the difference between $\chi_{12}$ and $\chi_{13}$. They described this as the $\Delta\chi$ effect. To eliminate this effect Su and Patterson suggested that in order to analyze polymer blends, probes that give $\chi_{12} = \chi_{13}$ must be selected.

Shi and Schreiber (1991) agreed that the probe dependence of IGC data is due to non-random partitioning of vapour phase molecules. They also suggested that a critical portion of the problem is attributed to the assumption that the surface composition of a mixed stationary phase is identical to its bulk composition. They observed that the

surface and bulk compositions in a multi-component polymer system generally differs, indicating that the partitioning of vapour phase molecules between the components of a solid's surface is likely to be non-random. Unless the volatile phase molecule partitions randomly between the components of the stationary phase, some perturbation in the energies at the polymer-polymer contacts should be expected. They suggested a procedure for establishing the true surface composition for a two-component polymer system. This was found to reduce probe dependence, but not eliminate it.

Lezcana et al. (1992) attributed the weakness of the Flory-Huggins lattice theory to be due to one of the major assumptions made in the theory the enthalpic part of the Gibbs function for the polymer-polymer system is simply an addition of the binary contributions. They proposed a method to correct for this problem by combining Flory's equation of state theory with the original Flory-Huggins theory. It did not eliminate the probe dependency, but it did help to reduce the effect. Prolongo et al. (1989) also observed the weakness of the approximation that the Gibbs mixing function for the ternary solvent-polymer-polymer system is additive with respect to the binary contributions.

Sanchez (1978) and Prolongo et al. (1989) applied equation of state approaches for the calculation of interaction parameters. A major deficiency of the Flory-Huggins theory that they investigated was the excess volume effect. Using their equation of state approaches, they independently determined that the deficiency of the Flory-Huggins theory does not have a significant effect on the observed probe dependency of the $\chi_{23}$ values.

Etxeberria et al. (1992) suggested that the probe dependence could be explained if the thermodynamic aspects of a ternary system are taken into account. They proposed that $\chi_{12}$ and $\chi_{13}$ should be obtained in their own ternary system instead of being calculated in the homopolymer-probe binary system. Therefore, the measured $\chi'_{23}$ parameter is an apparent parameter, which takes into account the real polymer-polymer interaction parameter and other ternary effects not reflected in $\chi_{12}$ and $\chi_{13}$.

Faroque and Deshpande (1992) implemented four different approaches to calculate interactions for a blend of polystyrene and polybutidiene. They used Flory's equation of state, Sanchez's equation of state, Chee's method, and a method of their own. It was concluded that the different methods were not in agreement with each other.

Numerous attempts have been reported to resolve the problem of probe dependent interaction parameters. To summarize all the methods is beyond the scope of this current review; however, the important finding has been that the methods have had limited success. Recently, Zhao and Choi (2001) suggested a new strategy for analyzing IGC data that appears to eliminate the probe dependency problem. This method is summarized in the following section.

## 2.6 A Modified Flory-Huggins Lattice Theory for IGC Measurements

In particular, the authors identified a weakness of the traditional data analysis as being how the reference volume ($V_o$) is chosen. Traditionally, when the Flory-Huggins lattice theory is applied to a solvent-polymer system, the molar volume of the solvent ($V_1$) is usually taken as $V_o$ to define the size of the lattice (as mentioned previously when discussing the Flory-Huggins theory). This is problematic when comparing interaction

strengths between different solvents with the same polymer since the interaction strengths are calculated using different lattice sizes. Therefore, the apparent differences in the interaction parameters among different solvents with the same polymer will not necessarily be due to the differences in the intermolecular interactions, but will also be due to the different lattice sizes used. This is especially problematic with studying ternary blends since solvent dependency error will appear in the terms for each polymer-solvent term as well as the polymer-polymer-solvent terms. To rectify this problem, the authors suggested that a common reference volume be chosen such that each probe used to characterize the polymer (or polymer blend) will be based upon the same $V_o$.

In accordance with the original Flory-Huggins lattice theory, the reference volume should be chosen as the smallest among the molar volumes of the solvents and polymers comprising the mixture. For a solvent-polymer system, they chose the $V_o$ to be the molar volume of the polymer repeat unit rather than that of whole molecule since it is smaller than the solvent molecule or whole polymer molecule. Using this approach, they believe it eliminated probe dependency.

By using such a reference volume, the Gibbs free energy change on mixing for a solvent polymer system is given as follows:

$$\Delta G_m = RT\left( n_1 \ln \phi_1 + n_2 \ln \phi_2 + n_1 \phi_2 \chi_{12} \frac{V_1}{V_0} \right) \tag{39}$$

This equation is identical to Equation 16 of the original Flory-Huggins theory if the $V_0$ is chosen as the solvent molar volume ($V_1$). In the case of a ternary system:

$$\Delta G_m = RT\left(\begin{array}{l} n_1 \ln\phi_1 + n_2 \ln\phi_2 + n_3 \ln\phi_3 + n_1\phi_2\chi_{12}\dfrac{V_1}{V_0} \\ \qquad + n_1\phi_3\chi_{13}\dfrac{V_1}{V_0} + n_2\phi_3\chi_{23}\dfrac{V_2}{V_0} \end{array}\right) \tag{40}$$

With the use of Equation 39 or 40 (depending on whether it is a binary or ternary system being analyzed), Flory-Huggins interaction parameters can be obtained from IGC analysis. The critical miscibility of a binary mixture is determined by taking the second and third derivatives of Equation 39 with respect to the volume fraction and setting them to zero and equating the results. After some manipulation the following is obtained:

$$(\chi_{12})_{crit} = \frac{1}{2}\left(\sqrt{\frac{V_0}{V_1}} + \sqrt{\frac{V_0}{V_2}}\right)^2 \tag{41}$$

For a solvent-polymer system $V_1$ is small and $V_2 \approx \infty$, therefore, $(\chi_{12})_{crit} = \frac{1}{2}\frac{V_0}{V_1}$. This result is the same as what is obtained for a solvent-polymer system using the original Flory-Huggins theory when $V_1$ is used as $V_0$. For a polymer-polymer blend it is noted from Equation 41 that $(\chi_{12})_{crit} \approx 0$.

With $V_0$ as the reference volume the derivative of $\Delta G_m$ with respect to $n_1$ for a pure liquid phase is:

$$\left(\frac{\partial \Delta G_{mix}}{\partial n_1}\right) = RT\left(\ln\phi_1 + 1 - \frac{V_1}{V_2} - \chi_{12}\frac{V_1}{V_0}\right) \tag{42}$$

For a binary polymer blend:

$$\left(\frac{\partial \Delta G_{mix}}{\partial n_1}\right) = RT\left(\begin{array}{l} \ln\phi_1 + 1 - \dfrac{V_1}{V_2}\phi_2 - \dfrac{V_1}{V_3}\phi_3 + \phi_2\chi_{12}\dfrac{V_1}{V_0} + \\ \qquad \phi_3\chi_{13}\dfrac{V_1}{V_0} - \phi_2\phi_3\chi_{23}\dfrac{V_1}{V_0} \end{array}\right) \tag{43}$$

Combining Equations 25, 28-30, and 42 for a single polymer system the following is obtained for the solvent-polymer interaction parameter:

$$\chi_{12} = \frac{V_0}{V_1}\left( \ln \frac{273.15 R \nu_2}{V_g^0 V_1 P_1^0} - 1 + \frac{V_1}{M_2 \nu_2} - \frac{(B_{11} - V_1)}{RT} P_1^0 \right) \tag{44}$$

By performing a similar manipulation of Equations 26, 28-30, and 43 for a ternary system to following expression is obtained:

$$\phi_2 \chi_{12} + \phi_3 \chi_{13} - \phi_2 \phi_3 \chi_{23} = \frac{V_0}{V_1}\left( \ln \frac{273.15 R (w_2 \nu_2 + w_3 \nu_3)}{V_g^0 V_1 P_1^0} - 1 + \frac{V_1}{M_2 \nu_2} + \frac{V_1}{M_3 \nu_3} - \frac{(B_{11} - V_1)}{RT} P_1^0 \right) \tag{45}$$

For simplicity, the following is defined:

$$\chi_{1(23)} = \phi_2 \chi_{12} + \phi_3 \chi_{13} - \phi_2 \phi_3 \chi_{23} \tag{46}$$

where $\chi_{1(23)}$ is the solvent-polymer blend interaction parameter, similar to Equation 38 from the original Flory-Huggins lattice theory approach. From Equation 46 it is observed that a plot of $\chi_{1(23)}$ versus $(\phi_2 \chi_{12} + \phi_3 \chi_{13})$ should produce a straight line with a slope of 1 and an intercept of $-\phi_2 \phi_3 \chi_{23}$. Therefore, obtaining probe-independent $\chi_{23}$ values, with known polymer concentrations $\phi_2$ and $\phi_3$, it can be accomplished by determining $\chi_{12}$, $\chi_{13}$, and $\chi_{1(23)}$ from equations 44 and 45. The other parameters in the equations were calculated in the same manner as outlined in the original Flory-Huggins lattice theory section.

It should be noted that the above approach did not correct for the assumption that there is no volume change on mixing, which is made in the original Flory-Huggins theory. The justification for this is due to the polymers of interest in their study being polyethylenes (as is the focus of this thesis). It is widely known that the volume change

on mixing comes from the differences in free volumes or degrees of thermal expansion of the components in a mixture. The justification for not accounting for this problem for polyethylenes is that it was reported by Rudin et al. (1970) that the specific volume of different types of polyethylenes are equivalent in the melt state. This indicates that the different types of polyethylenes have the same thermal expansion coefficient in the melt state, regardless of the branch characteristic or content of the type of polyethylene. For a polyethylene in the melt state, for temperatures from 150 to 260°C, the expansion coefficient is $9.0*10^{-4}\frac{cm^3}{g\,°C}$. Consequently, it is believed that the volume change on mixing for polyethylene should be negligible. This assumption is further supported by observations of other researchers, such as Patterson and Robard (1978), who observed that the volume change on mixing for polymer blends is relatively small compared to polymer-solvent systems. Consequently, the volume change on mixing should not be the cause of obtaining probe dependent interaction parameters when using the original Flory-Huggins theory.

## 2.7 Experimental Methods

### 2.7.1 Materials

NOVA chemicals (Calgary, Canada) supplied all of the polyethylene samples used in this work. Two HDPE samples (with different molecular weight averages) were used. Five different LLDPE samples were used each having different branch contents. All of the LLDPE samples were produced using metallocene catalysts. The specific details regarding each prepared sample studied are summarized in Table 2.1.

**Table 2.1. Polyethylene Samples Studied**

| Sample | $M_n$ | $M_w$ | Branch Content Per 1000 Carbon Atoms |
|---|---|---|---|
| HDPE-1 | 13,700 | 49,400 | ------ |
| HDPE-2 | 28,000 | 137,000 | ------ |
| LLDPE-1 | 34,600 | 69,200 | 3.1 |
| LLDPE-2 | 38,700 | 77,400 | 11.4 |
| LLDPE-3 | 20,300 | 69,000 | 18.1 |
| LLDPE-4 | 53,800 | 96,900 | 49.7 |
| LLDPE-5 | 52,000 | 104,000 | 87.2 |

The solvents used to characterize the polymer samples were reagent grade solvents purchased from Fisher Scientific and were used without further purification. They were 1-hexene, 1-octene, benzene, cyclohexane, n-hexane, n-dodecane, n-heptane, n-nonane, n-pentadecane, n-pentane, n-octane, toluene, and xylene. Methane was used as the marker in order to determine the net retention time of the other solvents. It was assumed that methane's interaction with the polymer being studied was negligible. Therefore, it was used to determine the time that it takes for an non-interacting molecule to elude the system.

The 13 non-polar solvents were chosen based on previous work on similar blend systems by Zhao (2002) and Silveria (2001). As was illustrated in the discussion regarding the Flory-Huggins theory (Equation 21), for a solvent-polymer mixture the solvent should be miscible with the polymer if $\chi_{12,crit} < 0.5$. Silveria justified using these solvents because the solvents demonstrated good miscibility with the samples since in the majority of cases $\chi_{12} < 0.5$. Silveria also verified that polar solvents are not useful for

characterizing the blends by using two very polar solvents (methanol and ethanol). These solvents resulted in much higher $\chi_{12}$ values than what was obtained for non-polar probes.

### 2.7.2 Column Preparation

Each pure polymer and polymer blend was first dissolved in xylene at 120°C in a rotary evaporator. It was important to have the temperature high enough to dissolve the polymer sample, but not too high that it would degrade the sample. For every 1 g of polymer to be dissolved, 150 mL of xylene was used. Once the sample was completely dissolved by the xylene, an inert solid support (Chromosorb WAW 60/80 mesh) was added to the polymer solution. It was added at a polymer to support ratio of approximately 10%. This was done to ensure that the final amount of polymer coated on the solid support would be within the optimal loading range of 6 to 10% resulting in a coating thickness of roughly 20-50 nm. This optimal loading range was recommended from previous studies where it was determined that if the loading was too low (<5%) the solid support will not be totally covered by the polymer, which will affect the retention time of the probe. If the polymer loading is too high (>12%) the layer of the polymer covered on the support will be too thick. Consequently, the probe will not penetrate into the whole layer and reach thermodynamic equilibrium with all polymers. As mentioned previously, thermodynamic equilibrium is a key requirement for the justification of using equations described in this chapter. After the solid support was added to the polymer solution, it was mixed at approximately 120°C in the rotary evaporator for 3 hours to coat the polymer onto the support. The xylene was then slowly evaporated using a vacuum at the same temperature while the mixture was still constantly stirring. Once all the xylene

evaporated from the flask, the sample was removed from the rotary evaporator. This took roughly 1 to 2 hours to complete. The coated support was then dried overnight in a vacuum oven at –20 kPa and 80°C to remove most of the residual solvent. The temperature was kept lower than the polymer melting temperature to ensure that the coating of the polymer (or polymer blend) on the chromosorb was not compromised. The resultant coated support was then packed into an acetone washed stainless steel tubing by first ended (i.e., plugging) one end of the column with glass wool. The coated supported was added slowly to the column, using a funnel, while continually tapping the column to move the solid down the column. This process was performed slowly in order to prevent the solid from clogging and thus causing an even packing throughout the column. Once the column was full the other end of the column was ended with glass wool. It was essential to record the amount of coated support added to the column precisely since it is a key component in the thermodynamic analysis of the sample. Three lengths of stainless steel tubing were used for the columns; 1 m, 3 m and 6 m. All of the tubing used was 0.18 cm in diameter. The columns were then "conditioned" with pre-purified Helium for 2 days at 60°C in a gas chromatograph in order to further eliminate any residual solvent before data collection.

### 2.7.3 Mass Determination of Sample

The percent loading of the polymer on the solid support was determined by calcinations of 2 to 3 g of the coated support in a furnace operated at 850°C for 12 hours. All samples were calcinated in triplicate and an average loading for the sample was determined from the results. Blank (uncoated chromosorb) corrections were made since it

has been widely observed in the IGC literature that when uncoated chromosorb is calcinated a mass loss occurs. Therefore, blank samples were calcinated in triplicate and the mass loss of the blank sample was used to correct the observed mass loss of the coated sample.

### 2.7.4 Equipment

IGC measurements were conducted using a Hewlett-Packard 4890 gas chromatograph equipped with a flame ionization detector (FID). Pre-purified Helium was used as the carrier gas at flow rates ranging from 20 to 26 mL/min. The flow rate of the carrier gas was measured using a soap bubble flowmeter. The solvents used as probes were injected manually using 10μL Hamilton syringes with removable needles (bevel tip #2). Small volumes of solvent (~1μL) were injected in order to ensure that the infinite dilution conditions of the solvent were satisfied. Injections were done in triplicate with a reproducibility within 3%. The times for the solvents to elude the system were recorded using a PC computer with a HP 3365 Series II ChemStation interface. Approximately 1μL of methane was injected in triplicate and the average was used in order to determine the marker elution time. The experiments were conducted at oven temperatures of 170, 190, 210, and 230°C for each column. The inlet pressure was measured using the pressure gauge on the gas chromatograph and the outlet pressure was measured using a Fisherbrand digital barometer.

## 2.8 References


Al-Saigh, Z.Y. (1997) Review: Inverse Gas Chromatography for the Characterization of Polymer Blends, *Int. J. Polym. Anal. Charact.*, 3, 269-291.

Al-Saigh, Z.Y. (1997) Errata: Review: Inverse Gas Chromatography for the Characterization of Polymer Blends, *Int. J. Polym. Anal. Charact.*, 4, 263-264.

Al-Saigh, Z.Y. (1997) The Characterization of Polymer Blends by Inverse Gas Chromatography, *TRIP*, 5,3, 97-102.

Al-Saigh, Z.Y. and Munk P. (1984) Study of Polymer-Polymer Interaction Coefficients in Polymer Blends Using Inverse Gas Chromatography, *Macromolecules*, 17, 803-809.

Al-Saigh, Z.Y. and Chen, P. (1991) Characterization of Semicrystalline Polymers by Inverse Gas Chromatography. 2. A Blend of Poly(vinylidene fluoride) and Poly(ethyl methacrylate), *Macromolecules*, 24, 3788-3795.

Braun, J.M. and Guillet, J.E., (1976) Advances in Polymer Science; Spring-Verlag, Berlin.

Card, T.W., Al-Saigh, Z.Y. and Munk, P. (1985) Inverse Gas Chromatography. 2. The Role of Inert Support, *Macromolecules*, 18, 1034-1039.

Chee, K.K. (1990) Estimation of Polymer-Polymer Interaction Density Parameter by Inverse Gas Chromatography, *Polymer*, 31, 1711-1714.

Chen, C. and Al-Saigh, Z.Y. (1989) Characterization of Semicrystalline Polymers by Inverse Gas Chromatography. 1. Poly(vinylidene fluoride), *Macromolecules*, 22, 2974-2981.

Choi, P., Kavassalis, T. and Rudin, A. (1996) Measurement of Three-Dimensional Solubility Parameters of Nonyl Phenol Ethoxylates Using Inverse Gas Chromatography, *Journal of Colloid and Interface Science*, 180, 1-8.

Deshpande, D.D., Patterson, D., Schreiber, H.P. and Su, C.S. (1974) Thermodynamic Interactions in Polymer Systems by Gas-Liquid Chromatography. IV. Interactions Between Components in a Mixed Stationary Phase, *Macromolecules*, 7,4,530-535.

DiPaola-Baranyi, G. and Degre, P. (1981) Thermodynamic Characterization of Polystyrene-Poly(normal-butyl Methacrylate) Blends, *Macromolecules*, 14, 5, 1456-1460.

Du, Q. and Chen, W. (1999) Inverse Gas Chromatography. 8. Apparent Probe Dependence of $\chi_{23}$ for a Poly(vinyl chloride)-Poly(tetramethylene glycol)Blend, *Macromolecules*, 32, 1514-1518.

Etxeberria, A., Alfageme, J., Uriarte C., Iruin, J.J. (1992) Inverse Gas Chromatography in the Characterization of Polymeric Materials, *Journal of Chromatography*, 607, 227-237.

Etxeberria, A., Uriarte, C., Fernadez-Berridi, M.J. and Iruin, J.J. (1994) Probing Polymer-Polymer Interaction Parameters in Miscible Blends by Inverse Gas Chromatography: Solvent Effect, *Macromolecules*, 27, 1245-1248.

Etxeberria, A., Iriarte, M, Uriarte, C. and Iruin, J.J. (1995) Lattice Fluid Theory and Inverse Gas-Chromatography in the Analysis of Polymer-Polymer Interactions, *Macromolecules*, 28, 21, 7188-7195.

Farooque, A.M. and Deshpande, D.D. (1992) Studies of Polystyrene-Polybutadiene Blend System by Inverse Gas Chromatography, *Polymer*, 33,23, 5005-5018.

Flory, P.J. (1941) Thermodynamics of High Polymer Solutions, *J., Chem. Phys.*, 9, 660.

Flory, P.J. (1953) Principles of Polymer Chemistry, Cornell University Press, New York, NY.

Fried, J.R. (1995) Polymer Science and Technology, Prentice Hall, Englewood Cliffs, NJ.

Huggins, M.L. (1941) Solutions of Long Chain Compounds, *J. Chem. Phys.*, 9, 440.

Lipson, J.E.G. and Guillet, J.E. (1981) Studies of Polar and Nonpolar Probes in the Determination of Infinite-Dilution Solubility Parameters, *Journal of Polymer Science: Polymer Physics Edition*, 19, 1199-1209.

Olabisi, O. (1975) Polymer Compatibility by Gas-Liquid Chromatography, *Macromolecules*, 8, 3, 316-322.

Patterson, D., Tewari, Y.B., Schreiber, H.P. and Guillet, J.E. (1971) Application of Gas-Liquid Chromatography to the Thermodynamics of Polymer Solutions, *Macromolecules*, 4, 3, 356-359.

Prolongo, M.G., Masegosa, R.M. and Horta, A. (1989) Polymer Polymer Interaction Parameters in the Presence of a Solvent, *Macromolecules*, 22, 4346-4351.

Reid, R.C., Prausnitz, J.M. and Poling, B.E. (1987) The Properties of Gases and Liquids, 4$^{th}$ Edition, McGraw-Hill Book Company, New York, NY.

Rudin, A. (1998) The Elements of Polymer Science and Engineering, 2$^{nd}$ Edition, Academic Press, New York, NY.

Rudin, A., Chee, K.K. and Shaw, J.H. (1970) Specific Volume and Viscosity of Polyolefin Melts, *Journal of Polymer Science Part C*, 30, 415-427.

Schreiber, H.P., Tewari, Y.B. and Patterson, D. (1973) Thermodynamic Interactions in Polymer Systems by Gas-Liquid Chromatography. III. Polyethylene-Hydrocarbons, *Journal of Polymer Science: Polymer Physics Edition*, 11, 15-24.

Shi, Z.H. and Schreiber, H.P. (1991) On the Application of Inverse Gas Chromatography to Interactions in Mixed Stationary Phases, *Macromolecules*, 24, 3522-3527.

Silveira, M.D.L.V. (2001) Solubility Properties of LDPE and LLDPE Liquids and their Melt Miscibility by Inverse Gas Chromatography, *University of Alberta M.Sc. Thesis*.

Smidsrod, O. and Guillet, J.E. (1969) Study of Polymer-Solute Interactions by Gas Chromatography, *Macromolecules*, 2, 3, 272-277.

Tsonopoulos, C. (1974) An Empirical Correlation of Second Virial Coefficients, *AICHE Journal*, 20, 2, 263-272.

Tyagi, O.S., Sajjad, S.M. and Husain, S. (1987) Polymer-Polymer Interaction Parameter Determined by Inverse Gas Chromatography, *Polymer*, 28, 2329-2334.

Voelkel, A. (1991) Inverse Gas Chromatography: Characterization of Polymers, Fibers, Modified Silicas, and Surfactants, *Critical Reviews in Analytical Chemistry*, 22, 5, 411-439.

Young, C.L. (1968) The Use of Gas Liquid Chromatography for the Determination of Thermodynamic Properties, *Chromatog. Rev.*, 10, 129-158.

Zhao, L. and Choi, P. (2001) Determination of Solvent-Independent Polymer-Polymer Interaction Parameter by an Improved Inverse Gas Chromatographic Approach, *Polymer*, 42, 1075-1081.

# Chapter 3

# Miscibility of HDPE/LLDPE Blends Review

## 3.1 Introduction

In order to optimize the design of HDPE/LLDPE blends, a great deal of attention has been focused on improving our understanding of the phase behaviour (miscibility) of the blends in order to achieve desirable physical and mechanical properties. Several researchers have implemented numerous techniques in order to achieve an understanding of the phase behaviour of HDPE/LLPDE blends.

Traditionally, the phase behaviour of these blends was studied in the solid state since the blends are used in the solid state. However, it is believed that melt miscibility can significantly influence the solid-state morphology and mechanical properties of the polymer blend, especially under rapid cooling conditions, therefore, it is important to be able to accurately measure the melt state miscibility of these blends.

Several different techniques have been implemented in order to analyze the melt state miscibility. Typically, the study of the melt state is restricted to indirect methods of analysis since the components in a melt of HDPE/LLDPE are very similar and are difficult to distinguish from each other using traditional methods such as Light Scattering (LS). Consequently, the melt state miscibility of the blends is usually inferred from solid samples that are rapidly quenched from the melt state. It is believed that this rapid quenching process is fast enough to effectively "freeze" the morphology of the melt in the solid sample. Molecular simulations have also been used to predict the melt state miscibility.

More recently, direct analysis techniques have been developed to analyze the sample directly in the melt. This has typically been limited to the use of small angle neutron scattering (SANS), which is an expensive analysis method and also has some inherent flaws, which is the subject of debate. An alternative method of analysis is inverse gas chromatography (IGC), which has traditionally been flawed due to the probe dependence of the results (see Chapter 2). However, with the recent developments of Zhao and Choi (2001), this method may provide a cheaper alternative to SANS for the direct analysis of melt miscibility. A summary of previous studies of HDPE/LLDPE miscibility is presented in the following sections.

## 3.2 Literature Review

### 3.2.1 Solid State Miscibility

Datta and Birley (1982) implemented differential scanning calorimetry (DSC), X-ray diffraction (XD), and mechanical property testing to study blends of HDPE/LLDPE in the solid state. For both rapidly and slowly cooled samples, a single endothermic peak was observed suggesting that the samples are miscible in the crystalline state. This observation is further supported by XD analysis in which it is found that the unit cell dimensions for HDPE/LLDPE blends are identical to those of pure HDPE samples.

Hu et al. (1987) used a variety of indirect methods in order to study the miscibility of HDPE/butene-based LLDPE blends in the solid state. For their study, they used DSC, wide angle X-ray diffraction (WAXD), small angle X-ray scattering (SAXS), Raman longitudinal-acoustic-mode spectroscopy (LAM), dynamic mechanical analysis (DMA) and light scattering (LS). Using DSC, only one endothermic peak, which is dependent on

the composition of the blend, was observed whether the blends were rapidly quenched or slowly cooled from the melt state. This implied that co-crystallization occurs between the components. Therefore, the blends are miscible in the crystalline state. No separate peaks are observed in the WAXD, SAXS, LAM, and LS studies. This observation, along with the fact that no peak broadening is observed in the DSC measurements suggests that these peaks are associated with the presence of a single component. No double peaks or broadened peaks were observed, which would be associated with two closely spaced unresolved peaks. This result suggests that phase segregation does not take place at the structural levels of crystalline, lamellar, and spherulitic textures. A single step drop in the scattered intensity as a function of temperature was seen in the LS studies suggesting that cocrystallization between the HDPE and LLDPE components occurs. The $\alpha$, $\beta$, and $\gamma$ relaxations of a 50/50 blend, observed using DMA, displayed intermediate relaxation behaviour, which is consistent with the characteristics of a typical miscible blend. The LLDPE used had $M_w$ = 114,000, PDI = 4.5 and a branch content of 18 butene branches per 1000 backbone carbons. The HDPE had a $M_w$ = 160,000 and PDI = 7.1.

Tashiro et al. (1992, 1994) studied the crystallization behaviour of 50/50 weight % HDPE/LLDPE blends using DSC and Fourier transform infrared spectroscopy (FTIR). Since HDPE and LLDPE have almost the same chemical structure of carbon and hydrogen atoms, deuterated HDPE (DHDPE) was used. It is observed that the branch content of the LLDPE has an effect on the miscibility of the blend. When the branch content is 17 ethyl branches per 1000 backbone carbons, DHPE/LLDPE co-crystallizes over the whole composition region, even for slow cooling conditions. However, when the

branch content of LLDPE is increased to 41 ethyl branches per 1000 backbone carbons the system phase separates upon cooling from the melt.

Lee and Cho (1997) used DSC and DMA to study the miscibility of HDPE/LLDPE blends in the solid state by performing extensive studies of thermal and relaxational behaviour for both the crystalline and amorphous phases. The DSC results confirm that HDPE/LLDPE blends are miscible in the crystalline phase and DMA shows that the blends are miscible in the amorphous phase. The LLDPE used in this study was a low branch content LLDPE with 16 branches per 1000 backbone carbons.

Lee et al. (1997) studied blends of HDPE and octene-based LLDPE in the crystalline and amorphous phases. DSC and DMTA were used to perform extensive thermal and relaxational behaviour studies of the blends in the crystalline and amorphous phases to elucidate miscibility of the blends. A composition-dependent peak during melting and crystallization, and the heat of fusion vary linearly with composition supporting the incorporation of HDPE into LLDPE crystals, thus indicating the samples are miscible in the crystalline state. The dynamic mechanical $\alpha$, $\beta$, and $\gamma$ relaxations of the blends displayed an intermediate behaviour, which indicates miscibility in the crystalline and amorphous phases.

Wignall et al. (2000) used DSC, transmission electron microscopy (TEM), SANS and SAXS to investigate the solid state morphology of blends of HDPE and model short chain LLDPE. From their previously published work, they have determined that the blends are miscible in the melt when the ethyl branch content of the LLDPE is low (i.e. <40 branches per 1000 backbone carbons for $M_w \sim 10^5$). However, due to structural and melting point differences between HDPE and LLDPE, the blends may phase separate in

the solid state. It is believed that the degree of separation is controlled by crystallization kinetics. DSC, TEM, SAXS, and SANS were used to investigate the solid state morphology as a function of composition, the thermal history, and rate of cooling. The complementary information given by the different analysis methods was used to establish the morphology of HDPE/LLDPE blends that arise on cooling of a homogeneous melt. Using DSC and solvent extraction procedures, the co-crystallization behaviour was studied. A high degree of cocrystallization is observed in the rapidly crystallized mixtures, whereas segregated crystals form when the blends are isothermally crystallized. Wignall et al. concluded that the blends are homogeneous in the melt, but may phase separate in the solid state to different degrees depending on the rate of cooling and the initial composition of the blend.

### 3.2.2 Indirect Measurements of Melt State Miscibility

Hill and Barham (1992) studied HDPE/octene-based LLDPE blends using DSC and TEM. For systems with low branch content LLDPE (10 to 40 branches per 1000 backbone carbons) a closed loop phase diagram of liquid-liquid phase separation (LLPS) at lower HDPE concentrations was observed, which is similar to what they have observed for HDPE/LDPE systems they previously studied. Similar results were observed for butene-based LLDPE/HDPE blends and hexene-based LLDPE/HDPE blends when the LLDPEs had comparable branch contents. From this observation, Hill and Barham concluded that the branch length is not the decisive factor for phase separation; rather, the branch content is. Additionally, TEM is found to be capable of detecting phase separation

in blends containing as low as 5 branches per 1000 backbone carbons, which is lower than what is possible by DSC.

Hill and Barham (1993) blended HDPE with a series of octene-based LLDPEs, with differing octene content, and studied the melt miscibility using DSC and TEM by observing surface replicas of quenched and some isothermally crystallized samples. Melts of the blends with the lowest branch contents (2, 3, 5, and 8 mol%) displayed liquid-liquid phase separation (LLPS) at some temperatures and for some compositions. The phase-separated regions are closed loops and asymmetrically placed at low HDPE contents, which is in agreement with their previous experiments. Their results indicate that when the molecular weight of the polymers are roughly equal, the size of the LLPS region becomes smaller as the number of octene branches increases from 2 to 8 mol% octene. However, blends of HDPE with 12 mol% octene LLDPE were observed to have extensive separation and rather different morphologies. The HDPE used had $M_w = 5*10^4$ and $M_n = 1.79*10^4$, while the LLDPE had octene mol% from 2.1 – 11.8% with $M_w$ ranging from 3.7 to $13*10^4$ and $M_n$ ranging from 1.85 to $6.5*10^4$.

Hill and coworkers have done extensive research on HDPE/LLDPE blend systems by studying over 65 different systems (Hill and Puig, 1997). They have used HDPE with $M_w$ ranging from $2*10^3$ to $2*10^6$ blended with both Ziegler-Natta and metallocene catalyst produced LLDPEs. The LLDPE were either butene, octene, or hexene based. The HDPE had PDI as low as 1.1, while the LLDPE had PDI as low as 2. For a high HDPE content, the blends are miscible in the melt (only one crystal type is present upon quenching from the melt), but at low HDPE content there is always a closed loop of LLPS. The phase separation is on a large spatial scale, with aggregates of minority

crystals typically being some microns in diameter and separated on a similar scale. Hill and Puig believe that the diffusion rates are not large enough to cause this large scale separation upon quenching from the melt. When the branch content is 8 mol% or less, the extent of phase separation observed for the binary blends is the same as when the molecular weight of the two components and the branch densities of the copolymers is similar. This was observed whether the LLDPEs were butene, hexene, or octene based, implying it is the number of branches, rather than the branch type that determines the phase behaviour. They also found that when two random copolymers of different branch content (both 8 mol% or less) are blended together the phase behaviour is similar to that observed for the HDPE/LLDPE blends.

Morgan et al. (1997) have extensively studied HDPE/LLDPE blends in the melt state using indirect techniques that they largely developed. It is difficult to detect phase separation directly in the melt due to the similarity of the components. For example, the usual light scattering methods are not sufficiently sensitive due to the similarity of the refractive indices of the components. Their indirect methods involve the examination of rapidly quenched melts by DSC and TEM. They believe that the phase structure of the resultant crystalline polymer after rapid quenching closely resembles the melt. The justification for this assumption is that it should take the polymer several minutes to separate on the scale that is observed, whereas the time of the quench is less than a second (Hill and Barham, 1992). Others have argued that the observed phase separation occurs upon crystallization (e.g. Alamo et al., 1997). The three main reasons that Morgan et al. (1997) disagree that the observed phase separation occurs upon quenching from the melt are:

1. The diffusion rates are too slow to allow phase separation, on the scale observed, to take place during the quench.
2. They observed that single uniform morphologies can be obtained by quenching some blends from higher temperatures, whereas biphasic morphologies are obtained from lower temperatures. If all melts were mixed, and separation took place only on crystallization, this observation would be hard to explain.
3. Experiments showed that the average size of the dispersed phase increase with time in the melt, while the overall amount of the dispersed phase remains constant. If the blends were not separated in the melt, no such ripening process would be observed.

The majority of the published attempts to search for melt phase separation directly in the melt have typically been with using SANS, where one component is deuterated. Morgan et al. believe that unless the experiments are carried out at very low angles, the large scale phase separation that they believe to be present cannot be detected by SANS. Using their indirect methods for the HDPE/LLDPE blends, in every case where the $M_w$ of HDPE is more than ~ $10^4$, melt phase separation of a closed-loop of liquid-liquid phase separation (LLPS) at low HDPE content is observed. They found that the extent of the phase separated loop depends only weakly on the molecular weight of the HDPE. However (for octene-based LLDPE blend sample) the extent of phase separation depends strongly on the degree of branching of the LLDPE. The LLPS region is wider when the copolymer contained less branches. Although this observation is counter intuitive, Morgan et al. explained this observation by adding an extra asymmetric free energy term to the usual

Flory-Huggins model. They also determined that the type of branches on the LLDPE is of secondary importance in determining the phase behaviour. Therefore, it was concluded that for HDPE/LLDPE blends, it is the number of branches that is the most important factor influencing the extent of phase behaviour.

In order to confirm that it is the branch content that effects phase separation most strongly, rather than the branch type, Hill and Barham (2000) studied binary blends of LLDPEs produced by metallocene catalysts. The three LLDPEs used were two butene-based LLDPEs of different butene contents, and a hexene-based LLPDE with the same branch content as the more lightly branched LLDPE. The components of one system studied differ in both branch type and branch content, one in branch content but not type, and the third in branch type only. These samples were analyzed for the melt using DSC and TEM. When the two components have the same branch content, only one crystal type is seen on quenching melts of all compositions from all temperatures. When the branch content is varied, two crystal types are seen for blends of some compositions when quenched from some temperatures. The morphology maps of the phase separated systems closely resembled those found when HDPE is blended with LLDPE. These findings confirmed the view that it is the branch content that effects the morphology of the melt most strongly and that the branch type is of secondary importance.

Excimer fluorescence was used by Zhao et al. (1998) to study the miscibility of HDPE/LLDPE blends in the amorphous phase. In order to use excimer fluorescence, it is required that one of the components be labelled by chromophore. Chromophore labelled LLDPE/HDPE blend samples annealed at 140°C and rapidly quenched to room temperature were both found to be miscible in the solid state indicating that the blends

are miscible in the solid and melt state. However, the influence of the chromophore label on the phase behaviour of the blend was not discussed nor was the branch content of LLDPE reported.

Lee and Denn (2000) used rheological measurements in the melt and solid state together with a thermal analysis technique to study the phase separation behaviour of HDPE/LLDPE blends. The blends exhibit one single melting point at all compositions with no indication of superposition of two peaks. Therefore, they concluded that HDPE/LLDPE blends co-crystallize and form a single phase in the melt. For the binary blends tested, the phase behaviour appears to be insensitive to the PDI, molecular weight and branch content of the blend components. The $M_w$ and PDI of HDPE were 40,000 and 3.1, and of LLDPE 68,300 and 3.2 respectively. The LLDPE was a low branch content LLDPE with 10 branches per 1,000 for backbone carbons.

Tanem and Stori (2001) studied rapidly quenched blends of HDPE/LLDPE using DSC, TEM and Atomic force microscopy (AFM). Two different HDPEs were used. One was $M_w$ of 26,000 g/mol and the other was 435,000 g/mol. Four different hexene based LLDPEs of different branch contents were used. The extent of phase separation is wider (both in temperature and composition) than what was observed in previous studies. There is no clear indication of the existence of a closed loop of phase separation of the blend systems (as has been reported by Hill and coworkers). However, the phase separation was found to be limited in composition and partly by temperature. The type of short chain branches on the LLDPE for a fixed molecular weight and amount of LLDPE in the blend is of little (if any) importance on the miscibility of the system. The extent of phase separation is reduced if the amount of branches in the LLDPE is reduced for a fixed

molecular weight and type of comonomer. When the difference in molecular weight between the blend samples is increased, the extent of phase separation is found to increase for a fixed type and amount of comonomer. This observation is independent of which one of the blend components' molecular weight is increased. In order to illustrate that changing the molecular weight among the blend components is not enough in itself to initiate phase separation in the melt, Tanem and Stori blended two HDPEs of considerably different molecular weights and no phase separation was observed. The same observation is also true for a blend of two LLDPEs of different molecular weights (but with equal amounts of comonomer). For HDPE/LLDPE blends, Tanem and Stori observed that the extent of phase separation increased when the amount of comonomer in the branched blend component is increased. This is observed for ethyl and butyl type short chain branches and is valid as long as the amount of the comonomer is less than approximately 5 mol%. For higher amounts of comonomer incorporation, the extent of phase separation is approximately fixed. Tanem and Stori suggested that these observations might be partly predicted from theory if an extra repulsive potential is added to the original Flory-Huggins equation. They found that the amount of phase separation in the melt (i.e. how widespread in temperature and composition the phase separation is found to be) is dependent on the molecular weight of the blend components and the amount of branches in the LLDPE. Their results indicate that the extent of phase separation in the melt was both wider in temperature and composition than reported previously by others. Tanem and Stori (2001) also found that the extent of phase separation is essentially independent of the type of short chain branches of the LLDPE, rather the difference in molecular weight of blend components seems to affect the extent

of phase separation. In blends containing butyl branches, the extent of phase separation is reduced if the amount of comonomer is reduced.

The degree of miscibility of HDPE/LLDPE blends containing only lightly branched LLDPE has generated some controversy. Morgan et al. (2001) addressed this issue using micro-Raman imaging. The use of micro-Raman imaging is done to gain compositional information on the polyethylene blends. In order to distinguish the spectra of the two blend components, the blends of a deuterated HDPE and hydrogeneous LLDPE were investigated. Both isothermally crystallized and rapidly quenched blends were studied and the results were compared to those previously obtained by TEM. The isothermally crystallized blends were prepared at very low undercooling to generate large compositional differences on a large spatial scale. Both the compositional phase structures detected by the isothermally quenched blends agree closely with the morphological phase structures detected using TEM. Compositional differences are not, however, detected by Raman imaging in rapidly quenched blends. The Raman data clearly shows that in rapidly quenched samples where a biphasic morphology is seen by TEM, there are two distinct regions separated on a similar scale to the morphologically distinct regions seen in the electron microscope. The Raman data also clearly demonstrates that the distinguishing feature of these regions is not their relative branch content, but rather the degree of crystallinity of the two components. Accordingly, they concluded that the morphological differences that they previously assigned to differences in branch content should, correctly, be attributed to differences in the crystallinity of both the branched and linear molecules. It is clear from all previous evidence that the branch content of LLDPE, the actual blend composition, the temperature at which the melt is

held, and the time for which the blend sample is help in the melt, all affect the morphologies observed upon quenching. It is unknown if this phase separation occurs on the basis of molecular weight, nucleation, or some other reason. However, the Raman imaging results indicate that phase separation does not occur on the basis of branch content as they previously concluded.

### 3.2.3 Simulations of Melt State Miscibility

Choi (2000) studied the miscibility of HDPE/butene-based LLDPE (of different branch contents) blends using molecular dynamics (MD) simulations. Hildebrand solubility parameters ($\delta$) at elevated temperatures were computed and then used to calculate $\chi$ values in order to determine the blend system's miscibility. The results indicate that when the branch content of the LLDPE is roughly 40 branches per 1,000 backbone carbons (or greater), the blends will phase separate in the liquid state regardless of temperature. This finding is consistent with the SANS findings of Alamo et al. (1997).

### 3.2.4 Direct Measurements of Melt State Miscibility

The miscibility of the molten and crystalline state of HDPE/LLDPE blends was measured using SANS by Tashiro et al. (1995). In order to implement SANS for analysis, the HDPE sample was deuterated (D), while the LLDPE was left as hydrogeneous (H) or normal LLDPE. For the blends, different LLDPEs of varying branch content were used. LLDPE(2) had 17 ethyl groups per 1,000 backbone carbons and LLDPE(3) had 41 ethyl branches per 1,000 backbone carbons. Utilization of the deuterated sample was originally aimed at observing the crystallization behaviour of the individual components of the

blends separately. The crystallization behaviour of the blends between the DHDPE and LLDPE is dependent on the branch content of LLDPE. In previous papers, Tashiro et al. investigated the crystallization behaviour of DHDPE/LLDPE blends using XD, FTIR, DSC, and so on. Using those methods, the DHDPE/LLDPE(2) blends cocrystallized (i.e. they pack together in a common lamella) even when the sample is slowly cooled from the melt state. While, for DHDPE/LLDPE(3) blends the components crystallized in separate lamella (i.e. phase separated). SANS was implemented in order to determine whether or not this observed phase separation occurs in the melt or upon crystallization from the melt. It was observed that both blends are miscible in the melt state. This result suggests that the difference in the crystallization behaviour between DHDPE/LLDPE(2) and DHDPE/LLDPE(3) is not determined by chain aggregation state in the melt, but is governed more significantly by the kinetic effect during the crystallization process from the melt.

Melt state miscibility of HDPE/LLDPE blends were studied by Alamo et al. (1997) using SANS. They studied the level of branching (of the LLDPE) that is required for the system to phase separate. Their results confirm that when the branch content is low (i.e. <40 branches per 1000 backbone carbons for $M_w \sim 10^5$) the blends are homogeneous, but when the branch content is high (typically ≥ 80 branches per 1000 backbone carbons for $M_w \sim 10^5$) phase separation of the melt occurs. In order to use SANS, the HDPE sample is deuterated (D), while the LLDPE is left in the hydrogeneous (H) or normal state. SANS can supply information on the melt homogeneity of polymer blends via the contrast achieved by deuterating one of the components, as there are large differences in both the shape and absolute magnitude of the scattering between phase

separated and homogeneous systems. Phase separation on a scale up to 100 nm is detected by SANS and an interaction parameter was calculated for the blend. However, phase separation is also observed for blends for DHDPE with HDPE and an interaction parameter of a similar magnitude is obtained ($\chi \sim 4*10^{-4}$). The observed phase separation of the DHDPE/HDPE blends is therefore considered to be an isotope effect. Consequently, after allowance for the effect of deuteration on phase behaviour, Alamo et al. concluded that the HDPE and lightly branched LLDPE are fully miscible in the melt. It was also shown that for heterogeneous LLDPE blends with a wide range of branch contents, a fraction of the highly branched chains (e.g. > 80 branches per 1,000 backbone carbons) phase separate from the lightly branched majority even when the average branch content is low (e.g. 10 to 20 branches per 1,000 backbone carbons). Therefore, when the branch content of a binary mixture is low, the blend should be miscible, but it should be immiscible when it is high. Alamo et al. suggest that the segregation of the components in the solid state reported by Hill et al. is due to crystallization mechanisms, rather than an incompatibility in the melt.

For SANS measurements, the maximum spatial resolution of pinhole cameras is ~10 Å. It has therefore been suggested that data might also be interpreted as arising from a bi-phasic melt with a large particle size (~1 μm) since most of the scattering from the different phases would not be resolved. Agamalian et al. (2000) addressed this hypothesis through the use of ultra-small angle neutron scattering (USANS). They confirmed that for HDPE/LLDPE blends phase separation occurs when the branch content is sufficiently high.

Zhao (2001) studied the effect of branch content of LLDPE on its miscibility with HDPE using Inverse Gas Chromatography (IGC) and a modified Flory-Huggins theory (as described in Chapter 2). Zhao also studied HDPE/LDPE, HDPE/i-PP, and HDPE/PS blends. For those blends, the measured polymer-polymer interaction parameters ($\chi_{23}$) are one to two orders of magnitude larger than those obtained by other methods (such as SANS). She believes that this deviation may be due to the use of the third solvent in IGC experiments. Since this deficiency is inherent in all IGC measurements, the $\chi_{23}$ values obtained from IGC may systematically be shifted and any observed functional dependence of $\chi_{23}$ may be retained. Five different octene-based LLDPEs were studied with branch contents ranging from 2 to 87 branches per 1,000 backbone carbons. For the same pair of HDPE and LLDPE, 50/50 blends are more miscible than those at other compositions. The effect of temperature on the miscibility depends on the composition of the blend and the branch content of LLDPE. The branch content of LLDPE has a significant effect on the miscibility of the blend. When the branch content of LLDPE is greater than 50 branches per 1000 backbone carbons, phase separation is observed. Although, it is observed that branch content induces phase separation, as is observed by other methods, the resulting $\chi_{23}$ values are noted to be much larger than those observed by other methods (e.g. two orders of magnitude) and the corresponding error values associated with the $\chi_{23}$ values are very large as well.

### 3.2.5 Summary

Due to the chemical similarity of HDPE/LLDPE blends there are a limited number of techniques that can be used to determine the miscibility of the blends. Most of

the available techniques are indirect methods that can not be used to study the blends directly in the melt state, therefore requiring the investigation of solidified samples. Melt miscibility of the blends is limited to indirect methods, molecular simulation and direct methods. However, all of the methods have their limitations. Indirect methods require the analysis of solidified samples, which is controversial since the morphology of the sample may change upon quenching. Molecular simulations are limited due to the computer resources. Traditionally, direct analysis of the blends has been limited to using SANS. This is also a limitation since SANS equipment is not readily available to most researchers and is very expensive. Consequently, the development of IGC as an analysis method is desirable since it may provide an inexpensive and readily available alternative; however, it is still in a developmental stage. Due to the limitations of all the different techniques, consistent results between techniques have not been obtained.

## 3.3 References


Agamalian, M.M., Alamo, R.G., Londono, J.D., Mandelkern, L., and Wignall, G.D. (1999) Phase Behaviour of Blends of Linear and Branched Polyethylenes on Micron Length Scales via Ultra-Small Angle Neutron Scattering, *Macromolecules*, 32, 3093-3096.

Agamalian, M.M., Alamo, R.G., Londono, J.D., Mandelkern, L., and Wignall, G.D. (2000) Phase Behaviour of Blends of Linear and Branched Polyethylenes on Micron Length Scales Via Ultra-Small Angle Neutron Scattering (USANS), *J. Appl. Cryst.*, 33, 843-846.

Alamo, R.G., Chan, E.K.M, Mandelkern, L., and Voigt-Martin, I.G. (1992) Influence of Molecular Weight on the Melting and Phase Structure of Random Co-polymer of Ethylene, *Macromolecules*, 25, 6381-6394.

Alamo, R.G., Londono, J.D., Mandelkern, L., Stehling, F.C., and Wignall, G.D. (1994) Phase Behaviour of Blends of Linear and Branched Polyethylenes in the Molten and Solid States by Small-Angle Neutron Scattering, *Macromolecules*, 27, 411-417.

Alamo, R.G., Viers, B.D., and Mandelkern, L. (1995) A Re-examination of the Relation between the Melting Temperature and the Crystallization Temperature: Linear Polyethylene, *Macromolecules*, 28, 3205-3213.

Alamo, R.G., Graessely, W.W., Krishnamoorti, R., Lohse, D.J., Londono, J.D., Mandelkern, L., Stehling, F.C., and Wignall, G.D. (1997) Small Angle Neutron Scattering Investigations of Melt Miscibillty and Phase Segregation in Blends of Linear and Branched Polyethylenes as a Function of the Branch Content, *Macromolecules*, 30, 561-566.

Cho, K., Lee, B.H., Hwang, K., Lee, H. and Choe, S. (1998) Rheological and Mechanical Properties in Polyethylene Blends, *Polymer Engineering and Science*, 38, 12, 1969-1975.

Choi, P. (2000) Molecular Dynamics Studies of the Thermodynamics of HDPE/butene-based LLDPE Blends, *Polymer*, 41, 8741-8747.

Crist, B., and Hill, M.J. (1997) Recent Developments in Phase Separation of Polyolefin Melt Blends, *Journal of Polymer Science Part B – Polymer Physics*, 35, 2329-2353.

Datta, N.K., and Birley, A.W. (1982) Thermal Analysis of Polyethylene Blends, *Plastics and Rubber Processing and Application*, 2, 237-245.

Hill, M.J., Barham, P.J., and Keller, A. (1992) Phase Segregation in Blends of Linear with Branched Polyethylene: the Effect of Varying the Molecular Weight of the Linear Polymer, *Polymer*, 33, 12, 2530-2541.

Hill, M.J., and Barham, P.J. (1992) Liquid-Liquid Phase Separation in the Melts of Blends of Linear with Branched Polyethylenes: Morphological Exploration of the Phase Diagram, *Polymer*, 33, 19, 4099-4107.

Hill, M.J., and Barham, P.J. (1992) Diffusion Effects in Blends of Linear with Branched Polyethylenes, *Polymer*, 33, 23, 4891-4897.

Hill, M.J., Barham, P.J., and Van Ruiten, J. (1993) Liquid-Liquid Phase Segregation in Blends of Linear Polyethylene with a Series of Octene Copolymers of Differing Branch Content, *Polymer*, 34, 14, 2975-2980.

Hill, M.J., and Barham, P.J. (1995) Ostwald Ripening in Polyethylene Blends, *Polymer*, 36, 17, 3369-3375.

Hill, M.J., and Puig, C.C. (1997) Liquid-Liquid Phase Separation in Blends of Linear Low-Density Polyethylene with a Low-Density Polyethylene, *J. Appl. Poly. Sci.*, 65, 1921-1931.

Hill, M.J., Morgan, R.L., and Barham, P.J., (1997) Minimum Branch Content for Detection of Liquid-Liquid Phase Separation Using Indirect Techniques in Blends of Polyethylene with Ethylene-Octene and Ethylene-Butene Copolymers, *Polymer*, 38, 12, 3003-3009.

Hill, M.J., and Barham, P.J. (2000) Morphology Maps of Binary Blends of Copolymers Produced Using the Metallocene Catalyst Process, *Polymer*, 41, 1621-1625.

Hu, S.R., Kyu, T., and Stein, R.S. (1987) Characterization and Properties of Polyethylene Blends. 1. Linear Low-Density Polyethylene With High-Density Polyethylene, *Journal of Polymer Science Part B – Polymer Physics*, 25, 1, 71-87.

Kwang, H., Rana, D., Cho, K., Rhee, J., Woo, T., Lee, B.H., and Choe, S. (2000) Binary Blends of Metallocene Polyethylene with Conventional Polyolefins: Rheological and Morphological Properties, *Poly. Engr. Sci.*, 40, 7, 1672-1681.

Lee, H., Cho, K., Ahn, T., Choe, S., Kim, I., Park, I., and Lee, B.H. (1997) Solid-State Relaxations in Linear Low-Density (1-Octene Comonomer), Low-Density, and High-Density Polyethylene Blends, *Journal of Polymer Science Part B – Polymer Physics*, 35, 10, 1633-1642.

Lee, H.S., and Denn, M.M. (2000) Blends of Linear and Branched Polyethylenes, *Polymer Engineering and Science*, 40, 5, 1132-1142.

Morgan, R.L., Hill, M.J., Barham, P.J., and Frye, C.J. (1997) Liquid-Liquid Phase Separation in Ternary Blends of Linear Polyethylene With Two Ethyl-Butene Copolymers, *Polymer*, 38, 8, 1903-1909.

Morgan, R.L., Hill, M.J., Barham, P.J., van der Pol, A., Kip, B.J. Ottjes, R., and Van Ruitein, J. (2001) A Study of the Phase Behaviour of Polyethylene Blends Using Micro-Raman Imaging, *Polymer*, 42, 5, 2121-2135.

Tanem, B.S. and Stori, A. (2001) Investigation of Phase Behaviour in the Melt in Blends of Single-site Based Linear Polyethylene and Ethylene-1-alkene Copolymers, *Polymer*, 42, 4309-4319.

Tanem, B.S., and Stori, A. (2001) Phase Separation in Melt Blends of Single-Site Linear and Branched Polyethylene, *Polymer*, 42, 5689-5694.

Tashiro, K., Stein, R.S., and Hsu, S.L. (1992) Cocrystallization and Phase Segregation of Polyethylene Blends. 1. Thermal and Vibrational Spectroscopic Study by Utilizing the Deuteration Technique, *Macromolecules*, 25, 1801-1808.

Tashiro, K., Izuchi, M., Kabayashi, M., and Stein, R.S. (1994) Cocrystallization and Phase Segregation of Polyethylene Blends Between the D and H Species. 3. Blend Content Dependence of the Crystallization Behaviour, *Macromolecules*, 27, 1221-1227.

Tashiro, K., Izuchi, M., Kobayashi, M., and Stein, R.S. (1994) Cocrystallization and Phase Segregation of Polyethylene Blends Between the D and H Species. 4. The Crystllization Behaviour as Viewed From the Infrared Spectral Changes, *Macromolecules*, 27, 1228-1233.

Tashiro, K., Izuchi, M., Kobayashi, M., and Stein, R.S. (1994) Cocrystallization and Phase Segregation of Polyethylene Blends Between the D and H Species. 5. Structural Studies of the Blends as Viewed from Different Levels of Unit Cell to Spherulite, *Macromolecules*, 27, 1234-1239.

Tashiro, K., Imanishi, K., Izuchi, M., Kobayashi, M., Itoh, Y., Imai, M., Yamaguchi, Y., Ohashi, M. and Stein, R.S. (1995) Cocrystallization and Phase Segregation of Polyethylene Blends Between the D and H Species. 8. Small-Angle Neutron Scattering Study of the Molten State and the Structural Relationship of Chains Between the Melt and the Crystalline State, *Macromolecules*, 28, 8484-8490.

Wignall, G.D., Alamo, R.G., Londono, J.D., Mandelkern, L., Kim, M.H., Lin, J.S., and Brown, G.M. (2000) Morphology of Blends of Linear and Short-Chain Branched Polyethylenes in the Solid State by Small Angle Neutron and X-ray Scattering, Differential Scanning Calorimetry, and Transmission Electron Microscopy, *Macromolecules*, 33, 551-561.

Zhao, L. and Choi, P. (2001) Determination of Solvent-Independent Polymer-Polymer Interaction Parameter by an Improved Inverse Gas Chromatographic Approach, *Polymer*, 42, 1075-1081.

Zhao, H., Lei, Z., and Huang, B. (1998) Excimer Fluroescence Studies on the Miscibility of Polyolefins in the Amorphous Phase, *Polymer Journal*, 30, 2, 149-151.

# Chapter 4

# Miscibility of HDPE/LLDPE Blends

## 4.1 Background

A novel approach for obtaining solvent independent Flory-Huggins interaction parameters ($\chi_{23}$) using IGC was proposed by Zhao and Choi (2001). Promising results were obtained for a variety of polyolefin blends, including HDPE/i-PP, HDPE/PS, HDPE/LDPE, HDPE/LLDPE and LDPE/LLDPE blends. However, the measured $\chi_{23}$ were typically one to two orders of magnitude larger than values obtained using SANS for comparable blends (e.g. Alamo et al., 1997). The authors believed that the deviation between IGC and SANS measurements may be due to the use of the injected probe in IGC measurements. Since this deficiency is inherent in all IGC measurements, it is speculated that such $\chi_{23}$ values obtained from IGC may be systematically shifted and any observed functional dependence of $\chi_{23}$ may be retained, although not necessarily.

The authors decided to apply the modified IGC method to study the effect of branch content of octene-based LLDPE on its miscibility with HDPE at elevated temperatures. Since such systems have been extensively studied and the branch content dependence of $\chi_{23}$ has been established using other methods, it is possible to compare the results obtained by IGC with other methods. Therefore, if IGC is capable of capturing miscibility trends, this method could be a valuable analysis technique due to it being a quick and inexpensive method.

Zhao (2001) investigated five different octene-based LLDPE with branch contents ranging from 2 to 87 branches per 1,000 backbone carbons at three compositions and four

temperatures with a single HDPE (HDPE-1) of a low molecular weight ($M_w$ = 49,400, $M_n$ = 13,700).

She found that $\chi_{23}$ of blends containing low branch content LLDPE reaches a minimum value for the 50/50 blend regardless of the temperature indicating that blends are more miscible at 50% HDPE. However, for higher branch content blends, clear composition trends were not observed. In general, $\chi_{23}$ was at a minimum at 50% HDPE, but not always. Due to the associated errors of $\chi_{23}$ being large, there is some uncertainty regarding the blend composition dependence of $\chi_{23}$.

Zhao concluded that the effect of temperature on the miscibility is dependent on the composition of the HDPE-1/LLDPE blends and the branch content of LLDPE studied. For 30/70 blends, $\chi_{23}$ slightly decreased with temperature. For 50/50 and 70/30 blends no obvious trend was observed. Due to the large errors of the measured $\chi_{23}$, the ability of IGC to capture the temperature dependence of $\chi_{23}$ is questionable.

When $\chi_{23}$ values were plotted against the branch content of LLDPE, $\chi_{23}$ was negative for all temperatures and blend compositions if the branch content of LLDPE is < 50 branches per 1,000 backbone carbons. When the branch content of LLDPE was ≥50 branches per 1,000 backbone carbons, $\chi_{23}$ values became positive and deviated significantly from zero as the branch content was increased further. This indicated that phase separation may occur in blends when the branch content of LLDPE is sufficiently high (~50 branches per 1,000 backbone carbons). However, the magnitudes of the measured $\chi_{23}$ values were much larger than what is expected. At low branch contents, $\chi_{23}$ showed large negative values. It is expected that these systems should conform to the

geometric mean assumption and consequently, the interaction parameters are expected to be slightly positive.

In this chapter, the effect of increasing the molecular weight of HDPE on the blend miscibility was investigated using a higher molecular weight HDPE (HDPE-2, $M_w$ = 137,000, $M_n$=28,000). The same five octene-based LLDPE samples with branch contents ranging from 2 to 87 branches per 1,000 backbone carbons were analyzed. The branch content dependence of $\chi_{23}$ for the HDPE-2/LLDPE blends as well as the temperature dependence of the blends was investigated. By comparing these results with the results obtained by Zhao for HDPE-1/LLDPE blends, conclusions regarding the molecular weight dependence of HDPE on $\chi_{23}$ were made.

## 4.2 Experimental Methods

### 4.2.1 Materials

Two different HDPEs of different molecular weights and five different octene-based LLDPE samples of different branch contents were analyzed. HDPE-1 was a low molecular weight HDPE (analyzed previously by Zhao) while HDPE-2 was a higher molecular weight. Five different metallocene catalyst produced octene-based LLDPE samples with branch contents ranging from 2 to 87 branches per 1,000 backbone carbons were used. The molecular weights and branch contents of such polymers are presented previously in Table 2.1. The same 13 solvents that Zhao used to characterize the polymer samples were used in this study for consistency. The solvents were reagent grade solvents purchased from Fisher Scientific and used without further purification. They were 1-hexene, 1-octene, benzene, cyclohexane, n-hexane, n-dodencane, n-heptane, n-nonane, n-

pentadecane, n-pentane, n-octane, toluene, and xylene. The justification for using these solvents is summarized in Chapter 2.

### 4.2.2 Sample Preparation

Samples were prepared at 50/50 weight composition since it was observed that 50/50 blend compositions appear to be the most miscible (Zhao, 2001). The sample preparation technique is summarized in Section 2.7.2. To be consistent with Zhao's approach, 1 m long columns were used and the coated support was packed into the column to avoid any void spaces. The amount of mass coated on the solid support was determined using the ashing process described in Section 2.7.3 and blank corrections were implemented.

### 4.2.3 Operating Conditions

The experiments were conducted at oven temperatures of 170, 190, 210, and 230°C for each column. Inlet pressures ranged from 200 to 250 kPa and the outlet pressure was atmospheric. The flow rate of the carrier gas (helium) ranged between 23 to 29 $cm^3$/minute.

Injections of the solvents (in the vapour form) were made in small volumes (~1 μL) using a 10 μL Hamilton syringe with removable needles (bevel tip #2). Small volumes of solvent vapour were used to ensure that the infinite dilution condition was satisfied. Injections were performed in triplicate.

## 4.3 Results

### 4.3.1 Retention Time and Specific Retention Volume Measurements

The retention time of the injected probe is an important measured parameter that is required for the calculation of $\chi$ values. For each column at each experimental temperature, the retention time of the injected solvent was noted to increase as the molecular weight of the solvent increases for probes with linear chains. As the temperature of the system increased, the net retention time decreased. The specific retention volumes were calculated using the measured $t_r$, $F$, $P_i$, $P_o$, and $T$ for each injected solvent using Equations 22-24.

### 4.3.2 Interaction Parameters

The calculated specific retention volumes were then used to calculate the polymer-solvent interaction parameters ($\chi_{12}$ or $\chi_{13}$) and the polymer blend-solvent interaction parameters ($\chi_{1(23)}$). Sample calculations are presented in Appendix A. This data was then used to determine the $\chi_{23}$ for the blends by plotting $\chi_{1(23)}$ vs. ($\phi_2\chi_{12} + \phi_3\chi_{13}$) according to Equation 46. The corresponding plots of $\chi_{1(23)}$ vs. ($\phi_2\chi_{12} + \phi_3\chi_{13}$) for each HDPE/LLDPE blend follow a linear relationship. According to Equation 46, it is expected that the slope of the line should be unity for solvent independent $\chi$ values. However, this is not observed in most cases. Slopes are found to range from 0.7466 to 1.3577 for HDPE-1/LLDPE blends and from 0.7425 to 1.1215 for HDPE-2/LLDPE blends. The calculated coefficient of determination ($R^2$) of the data are typically close to unity, ranging from 0.9430 to 0.9936 for HDPE-1/LLDPE blends and from 0.8858 to 0.9975 for HDPE-2/LLDPE blends indicating that the data is adequately described by the

linear regression model. $R^2$ is the square of the correlation coefficients between X and Y and it is often referred to as the amount of variability in the data that is being represented by the regression model (Montgomery and Runger, 1994). An $R^2$ value close to unity should represent an accurate fit of the regression model. Thus, it is observed that the linear regression model accurately describes the data. However, the slopes that are observed to deviate significantly from unity are problematic since it may suggest that there is possibly solvent dependence (or an unidentified dependence) of the data that is causing the slope to deviate from unity.

From the intercept of the linear lines, the resultant $\chi_{23}$ was determined as per Equation 46. Sample calculations of the associated error values are presented in Appendix B.

### 4.3.3 Temperature Dependence of $\chi_{23}$

Figures 4.1 and 4.2 display plots of $\chi_{23}$ versus temperature for 50/50 weight composition HDPE-1/LLDPE and HDPE-2/LLDPE blends, respectively. For the HDPE-1/LLDPE blends, there was no clear temperature dependence for 50/50 composition blends. However, for the HDPE-2/LLDPE blends, curves of $\chi_{23}$ versus temperature show minima at 210°C for all the LLDPEs, indicating that the blends are comparatively more miscible at 210°C. Also, at 170°C, positive $\chi_{23}$ values were obtained for all of the HDPE-2/LLDPE blends indicating immiscibility of some of the blends. Due to the large error values in both sets of data as well as the absolute magnitude of $\chi_{23}$ being much larger than those obtained by other methods (e.g. SANS results for similar blends, $\chi_{23} = \sim 10^{-4}$). Therefore, it is difficult to make a conclusive statement regarding the temperature

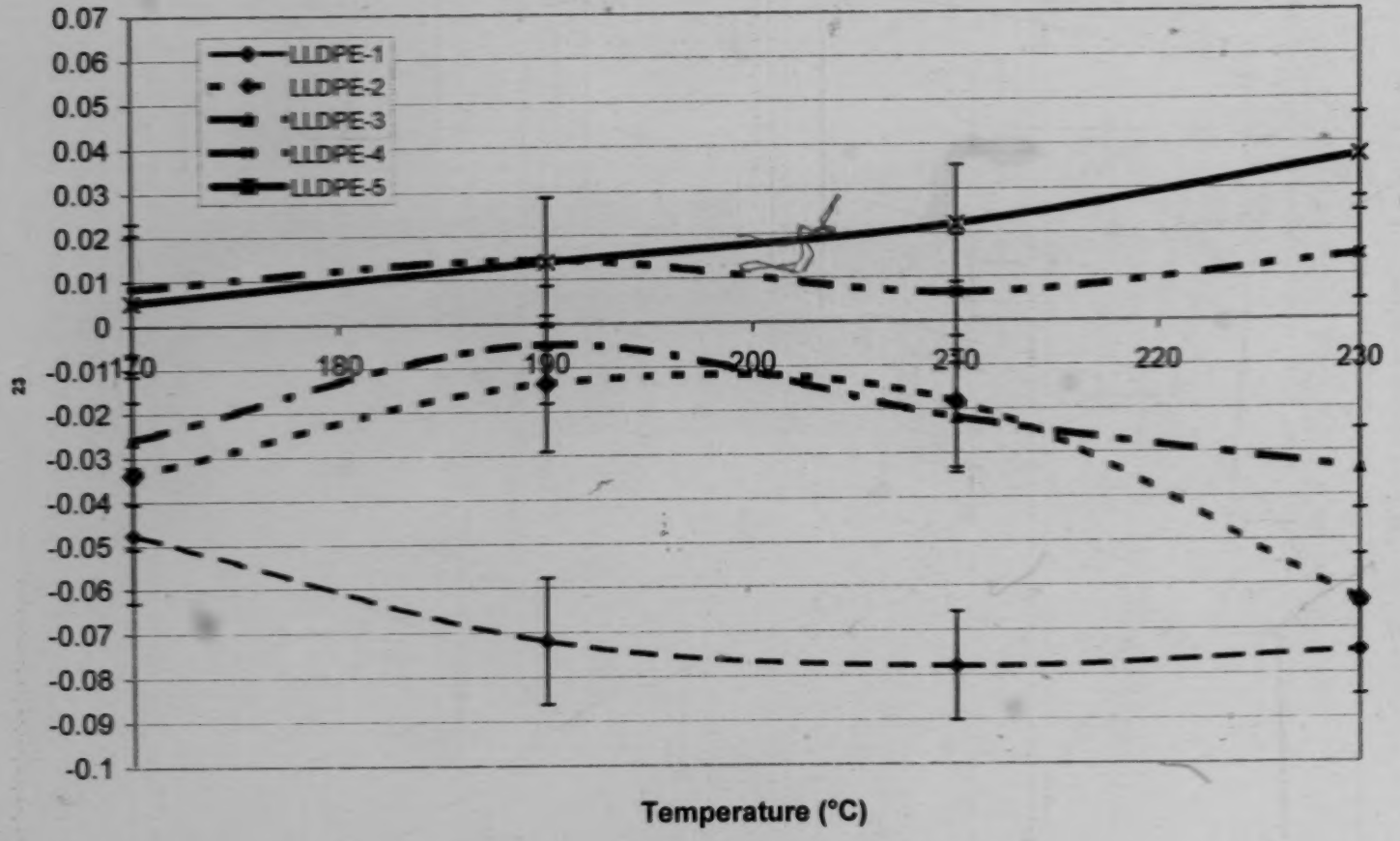


**Figure 4.1.** $\chi_{23}$ **Versus Temperature for HDPE-1/LLDPE Blends**

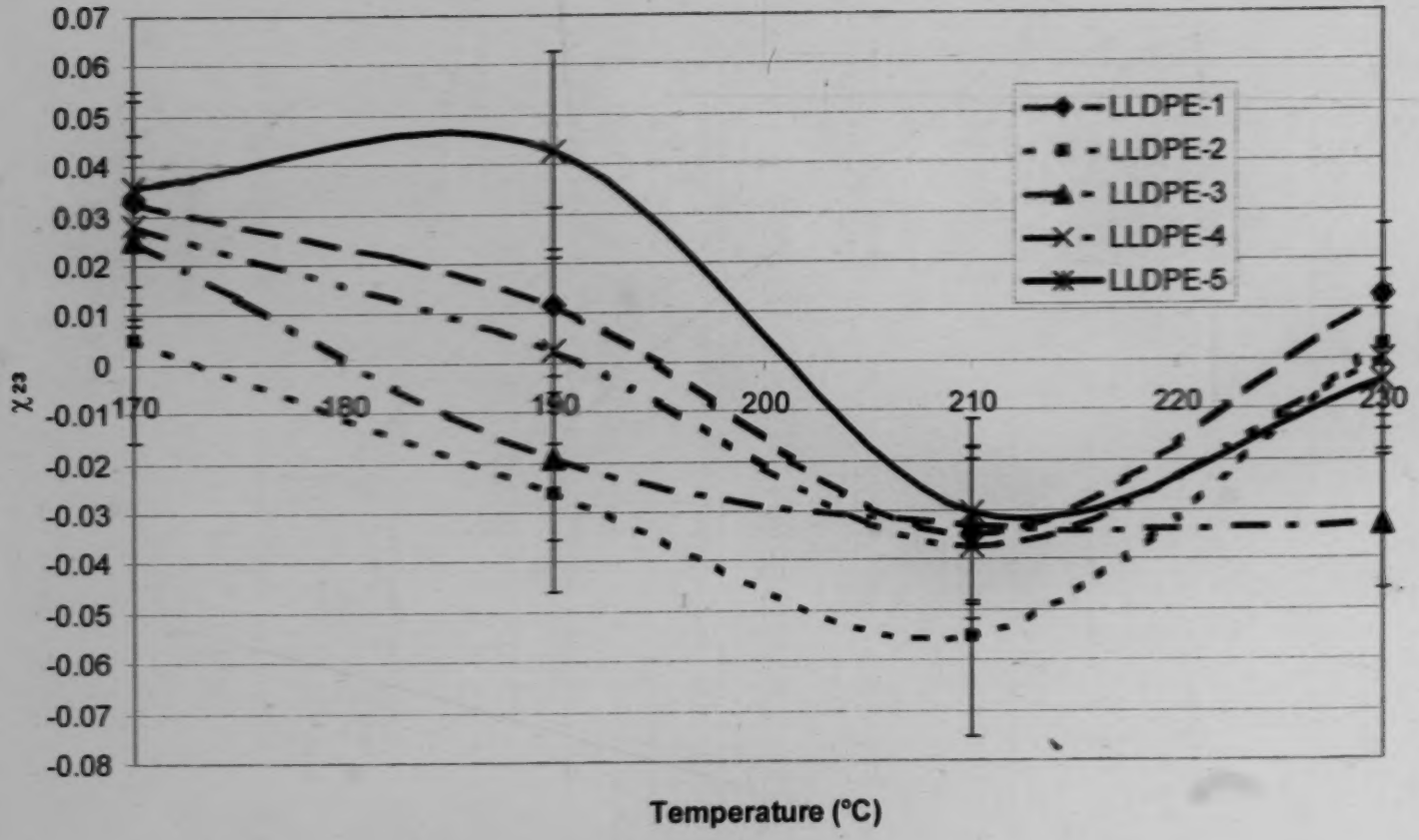


**Figure 4.2.** $\chi_{23}$ **Versus Temperature for HDPE-2/LLDPE Blends**

dependence of $\chi_{23}$ for HDPE/LLDPE blends. Further studies of the reproducibility of the data are needed.

### 4.3.4 Branch Content Effect of LLDPE on $\chi_{23}$ of HDPE/LLDPE Blends

Zhao (2001) observed that immiscibility of the HDPE-1/LLDPE blends occurred when the branch content of LLDPE was ≥ 50 branches per 1,000 backbone carbons (Figure 4.3). For the HDPE-2/LLDPE blends no clear branch content dependence was observed (Figure 4.4). All of the $\chi_{23}$ values generally tended to increase slightly as the branch content of LLDPE increased. Therefore, no clear conclusion regarding the branch content effect on HDPE-2/LLDPE blends can be made. Due to the large error values in both sets of data as well as the absolute magnitude of $\chi_{23}$ being much larger than those obtained by other methods (e.g. SANS), it is difficult to make a conclusive statement regarding the branch content dependence of $\chi_{23}$ for HDPE/LLDPE blends.

### 4.3.5 Molecular Weight Effect of HDPE on $\chi_{23}$ of HDPE/LLDPE Blends

By comparing the HDPE-1/LLDPE results of Zhao's with the HDPE-2/LLDPE blends studied, observations regarding the effect of increasing the molecular weight of HDPE on the blend miscibility can be inferred. As noted in the temperature dependence and branch content dependence discussions, the HDPE-1/LLDPE and HDPE-2/LLDPE blends are noted to behave fairly similarly. Therefore, the variation in molecular weight does not affect the miscibility significantly. The following may explain such an observation:

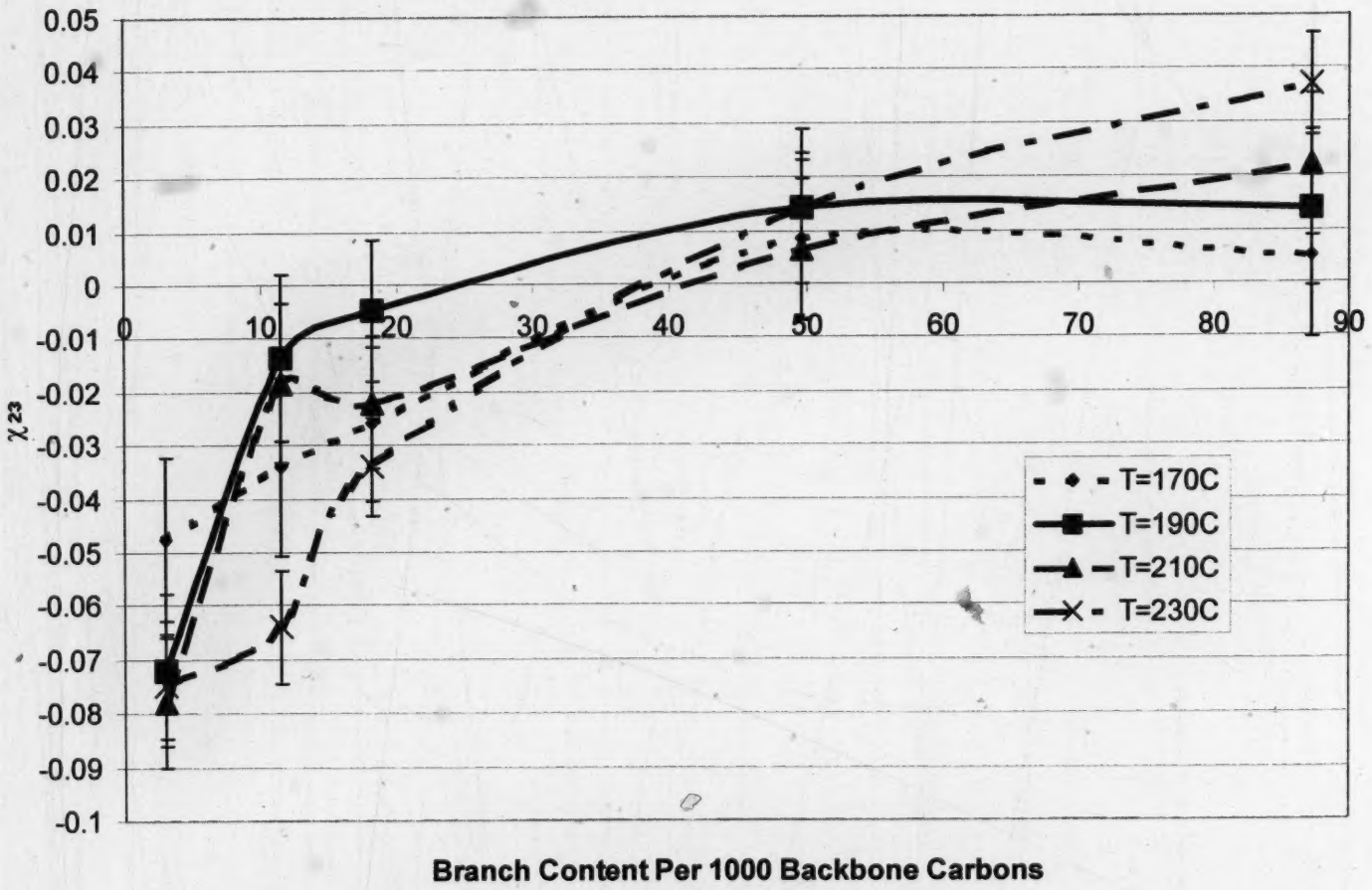


**Figure 4.3.** $\chi_{23}$ **versus Branch Content of LLDPE for HDPE-1/LLDPE Blends**

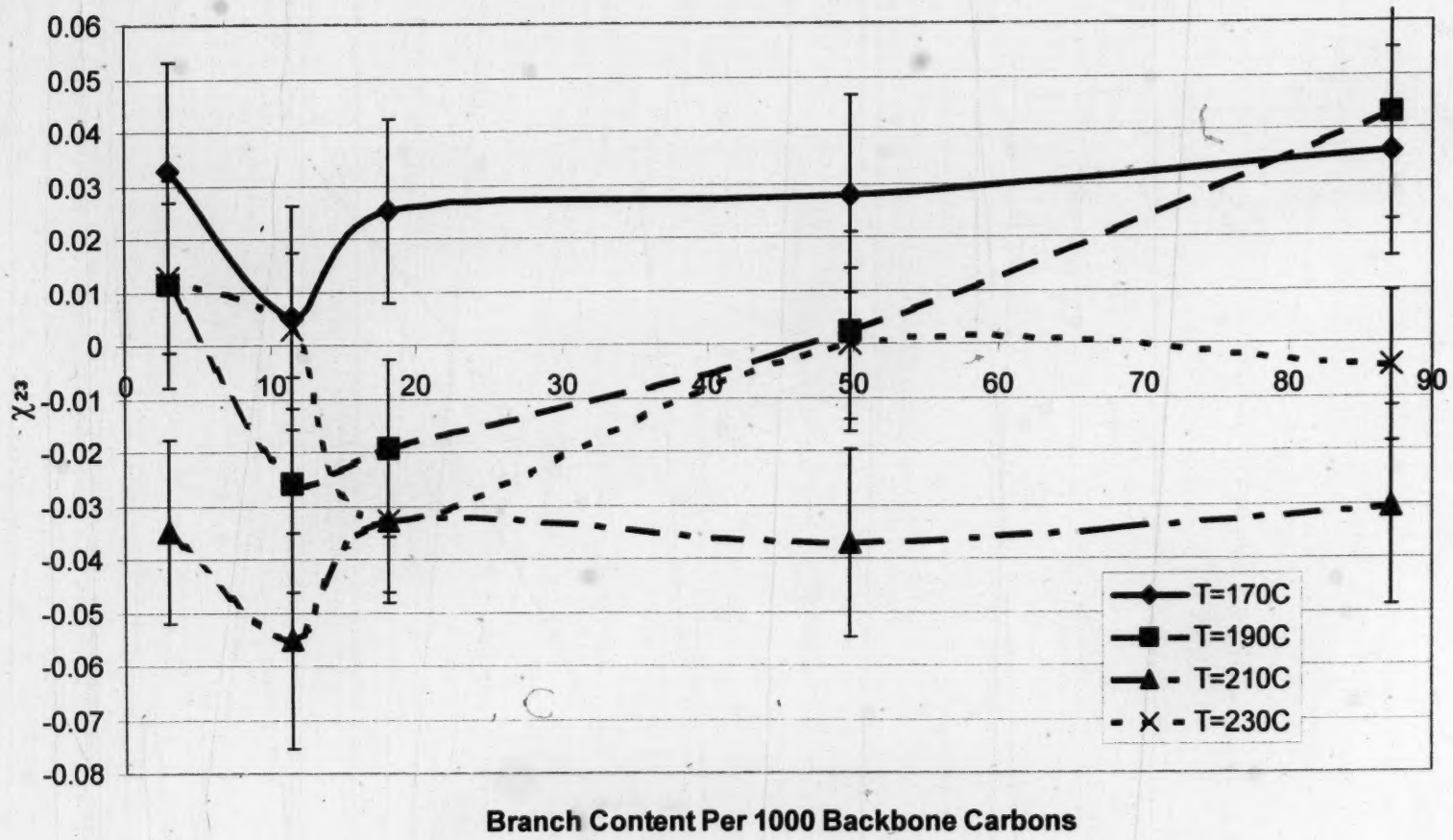


**Figure 4.4.** $\chi_{23}$ **versus Branch Content of LLDPE for HDPE-2/LLDPE Blends**

1. The molecular weight difference between HDPE-1 and HDPE-2 is not substantially large. The $M_w$ of HDPE is ~ 2.75 times larger than that of HDPE-1; however when compared to the LLDPE $M_w$, there is not substantial differences between the HDPE-1 and HDPE-2 molecular weight ranges. As stated by Tanem and Stori (2001) it is the molecular weight difference between the HDPE/LLDPE components that will effect the miscibility not the absolute $M_w$ of the components.
2. The error values of the $\chi_{23}$ and the absolute magnitude of $\chi_{23}$ make the results difficult to interpret and are possibly flawed.

Consequently, it is difficult to comment on the molecular weight dependence of the blends.

## 4.4 Summary

Due to the large error associated with the measured $\chi_{23}$ values, it is difficult to make concise conclusions regarding the miscibility of the HDPE-1/LLDPE and HDPE-2/LLDPE blends. The $\chi_{23}$ values for HDPE-1/LLDPE blends appeared to be independent of temperature and displayed a branch content dependence (similar to that observed in the literature) with phase separation occurring when the branch content of the LLDPE is ≥ 50 branches per 1,000 backbone carbons. For the HDPE-2/LLDPE blend, the observation was somewhat different. The $\chi_{23}$ was noted to be dependent on temperature (it was most miscible at 210°C); however, a branch content dependence was not as obvious as the blends with HDPE-1. It is possible that the differences observed for the HDPE-1/LLDPE and HDPE-2/LLDPE blends are due to the change of the HDPE molecular weight.

However, as stated previously, this is unlikely. Especially, when the magnitude of the $\chi_{23}$ errors (and the $\chi_{23}$ values themselves) are taken into account. Another factor that may cause the above observation is attributed to the slopes of the $\chi_{1(23)}$ versus $(\phi_2\chi_{12} + \phi_3\chi_{13})$ graphs not being unity, as is expected for solvent independency. This deviation of the slope indicates that the theories presented in Chapter 3 may be inadequate. It should be noted that any slight deviation in the slope of the resultant regression line can result in a large change in $\chi_{23}$ due to it being calculated from the y-intercept of the graph.

Due to the observed deficiencies and the lack of agreement between the data, error reduction methods were examined in order to obtain more conclusive data. The error reduction approaches and the corresponding results are presented in Chapter 5.

## 4.5 References


Alamo, R.G., Graessely, W.W., Krishnamoorti, R., Lohse, D.J., Londono, J.D., Mandelkern, L., Stehling, F.C., and Wignall, G.D. (1997) Small Angle Neutron Scattering Investigations of Melt Miscibility and Phase Segregation in Blends of Linear and Branched Polyethylenes as a Function of the Branch Content, *Macromolecules*, 30, 561-566.

Choi, P. (2000) Molecular Dynamics Studies of the Thermodynamics of HDPE/butene-based LLDPE Blends, *Polymer*, 41, 8741-8747.

Montgomery, D.C. and Runger, G.C. (1994) Applied Statistics and Probability for Engineers, John Wiley and Sons Inc., New York, N.Y..

Tanem, B.S. and Stori, A. (2001) Investigation of Phase Behaviour in the Melt in Blends of Single-site Based Linear Polyethylene and Ethylene-1-alkene Copolymers, *Polymer*, 42, 4309-4319.

Tanem, B.S. and Stori, A. (2001) Phase Separation in Melt Blends of Single-Site Linear and Branched Polyethylene, *Polymer*, 42, 5689-5694.

Zhao, L. (2001) PhD. Thesis, University of Alberta.

Zhao, L. and Choi, P. (2001) Determination of Solvent-Independent Polymer-Polymer Interaction Parameters by an Improved Inverse Gas Chromatographic Approach, *Polymer*, 42, 1075-1081.

# Chapter 5

# Error Analysis

## 5.1 Error Reduction Methods Implemented and Justification of Changes

In order to acquire meaningful $\chi_{23}$ values when using IGC, it is necessary to obtain precise $\chi_{12}$, $\chi_{13}$, and $\chi_{1(23)}$ values since any inaccuracies in those measurements will manifest themselves in the final $\chi_{23}$ calculated value. Small absolute errors in $\chi_{12}$, $\chi_{13}$, or $\chi_{1(23)}$ can result in a large relative error in the calculated $\chi_{23}$.

It is important that the collected data from IGC measurements be taken accurately to obtain meaningful results. In the case of thermodynamic data collection, all factors related to non-equilibrium effects must be eliminated as well as the effects due to experimental set up (e.g. support effects). The thermodynamic analysis of IGC data assumes that only the bulk polymer causes the retention of the probe and that there is an instantaneous equilibrium between the bulk polymer and mobile phase. In actual experiments, the probe may be retained also by the support, by the inner walls of the column and by the surface of the polymer. Slow equilibrium between the stationary and mobile phases may cause not only spreading of the peaks, but also reduce the measured retention time. All these effects must be taken into account when the thermodynamic analysis is contemplated (Munk, 1991 and Al-Saigh, 1997).

It has been suggested (Munk, 1991) that when calculating $\chi_{23}$ that all three columns used in the analysis should be studied under identical conditions to produce reliable measurements of $\chi_{12}$, $\chi_{13}$, and $\chi_{1(23)}$. In practice, it is impossible to study the columns under identical conditions, mainly due to the column loading. It is relatively

simple to control the carrier gas flow rate and the temperature of the column. However, due to the sample preparation, it is very difficult to precisely control the amount of solid that is loaded into the chromatographic column. The total amount of solid added to the column can be artificially controlled by always loading an arbitrarily specified mass. This has two drawbacks; (1) the percent loading of polymer on the solid differs from sample to sample due to the coating procedure that is used (as described in Chapter 2) resulting in different polymer amounts, and (2) by controlling the amount of solid added (rather than packing the column until it is full) will introduce void spaces. Void spaces are believed to be detrimental to the column analysis due to the injected solvents possibly interacting with the column walls (Al-Saigh, 1997). If the total amount of polymer, rather than the total amount of solid, is artificially controlled for each column, the void space problem will still be encountered. Consequently, it was decided that the columns should be packed as tightly as possible in order to avoid having void spaces. Therefore, the mass term ($w$) from column to column differs. As a result, the pressure drop across the columns also differs. Therefore, it is not possible to analyze the three columns under identical conditions for the determination of $\chi_{12}$, $\chi_{13}$, and $\chi_{1(23)}$. It should be unnecessary to analyze the column under identical conditions, as long as the variables are controlled accurately, since the calculated $\chi$ values should be independent of the mass, flowrate, etc. according to the theory (Chapter 2).

By examining Equation 32 from Chapter 2, it is observed that the only term, which is experimentally controlled once the temperature is set, is the specific retention volume ($V_g^\circ$), which was defined in Chapter 2 as:

$$V_g^\circ = \frac{273.15 t_n F J}{wT} \tag{22}$$

where $t_n$ is the net retention time; $F$ is the flow rate of the carrier gas measured at the experimental temperature $T$; $w$ is the mass of the polymer in the chromatographic column; and $J$ is the James-Martin correction factor that is used to correct for the pressure gradient across the column. The net retention time is defined as the difference between the retention time of the solute ($t_p$) and that of the unretained solute marker ($t_m$):

$$t_n = t_p - t_m \tag{23}$$

The James-Martin correction factor, $J$, is defined as:

$$J = \frac{3}{2}\left[\frac{\left(\frac{P_i}{P_o}\right)^2 - 1}{\left(\frac{P_i}{P_o}\right)^3 - 1}\right] \tag{24}$$

where $P_i$ and $P_o$ are the inlet and outlet pressures of the column. Therefore, the experimental variables that require precise measurement are: $F$, $P_i$, $P_o$, $t_p$, $t_m$, $w$, and $T$. The temperature of the column is known accurately to ± 0.05°C (< 0.03% absolute error for the temperature range studied). $P_o$ is the outlet pressure (atmospheric pressure) and is measured using a digital barometer to an accuracy of ± 0.05 kPa (< 0.05% absolute error). Consequently, no changes were made to improve the accuracy of $T$ or $P_o$ since it would have little (if any) effect.

With the existing equipment, the $P_i$ is known to roughly ± 5 kPa (roughly ~2.5% absolute error) due to the inaccuracy of the pressure gauge. With this current error, significant operator error (i.e. operator dependent results) can occur depending on how the pressure gauge is read, thereby introducing error to $\chi_{12}$, $\chi_{13}$, and $\chi_{1(23)}$. With some

modifications, a more accurate pressure gauge, such as a U-Tube mercury manometer as suggested by Farooque and Deshpande (1992), could be installed. However, such a change was not within the time frame of the current work.

The accuracy of the $t_n$ is also limited by the IGC since time measurements are measured to 0.001 min. Further inaccuracies are introduced due to the manual injection of the probe and starting of the time measurement. Also, since $t_n$ is determined from $t_m$ and $t_p$ the errors associated with $t_m$ and $t_p$ are additive. Therefore, $t_n$ measurements are known to have an error in the range of ± 0.01 minutes. Since all $t_n$ measurements were made in triplicate and are noted to be in good agreement with one another, direct changes to improve the accuracy of the measurements were deemed to be unnecessary.

A problem that is difficult to quantify is the accuracy of the retention time of the marker (methane), $t_m$, which is used in the calculation of $t_n$. The marker is assumed to be a non-interacting probe; however, methane is known to interact with the polymer, therefore introducing an unknown amount of error. Since methane is a very small molecule, this interaction is assumed to be negligible for this work. To overcome this problem a thermal conductivity (TC) detector could be used so that nitrogen could be used as the carrier gas and air as the marker. This change was not explored since substantial changes to the IGC equipment would be required. Additionally, when using a TC detector capillary columns are used in the analysis, which are known to have their own associated problems. Consequently, this change was not explored.

The accuracy of the $w$ and $F$ measurements are more difficult to quantify. For the results presented in Chapter 4, the error of $F$ was assumed to be ± 0.2 $cm^3$/min and for $w$ ± 0.001 g. The error in $F$ was taken to be due to the manual time measurements.

However, no other sources of error were considered for $F$. For $w$, the sources of error that were considered were measurement errors due to the balance used since a series of measurements were taken in the column loading process as well as in the ashing process (to determine the polymer loading). Also, since there is some mass that is likely lost during the loading process (e.g. due to the packing procedure a small amount of the coated support may spill). A corrective measure that was used to improve the accuracy of the $w$ measurement was blank corrections as suggested by Braun and Guillet (1976). Blank corrections are required when the polymer loading is determined by burning the coated support since some mass loss is observed when a blank (uncoated) support sample is burned under identical conditions. Failure to correct for this effect could bring about a sizeable error.

For the analysis in Chapter 4, it was assumed that performing blank corrections would result in accurate enough measurements for the precise calculation of $\chi_{23}$. However, from the obtained results, in which, large $\chi_{23}$ values and large error values are observed, as well as no distinct branch content trend being observed in the HDPE-2/LLDPE blends, it is questionable as to whether the experimental variables are controlled to a high enough accuracy in order to precisely calculate $\chi_{23}$.

Munk (1991) suggested that the use of a bubble flow meter with helium gas can result in errors of roughly 0.3 $cm^3$/minute due to the diffusion of helium through the soap bubble. By attaching an inverted U-tube to the outlet of the bubble flow meter, this effect was eliminated. Munk also suggested that the flowmeter should be thermostated to suppress the effects of the volume change of the gas in flow measurements. Daily fluctuations of the ambient temperature can also lead to an unacceptably high fluctuation

of flow rate. This problem can be solved by thermostating the valves by enclosing them in a Styrofoam box, thermostated by a copper coil through which a thermostated liquid is circulated. For the current work, to improve upon the accuracy of $F$, a digital flowmeter was purchased which was fitted with an inverted U-tube to prevent the effect of helium diffusion through the bubble. The flowmeter is calibrated to ~1.69% error at 25°C. Other changes were not implemented due to time constraints in modifying the equipment.

To further improve upon the accuracy of $w$, the length of the chromatographic columns used was increased from 1 m to 3m and also 6m. This was done in order to reduce the effects of measurement errors from the weigh scale since the overall mass error value due to the scale will be the same regardless of the length of column used. Consequently, with a longer column there is more polymer mass so the overall effect of the measurement errors on the $w$ term should be reduced. Additionally, by increasing the mass of polymer in the system, it will also increase the retention times of injected solvents. Therefore, the overall effect of the measurement errors for $t_n$ will also be reduced. Thus, the error due to $w$ and $t_n$ should be improved upon by increasing the column length.

Munk (1991) believes that the coating method described in Chapter 2 is problematic since during this procedure the polymer coats not only the support, but also the walls of the evaporating vessel and the quantitative relationship between the masses of the support and the polymer is lost. Therefore, it is required that the support be analyzed for polymer content by either extraction, calcination, or ignition; however, these methods are subject to much larger errors than are acceptable for thermodynamic purposes. In Munk's experience, even 1% error in a single experimental parameter is not

acceptable. To overcome this problem, Munk suggested that the samples be prepared by the "soaking method" that was devised by Al-Saigh and Munk (1984), which enables the whole polymer sample to be deposited on the support and into the column. In this method the polymer is dissolved in a solvent as usual. The support is piled on a watch glass or a similar dish and a small amount of solution is applied to the top of the support pile. Care is taken to wet the pile as much as possible without letting the solution touch the surface of the dish, either around or under the pile. The solvent is allowed to evaporate and the pile is thoroughly mixed. Then the next portion of the solution is applied and the whole procedure is repeated until all the solution (including risings of the solution flask) is used up. It takes typically 10-20 applications and requires only a few hours. In their experience no polymer was left on the surface of the dish. Then the support was dried in an oven and quantitatively transferred into the column with standard precautions of quantitative analytical chemistry. The method is fast, the amount of polymer is precisely known and the analysis of the column material is avoided, which eliminates further measurement errors. It was decided that the method in Chapter 2 would be accurate for the current work because the coating and ashing procedure with blank corrections is widely used throughout the literature and is believed to provide accurate results. Therefore, changes to the method to improve on the accuracy of $w$ for the current work were deemed to be unnecessary for this work.

## 5.2 Effect of Using Different Column Lengths For the Calculation of $\chi$ Values

In order to test the effect of changing the mass of the polymer analyzed, several samples of HDPE-2 were analyzed using different column lengths. The columns were 1,

3, and 6 m long and were packed with HDPE-2 coated solid support (using the column preparation method described in Chapter 2). The samples were analyzed at four temperatures (170, 190, 210, and 230°C) with flow rates ranging from 21 to 30 $cm^3$/minute. Inlet pressures ranged from 228 to 383 kPa and the outlet pressure was atmospheric. The percent loading of polymer on the support ranged from 7.27% to 9.41%, which is within the recommended range of 6 to 10%. The total amount of polymer in each column is dependent on the length of the column, the packing, and the loading of the polymer on the inert support. The total mass of polymer for each column is summarized in Table 5.1. Also included in Table 5.1 are the calculated $\chi_{12}$ values for each sample.

**Table 5.1. $\chi_{12}$ Values For HDPE-2 Using Different Column Lengths and Polymer Loading**

| Sample # | 1 | 2 | 3 | 4 | 5 | 6 |
|---|---|---|---|---|---|---|
| Column Length | 1 m | 1 m | 3 m | 3 m | 6 m | 6 m |
| Polymer Loading | 8.31% | 9.41% | 7.27% | 7.80% | 7.80% | 8.82% |
| Mass of Polymer (g) | 0.0673 | 0.0690 | 0.1610 | 0.1683 | 0.2252 | 0.2262 |
| Mass of Solid (g) | 0.8099 | 0.7333 | 2.2135 | 2.1575 | 2.8867 | 2.5633 |
| | | | | | | |
| T = 170°C | $\chi_{12}$ | $\chi_{12}$ | $\chi_{12}$ | $\chi_{12}$ | $\chi_{12}$ | $\chi_{12}$ |
| 1 - hexene | 0.0778 | 0.1035 | 0.1031 | 0.1190 | 0.1382 | 0.1225 |
| 1-octene | 0.0632 | 0.0759 | 0.0868 | 0.1008 | 0.1218 | 0.1083 |
| Benzene | 0.1414 | 0.1589 | 0.1821 | 0.2062 | 0.2421 | 0.2219 |
| cyclohexane | 0.0872 | 0.0935 | 0.1103 | 0.1306 | 0.1586 | 0.1427 |
| Hexanes | 0.0821 | 0.0838 | 0.0922 | 0.1123 | 0.1361 | 0.1143 |
| n-dodecane | 0.0355 | 0.0443 | 0.0578 | 0.0659 | 0.0830 | 0.0762 |
| n-heptane | 0.0672 | 0.0717 | 0.0856 | 0.1030 | 0.1265 | 0.1088 |
| n-nonane | 0.0500 | 0.0610 | 0.0757 | 0.0857 | 0.1075 | 0.0949 |
| n-pentadecane | 0.0267 | 0.0368 | 0.0520 | 0.0570 | 0.0716 | 0.0684 |
| n-pentane | 0.0755 | 0.0816 | 0.0814 | 0.0947 | 0.1309 | 0.1055 |
| Octane | 0.0562 | 0.0692 | 0.0786 | 0.0935 | 0.1158 | 0.1031 |
| Toluene | 0.0990 | 0.1157 | 0.1373 | 0.1573 | 0.1912 | 0.1760 |
| Xylenes | 0.0769 | 0.0983 | 0.1189 | 0.1311 | 0.1611 | 0.1509 |
| | | | | | | |
| T = 190°C | $\chi_{12}$ | $\chi_{12}$ | $\chi_{12}$ | $\chi_{12}$ | $\chi_{12}$ | $\chi_{12}$ |
| 1 - hexene | 0.0693 | 0.0861 | 0.1077 | 0.1160 | 0.1439 | 0.1187 |
| 1-octene | 0.0744 | 0.0830 | 0.0962 | 0.1087 | 0.1269 | 0.1088 |

| | | | | | | |
|---|---|---|---|---|---|---|
| Benzene | 0.1360 | 0.1617 | 0.1950 | 0.2142 | 0.2427 | 0.2162 |
| cyclohexane | 0.0901 | 0.0890 | 0.1245 | 0.1390 | 0.1592 | 0.1395 |
| Hexanes | 0.0716 | 0.0771 | 0.0989 | 0.1105 | 0.1319 | 0.1103 |
| n-dodecane | 0.0399 | 0.0503 | 0.0664 | 0.0746 | 0.0850 | 0.0767 |
| n-heptane | 0.0706 | 0.0784 | 0.0972 | 0.1063 | 0.1245 | 0.1040 |
| n-nonane | 0.0643 | 0.0657 | 0.0845 | 0.0936 | 0.1080 | 0.0932 |
| n-pentadecane | 0.0353 | 0.0429 | 0.0589 | 0.0648 | 0.0734 | 0.0687 |
| n-pentane | 0.0348 | 0.0385 | 0.0689 | 0.0742 | 0.0991 | 0.0747 |
| Octane | 0.0595 | 0.0739 | 0.0895 | 0.0998 | 0.1162 | 0.0991 |
| Toluene | 0.1009 | 0.1344 | 0.1543 | 0.1682 | 0.1914 | 0.1717 |
| Xylenes | 0.0811 | 0.1001 | 0.1321 | 0.1433 | 0.1634 | 0.1475 |
| | | | | | | |
| T = 210°C | $\chi_{12}$ | $\chi_{12}$ | $\chi_{12}$ | $\chi_{12}$ | $\chi_{12}$ | $\chi_{12}$ |
| 1 - hexene | 0.0650 | 0.0882 | 0.0966 | 0.1032 | 0.1176 | 0.1067 |
| 1-octene | 0.0953 | 0.0858 | 0.1062 | 0.1122 | 0.1299 | 0.1189 |
| Benzene | 0.1721 | 0.1680 | 0.1993 | 0.2157 | 0.2412 | 0.2273 |
| cyclohexane | 0.1035 | 0.1010 | 0.1321 | 0.1418 | 0.1644 | 0.1504 |
| Hexanes | 0.0695 | 0.0787 | 0.0918 | 0.1047 | 0.1224 | 0.1081 |
| n-dodecane | 0.0438 | 0.0581 | 0.0723 | 0.0801 | 0.0900 | 0.0866 |
| n-heptane | 0.0743 | 0.0795 | 0.0948 | 0.1084 | 0.1259 | 0.1134 |
| n-nonane | 0.0535 | 0.0719 | 0.0900 | 0.0998 | 0.1119 | 0.1051 |
| n-pentadecane | 0.0353 | 0.0470 | 0.0636 | 0.0697 | 0.0780 | 0.0778 |
| n-pentane | | | | | | |
| Octane | 0.0621 | 0.0744 | 0.0944 | 0.1033 | 0.1198 | 0.1091 |
| Toluene | 0.1100 | 0.1308 | 0.1588 | 0.1733 | 0.1979 | 0.1891 |
| Xylenes | 0.0814 | 0.1070 | 0.1389 | 0.1484 | 0.1702 | 0.1648 |
| | | | | | | |
| T = 230°C | $\chi_{12}$ | $\chi_{12}$ | $\chi_{12}$ | $\chi_{12}$ | $\chi_{12}$ | $\chi_{12}$ |
| 1 - hexene | 0.0303 | 0.0310 | 0.0464 | 0.0498 | 0.0629 | 0.0577 |
| 1-octene | 0.0662 | 0.0809 | 0.1007 | 0.1067 | 0.1239 | 0.1137 |
| benzene | 0.1418 | 0.1427 | 0.1883 | 0.2004 | 0.2238 | 0.2117 |
| cyclohexane | 0.0882 | 0.0891 | 0.1269 | 0.1374 | 0.1538 | 0.1403 |
| hexanes | 0.0510 | 0.0423 | 0.0614 | 0.0649 | 0.0785 | 0.0683 |
| n-dodecane | 0.0486 | 0.0621 | 0.0736 | 0.0794 | 0.0907 | 0.0857 |
| n-heptane | 0.0635 | 0.0753 | 0.0888 | 0.0969 | 0.1136 | 0.1007 |
| n-nonane | 0.0659 | 0.0768 | 0.0901 | 0.0933 | 0.1096 | 0.0998 |
| n-pentadecane | 0.0422 | 0.0511 | 0.0643 | 0.0700 | 0.0793 | 0.0764 |
| n-pentane | | | | | | |
| octane | 0.0636 | 0.0743 | 0.0879 | 0.0991 | 0.1138 | 0.1058 |
| toluene | 0.1107 | 0.1332 | 0.1549 | 0.1684 | 0.1878 | 0.1779 |
| xylenes | 0.0899 | 0.1130 | 0.1389 | 0.1444 | 0.1656 | 0.1600 |

For each column different HDPE-2 samples were prepared, except for Columns 4 and 5, which were the same sample, but different column lengths (3 and 6 m, respectively). It was observed that the $\chi_{12}$ values from column to column appear to be dependent on the mass of polymer that was analyzed. This trend is observed for all of the temperatures that the samples were analyzed at. Figure 5.1 displays the measured $\chi_{12}$

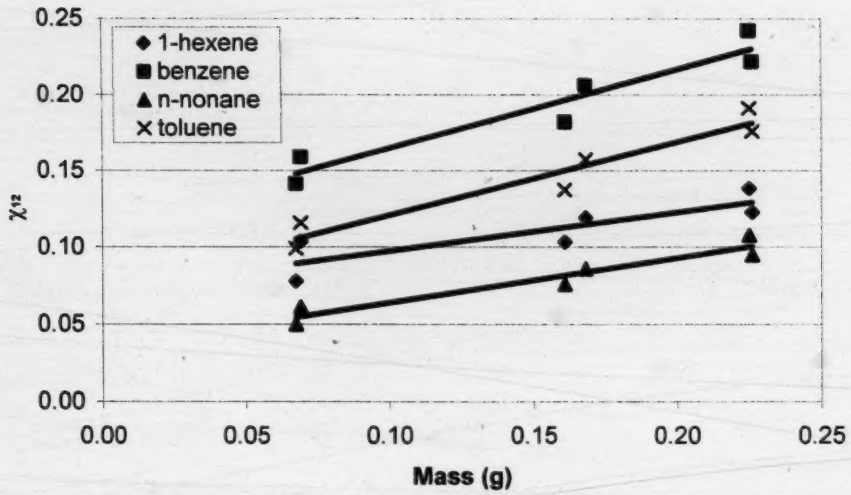
1-hexene
benzene
n-nonane
toluene
χ12
0.25
0.20
0.15
0.10
0.05
0.00
0.00
0.05
0.10
0.15
0.20
0.25
Mass (g)

(a)

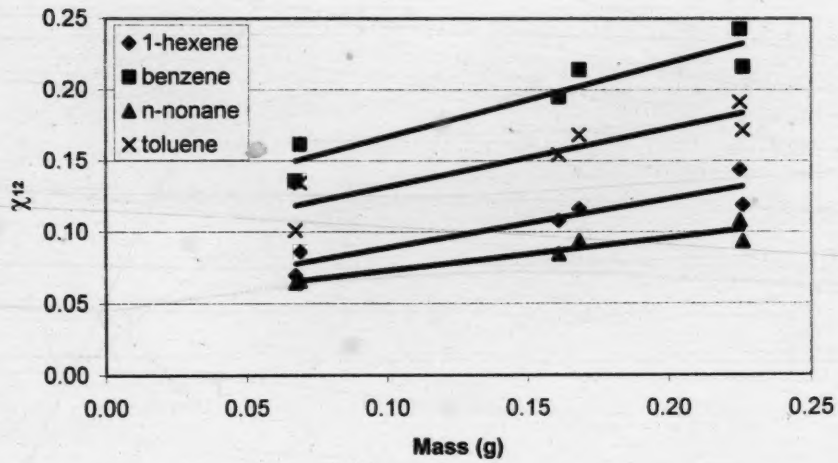
1-hexene
benzene
n-nonane
toluene
χ12
0.25
0.20
0.15
0.10
0.05
0.00
0.00
0.05
0.10
0.15
0.20
0.25
Mass (g)

(b)

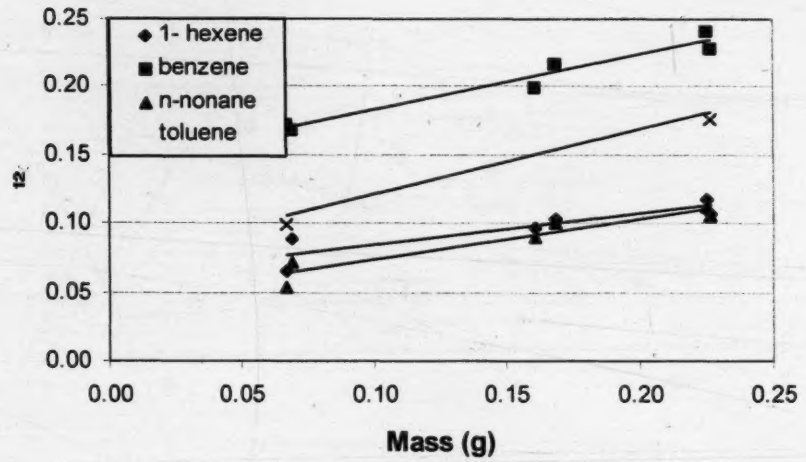


(c)

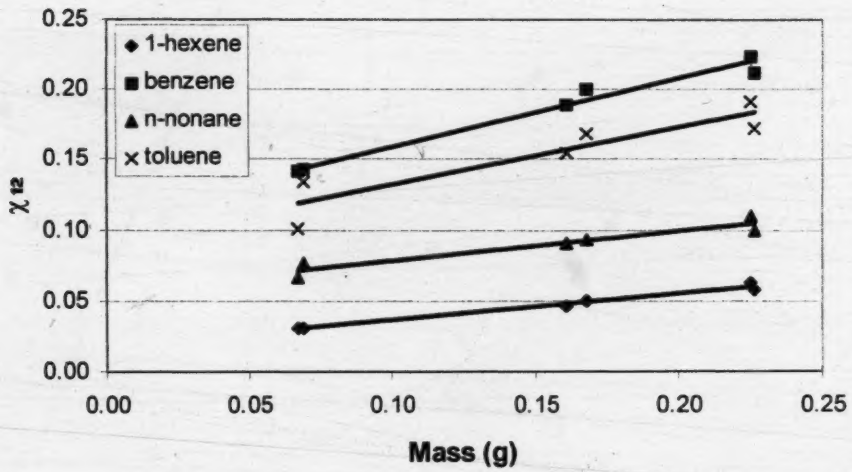


(d)

**Figure 5.1.** **$\chi_{12}$ Versus Polymer Mass (a) T = 170°C, (b) T = 190°C, (c) T = 210°C, (d) T = 230°C**

values for 1-hexene, benzene, n-nonane, and toluene plotted against the polymer mass. Other solvents' $\chi_{12}$ values were not included in the graphs for clarity. However, an increasing trend of $\chi_{12}$ is also observed for all solvents, not just those plotted in Figures 5.1. This trend is unreasonable since $\chi$ is a thermodynamic parameter that should not depend on the mass of polymer used in the experiment. Therefore, additional experiments were performed to determine the reason for such an observation.

## 5.3 Results for Pure HDPE Samples Using Different Column Loadings

In order to investigate mass dependence, several different HDPE-2 samples were analyzed using 3 and 6 m columns, which were packed tightly. Two 3 m columns (columns 5 and 6) were also prepared in order to determine if reproducible $\chi_{12}$ values could be obtained by preparing the column with a predetermined polymer mass. They were prepared with a mass of polymer within 2% or each other but had different void spaces. The measured $\chi_{12}$ values for all six samples are presented in Table 5.2.

**Table 5.2. $\chi_{12}$ For HDPE-2 Samples Using Different Column Loadings**

| Sample | 1 | 2 | 3 | 4 | 5 | 6 |
|---|---|---|---|---|---|---|
| Column Length | 3 m | 6 m | 3 m | 6 m | 3m | 3 m |
| Polymer Loading | 7.27% | 7.27% | 7.80% | 7.80% | 7.27% | 8.82% |
| Mass of Polymer (g) | 0.1610 | 0.2485 | 0.1683 | 0.2252 | 0.0953 | 0.0964 |
| Mass of Solid (g) | 2.2147 | 3.4180 | 2.1578 | 2.8871 | 1.3102 | 1.0935 |
| | | | | | | |
| T = 170 | $\chi_{12}$ | $\chi_{12}$ | $\chi_{12}$ | $\chi_{12}$ | $\chi_{12}$ | $\chi_{12}$ |
| 1 - hexene | 0.1031 | 0.1034 | 0.1190 | 0.1382 | 0.0978 | 0.1230 |
| 1-octene | 0.0868 | 0.0904 | 0.1008 | 0.1218 | 0.0880 | 0.0999 |
| benzene | 0.1821 | 0.1900 | 0.2062 | 0.2421 | 0.1875 | 0.2248 |
| cyclohexane | 0.1103 | 0.1154 | 0.1306 | 0.1586 | 0.1154 | 0.1372 |
| hexanes | 0.0922 | 0.1014 | 0.1123 | 0.1361 | 0.1044 | 0.1186 |
| n-dodecane | 0.0578 | 0.0602 | 0.0659 | 0.0830 | 0.0554 | 0.0697 |
| n-heptane | 0.0856 | 0.0936 | 0.1030 | 0.1265 | 0.0916 | 0.1045 |
| n-nonane | 0.0757 | 0.0781 | 0.0857 | 0.1075 | 0.0752 | 0.0890 |
| n-pentadecane | 0.0520 | 0.0533 | 0.0570 | 0.0716 | 0.0486 | 0.0619 |

| | | | | | | |
|---|---|---|---|---|---|---|
| n-pentane | 0.0814 | 0.1060 | 0.0947 | 0.1309 | 0.1110 | 0.1470 |
| octane | 0.0786 | 0.0861 | 0.0935 | 0.1158 | 0.0910 | 0.0988 |
| toluene | 0.1373 | 0.1483 | 0.1573 | 0.1912 | 0.1528 | 0.1697 |
| xylenes | 0.1189 | 0.1228 | 0.1311 | 0.1611 | 0.1218 | 0.1415 |
| | | | | | | |
| T = 190 | $\chi_{12}$ | $\chi_{12}$ | $\chi_{12}$ | $\chi_{12}$ | $\chi_{12}$ | $\chi_{12}$ |
| 1 - hexene | 0.1077 | 0.0974 | 0.1160 | 0.1439 | 0.0885 | 0.1379 |
| 1-octene | 0.0962 | 0.0939 | 0.1087 | 0.1269 | 0.0828 | 0.1173 |
| benzene | 0.1950 | 0.1838 | 0.2142 | 0.2427 | 0.1718 | 0.2496 |
| cyclohexane | 0.1245 | 0.1181 | 0.1390 | 0.1592 | 0.1064 | 0.1538 |
| hexanes | 0.0989 | 0.1026 | 0.1105 | 0.1319 | 0.0808 | 0.1184 |
| n-dodecane | 0.0664 | 0.0662 | 0.0746 | 0.0850 | 0.0582 | 0.0761 |
| n-heptane | 0.0972 | 0.1038 | 0.1063 | 0.1245 | 0.0842 | 0.1177 |
| n-nonane | 0.0845 | 0.0843 | 0.0936 | 0.1080 | 0.0749 | 0.0988 |
| n-pentadecane | 0.0589 | 0.0587 | 0.0648 | 0.0734 | 0.0526 | 0.0686 |
| n-pentane | 0.0689 | 0.0800 | 0.0742 | 0.0991 | 0.0889 | 0.1329 |
| octane | 0.0895 | 0.0907 | 0.0998 | 0.1162 | 0.0895 | 0.1065 |
| toluene | 0.1543 | 0.1534 | 0.1682 | 0.1914 | 0.1543 | 0.1839 |
| xylenes | 0.1321 | 0.1306 | 0.1433 | 0.1634 | 0.1274 | 0.1546 |

| T = 210 | $\chi_{12}$ | $\chi_{12}$ | $\chi_{12}$ | $\chi_{12}$ | $\chi_{12}$ | $\chi_{12}$ |
|---|---|---|---|---|---|---|
| 1 - hexene | 0.0966 | 0.0891 | 0.1032 | 0.1176 | 0.0741 | 0.1208 |
| 1-octene | 0.1062 | 0.0999 | 0.1122 | 0.1299 | 0.0816 | 0.1095 |
| benzene | 0.1993 | 0.1892 | 0.2157 | 0.2412 | 0.1629 | 0.2326 |
| cyclohexane | 0.1321 | 0.1238 | 0.1418 | 0.1644 | 0.1002 | 0.1498 |
| hexanes | 0.0918 | 0.0883 | 0.1047 | 0.1224 | 0.0756 | 0.1178 |
| n-dodecane | 0.0723 | 0.0702 | 0.0801 | 0.0900 | 0.0631 | 0.0798 |
| n-heptane | 0.0948 | 0.0934 | 0.1084 | 0.1259 | 0.0799 | 0.1123 |
| n-nonane | 0.0900 | 0.0866 | 0.0998 | 0.1119 | 0.0809 | 0.0942 |
| n-pentadecane | 0.0636 | 0.0626 | 0.0697 | 0.0780 | 0.0536 | 0.0700 |
| octane | 0.0944 | 0.0919 | 0.1033 | 0.1198 | 0.0837 | 0.1062 |
| toluene | 0.1588 | 0.1580 | 0.1733 | 0.1979 | 0.1425 | 0.1999 |
| xylenes | 0.1389 | 0.1342 | 0.1484 | 0.1702 | 0.1209 | 0.1535 |
| | | | | | | |
| T = 230 | $\chi_{12}$ | $\chi_{12}$ | $\chi_{12}$ | $\chi_{12}$ | $\chi_{12}$ | $\chi_{12}$ |
| 1 - hexene | 0.0464 | 0.0390 | 0.0498 | 0.0629 | 0.0494 | 0.0511 |
| 1-octene | 0.1007 | 0.0942 | 0.1067 | 0.1239 | 0.0944 | 0.0965 |
| benzene | 0.1883 | 0.1835 | 0.2004 | 0.2238 | 0.2038 | 0.2074 |
| cyclohexane | 0.1269 | 0.1207 | 0.1374 | 0.1538 | 0.1441 | 0.1471 |
| hexanes | 0.0614 | 0.0588 | 0.0649 | 0.0785 | 0.0740 | 0.0758 |
| n-dodecane | 0.0736 | 0.0705 | 0.0794 | 0.0907 | 0.0734 | 0.0750 |
| n-heptane | 0.0888 | 0.0890 | 0.0969 | 0.1136 | 0.1044 | 0.1064 |
| n-nonane | 0.0901 | 0.0862 | 0.0933 | 0.1096 | 0.0928 | 0.0947 |
| n-pentadecane | 0.0643 | 0.0628 | 0.0700 | 0.0793 | 0.0642 | 0.0656 |
| octane | 0.0879 | 0.0884 | 0.0991 | 0.1138 | 0.1090 | 0.1110 |
| toluene | 0.1549 | 0.1493 | 0.1684 | 0.1878 | 0.1834 | 0.1866 |
| xylenes | 0.1389 | 0.1320 | 0.1444 | 0.1656 | 0.1473 | 0.1502 |

Columns 1 and 2, which were prepared using the same HDPE-2 coated sample, displayed $\chi_{12}$ values difference is typically less than 10% of each other (with the occasional outlying discrepancy). Typically, the $\chi_{12}$ values are within ~5% of each other suggesting that the $\chi_{12}$ values between the two columns are quite repeatable when the same HDPE-2 coated support sample is used for both columns regardless of whether 3m or 6m columns are used, as long as they are well packed.

Columns 3 and 4, which were prepared using the same polymer coated support sample display $\chi_{12}$ values that are typically within ~ 15 to 25% of each other. These observed discrepancies are much larger than those for columns 1 and 2. It is possible that the larger discrepancies may be due to void spaces in the column, since it should be noted that although column 1 and 3 were packed with solid to roughly the same extent (within about 3% total mass of each other), columns 2 and 4 differ in the total amount of packed solid by roughly 18%, which is substantially larger. This large discrepancy in the packed solid in the 6 m columns (columns 2 and 4) is a noted problem. This is because when long columns are prepared it is difficult to properly pack them due to the shear length.

In order to determine if void spacing has a significant effect on the calculated $\chi_{12}$ values, columns 5 and 6 were analyzed. The calculated $\chi_{12}$ values are noted to be quite different from one another, ranging from 9 to 63% difference between temperatures of 170 to 210°C. However, at T = 230°C, the $\chi_{12}$ values are typically within about 2% of each other.

Columns 1, 2 and 5 were prepared using the same HDPE-2 coated support. Columns 1 and 2 are believed to be well packed, while 5 is not. Comparing $\chi_{12}$ values for

columns 1 and 5, the $\chi_{12}$ values are in fairly good agreement for T = 170 and 230°C, typically being within 15% or less of each other (with the occasional outlying value). For T = 190°C, the differences are larger, ranging from 0 to 22% depending on the solvent, with the differences typically being ~15%. For T = 210°C, the differences range from 11 to 32%.

Similar results are obtained when comparing columns 2 and 5. For T = 170°C, the $\chi_{12}$ values are within 10% of each other. T = 190°C the values range from 1 to 27% with most of them being within 15% of each other. For T = 210°C it ranges from 7 to 24% and for T = 230°C from 0 to 21%. The discrepancies in the $\chi_{12}$ values between the well packed columns 1 and 2 with columns 5, which is known to have void spaces, does not appear to be soley due to void spaces. Considering the calculated experimental errors for the $\chi_{12}$ values, the differences between columns 1 and 5, and columns 2 and 5 are quite often within that range. Also, since the $\chi_{12}$ values between columns 5 and 6 (known to have void spaces) are typically much larger than those observed between columns 1 and 5, and columns 2 and 5, which are not much larger than those observed between columns 1 and 2 (well packed columns), it suggests that the errors are probably not due entirely to void spacing, but also the sample preparation itself (e.g. column loading, inaccuracies in the mass determination process, etc.). However, void spacing does appear to have a significant effect.

## 5.4 HDPE/LLDPE Blends Results Using 3 m Columns

The branch content dependence of LLDPE on the $\chi_{23}$ of HDPE/LLDPE blends, the temperature dependence of $\chi_{23}$, and the molecular weight dependence of HDPE on

the $\chi_{23}$ of HDPE/LLDPE blends was re-examined due to the ambiguities discussed in Chapter 4. Samples of both HDPEs (HDPE-1 and HDPE-2) and four of the LLDPEs (LLDPE-1, 3, 4 and 5) that were used in Chapter 4 were analyzed as pure components and as 50/50 composition HDPE/LLDPE blends. However, instead of preparing the samples in 1 m columns, 3 m columns were used. This length of column was used since the increase in column length from 1 to 3 m was noted to decrease the magnitude of experimental errors on the calculated $\chi$ values. 6 m long columns were not used since they were difficult to pack properly (i.e. no void spaces) due to the shear length. Additionally, the time it took to analyze the 6 m columns was substantially longer than for the 3 m columns. Therefore, it was decided that the 3 m columns were be prepared for subsequent experiments.

Using the same approach as in Chapter 4, the samples' retention values were measured, the corresponding $\chi$ values were then calculated as described in Chapter 2. As observed in Chapter 4, slopes of the graphs used to calculate $\chi_{23}$ also deviate significantly from unity.

### 5.4.1 HDPE-2/LLDPE Blends

As shown in Figure 5.2, the HDPE-2/LLDPE blends show weak temperature dependence. However, it is obvious that $\chi_{23}$ values for the blends containing LLDPE-1, LLDPE-3, and LLDPE-4 are significantly smaller than zero indicating that they are all miscible over the temperature range of interest. Rather, for HDPE-2/LLDPE-5, immiscibility was observed for the complete temperature range except for at T = 230 °C

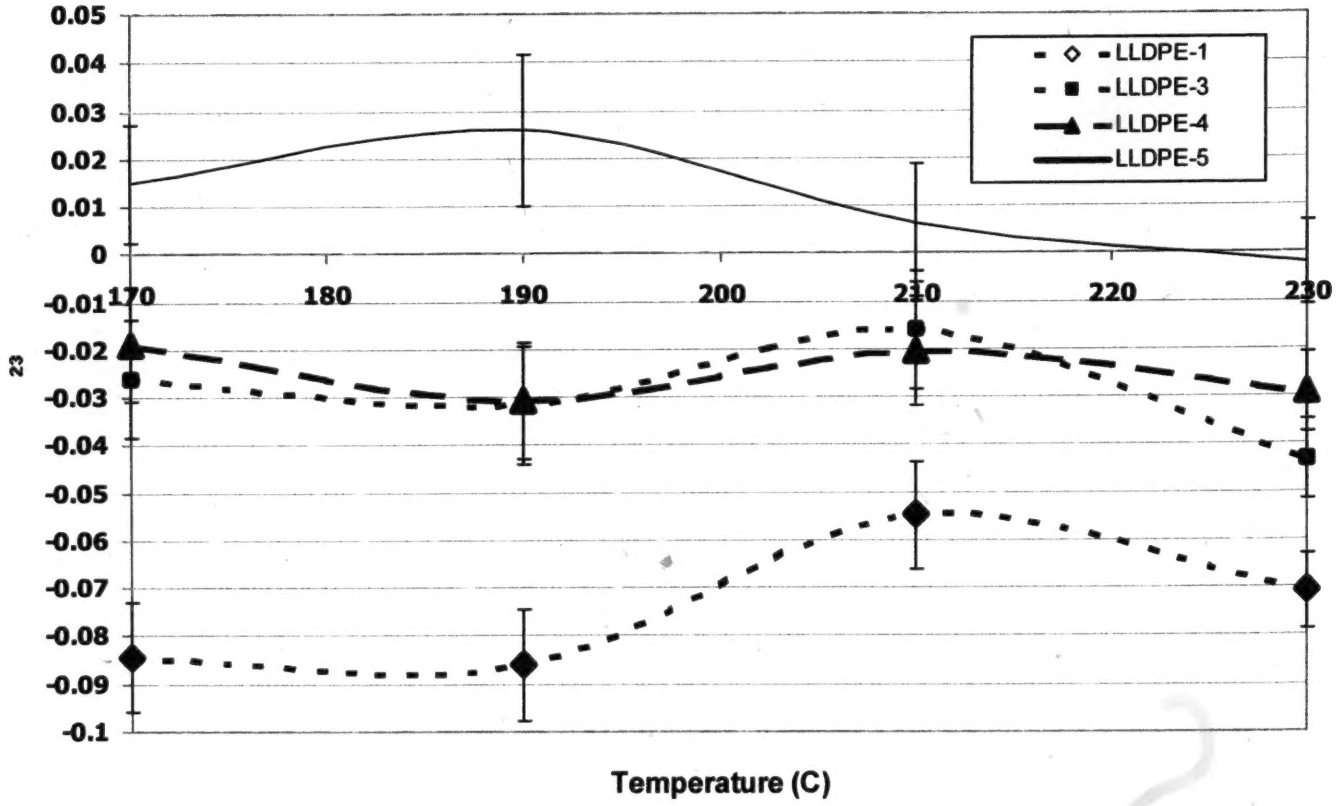


**Figure 5.2. Temperature Dependence of $\chi_{23}$ for HDPE-2/LLDPE Blends**

where miscibility is observed. It should be noted that the associated errors of the measured $\chi_{23}$ are slightly reduced (see Figures 4.2 and 5.2).

For the whole temperature range, $\chi_{23}$ appears to become more positive (less miscible) as the branch content of LLDPE is increased except in the branch content region of 20 to 50 branches per 1,000 carbons (Figure 5.3). The magnitude of $\chi_{23}$ values indicates that the blends are miscible for all branch contents except at 87.2 branches per 1,000 backbone carbons or higher.

In summary, the HDPE-2/LLDPE blends are observed to become immiscible as the branch content of LLDPE is increased. Immiscibility typically occurs at 87.2 branches per 1,000 backbone carbons for T = 170, 190, and 210°C, but not T = 230 °C. However, the trend of the graphs indicates that if the branch content is further increased, the T = 230°C should also become immiscible. Also, temperature dependence appears to be secondary to the branch content, since immiscibility cannot be induced solely by changing the temperature for a specific branch content (within the temperature range studied). However, increasing the branch content at a specific temperature is noted to induce phase separation.

### 5.4.2 HDPE-1/LLDPE Blends

For the HDPE-1/LLDPE blends, there appears to be temperature and branch content trends similar to those observed for the HDPE-2/LLDPE blends (Figures 5.4 and 5.5). In particular, the measured $\chi_{23}$ values are not sensitive to temperature. Similar to the HDPE-2/LLDPE blends, for all temperatures, the HDPE-1/LLDPE blends were immiscible at 87.2 branches per 1,000 backbone carbons. Based upon the results, shown

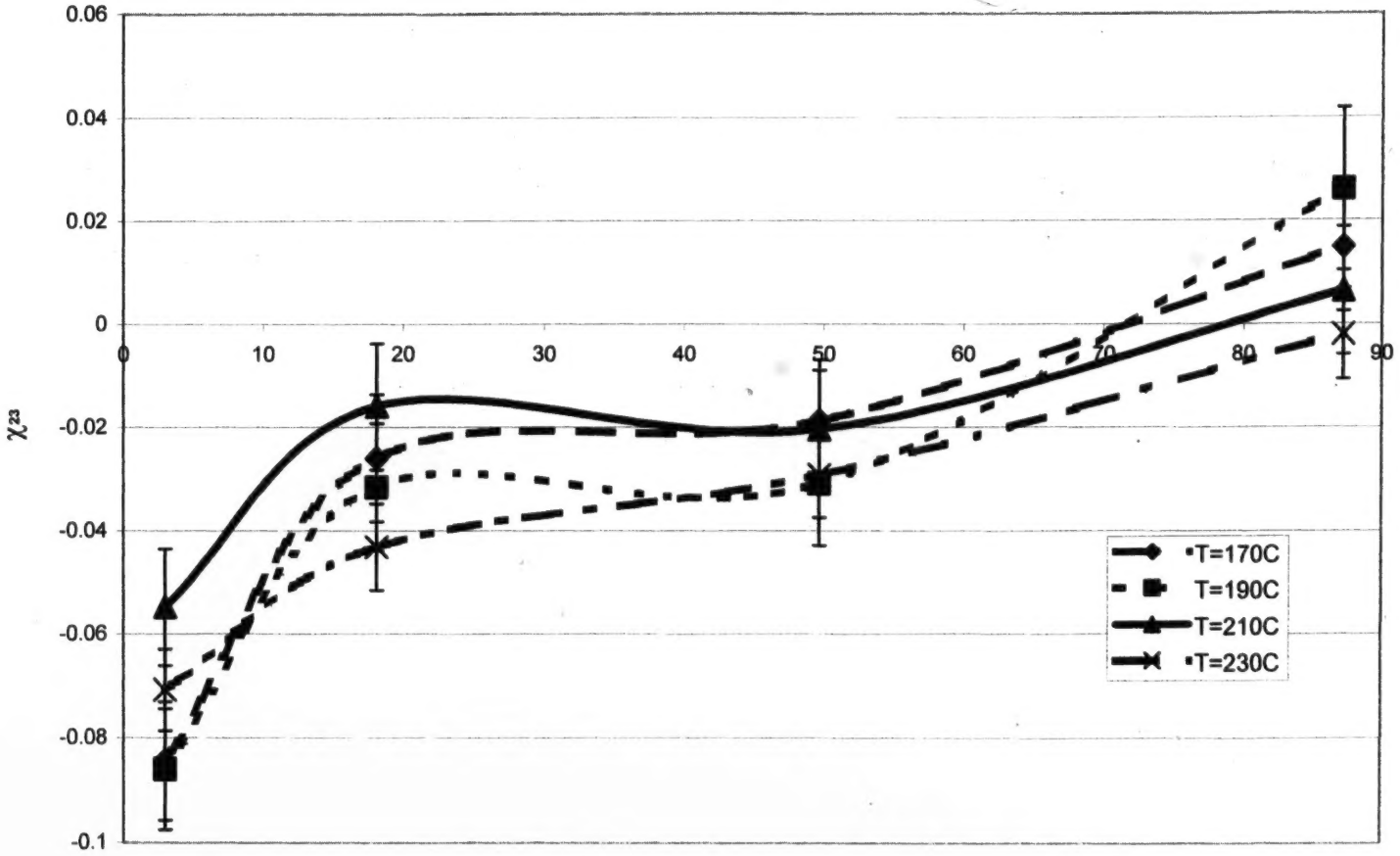


**Figure 5.3. Branch Content Dependence of $\chi_{23}$ for HDPE-2/LLDPE Blends**

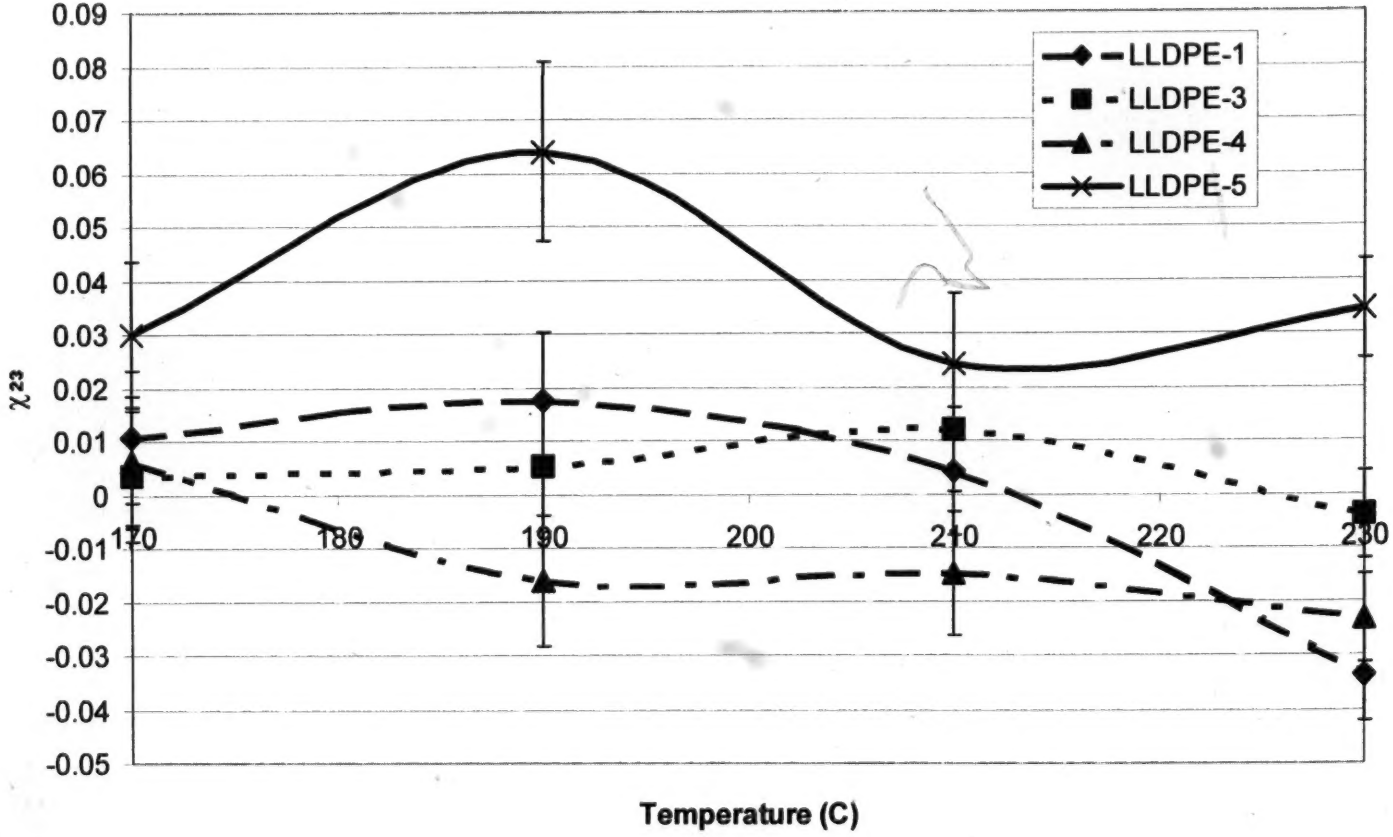


**Figure 5.4. Temperature Dependence of $\chi_{23}$ for HDPE-1/LLDPE Blends**

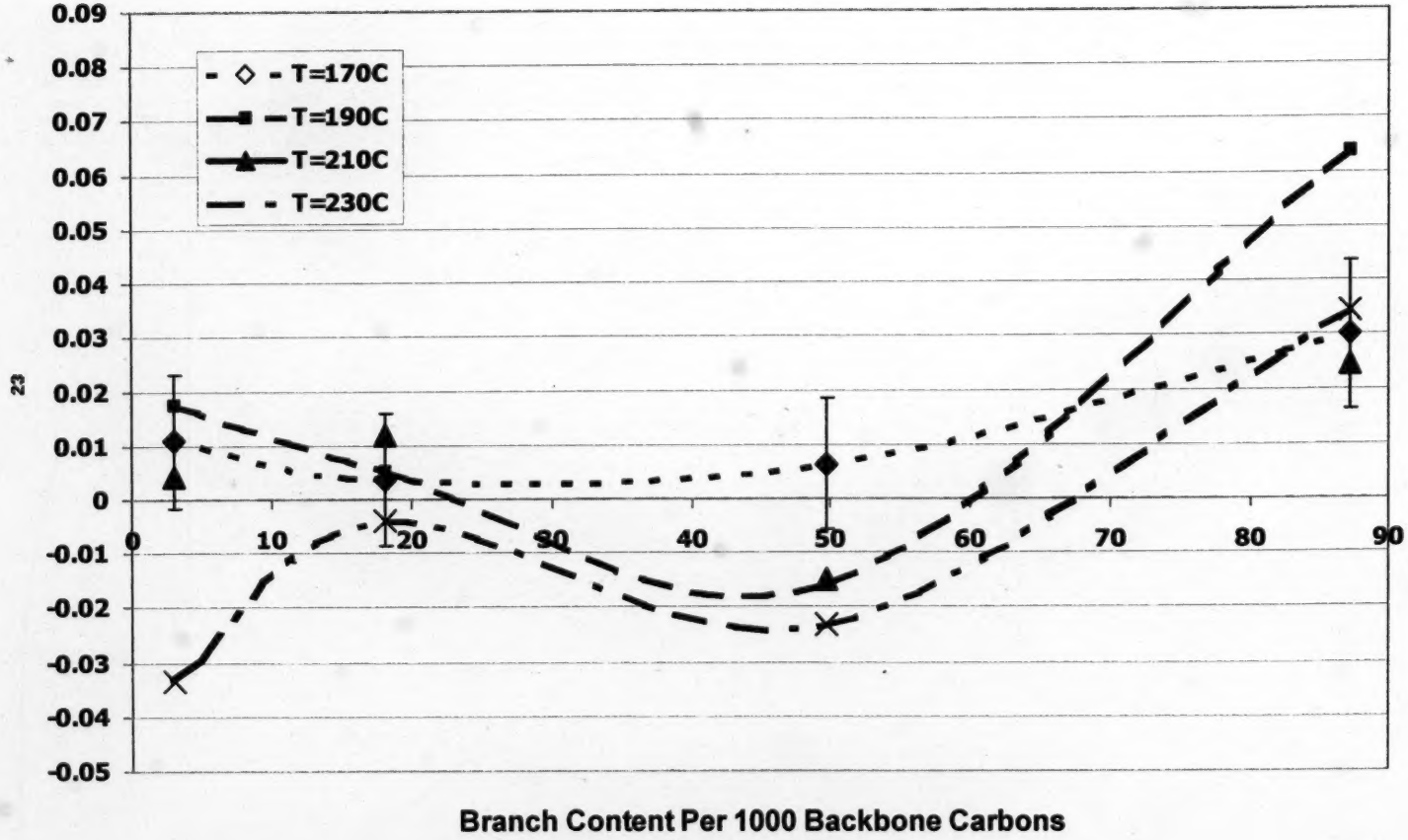


**Figure 5.5. Branch Content Dependence of $\chi_{23}$ for HDPE-1/LLDPE Blends**

in Figure 5.5, it appears that immiscibility occurs as the branch content increases. However, the trend observed is not as clear of a trend as was observed for HDPE-2/LLDPE. Additionally, the branch content dependence appears to occur at higher branch content (~87.2) than previously reported (~49.7). As for the HDPE-2/LLDPE blends, large $\chi_{23}$ values and associated errors are observed making the accuracy and reproducibility of the results questionable. Consequently, it is difficult to make conclusive statements regarding the HDPE-1/LLDPE miscibility dependence on the branch content of LLDPE and the temperature of analysis.

### 5.4.3 Molecular Weight Effect of HDPE on HDPE/LLDPE Blends

Both HDPE-1 and HDPE-2 blended with LLDPEs of different branch contents seem to follow a similar branch content and temperature dependence trends indicating that the molecular weight effect is not significant. According to Tanem and Stori (2001) the molecular weight difference between the two blend components (i.e. the HDPE and LLDPE in the blend) is what contributes to phase separation. Although the molecular weight between the two HDPEs was different, the difference between the LLDPEs and each HDPE is similar. Therefore, the molecular weight effect should be negligible, which appears to be what is observed. Also, the change in molecular weight did not appear to induce phase separation at a specific temperature or branch content.

## 5.5 References

Al-Saigh, Z.Y. (1997) The Characterization of Polymer Blends By Inverse Gas Chromatography, *TRIP*, 5, 3, 97-102.

Al-Saigh, Z.Y. (1997) Review: Inverse Gas Chromatography for the Characterization of Polymer Blends, *Int. J. Polym. Anal. Charact.*, 3, 269-291.

Al-Saigh, Z.Y., and Chen, P. (1991) Characterization of Semicrystalline Polymers by Inverse Gas Chromatography. 2. A Blend of Poly(vinylidene fluoride) and Poly(ethyl methacrylate), *Macromolecules*, 24, 3788-3795.

Al-Saigh, Z.Y., and Munk, P. (1984) Study of Polymer-Polymer Interaction Coefficients in Polymer Blends Using Inverse Gas Chromatography, *Macromolecules*, 17, 803-809.

Braun, J.M. and Guillet, J.E., (1976) Advances in Polymer Science; Spring-Verlag, Berlin.

Card, T.W., Al-Saigh, Z.Y., and Munk, P. (1985) Inverse Gas Chromatography. 2. The Role of the "Inert" Support, *Macromolecules*, 18, 1034-1039.

Chen, C.T., and Al-Saigh, Z.Y. (1989) Characterization of Semicrystalline Polymers by Inverse Gas Chromatography. 1. Poly(vinylidene fluoride), *Macromolecules*, 22, 2974-2981.

Deshpande, D.D., Patterson, D., Schreiber, H.P., and Su, C.S. (1974) Thermodynamic Interactions in Polymer Systems by Gas-Liquid Chromatography. IV. Interactions Between Components in a Mixed Stationary Phase, *Macromolecules*, 4, 530-535.

Du, Q., Chen, W., and Munk, P. (1999) Inverse Gas Chromatography. 8. Apparent Probe Dependence of $\chi_{23}'$ for a Poly(vinyl chloride) – Poly(tetramethylene glycol) Blend, *Macromolecules*, 32, 1514-1518.

Exteberria, A. Alfageme, J., Uriarte, C., and Iruin, J.J. (1992) Inverse Gas Chromatography in the Characterization of Polymeric Materials, *Journal of Chromatography*, 607, 227-237.

Exteberria, A., Uriarte, C., Fernandez-Berridi, M.J., and Iruin, J.J. (1994) Probing Polymer-Polymer Parameters in Miscible Blends by Inverse Gas Chromatography: Solvent Effects, *Macromolecules*, 27, 1245-1248.

Farooque, A.M., and Deshpande, D.D. (1992) Studies of Polystyrene-Polybutidiene Blend System by Inverse Gas Chromatography, *Polymer*, 33, 23, 5005-5018.

Munk, P. (1991) Polymer Characterization Using Inverse Gas Chromatography, *Modern Methods of Polymer Characterization*, 113, 151-200.

Shi, Z.H., and Schreiber, H.P. (1991) On the Application of Inverse Gas Chromatography to Interactions in Mixed Stationary Phases, *Macromolecules*, 24, 3522-3527.

Smidsrod, O., and Guillet, J.E. (1969) Study of Polymer-Solute Interactions by Gas Chromatography, *Macromolecules*, 2, 3, 272-277.

Voelkel, A. (1991) Inverse Gas Chromatography: Characterization of Polymers, Fibers, Modified Silicas, and Surfactants, *Critical Reviews in Analytical Chemistry*, 22, 5, 411-439.

Zhao, L. (2001) PhD. Thesis, University of Alberta.

# Chapter 6

# Conclusions and Future Work

## 6.1 Conclusions and Future Work

A new data analysis method suggested by Zhao and Choi (2001) for Inverse Gas Chromatography (IGC) measurements was used in order to obtain solvent independent polymer-polymer interaction parameters ($\chi_{23}$) for HDPE/LLDPE blends. The blends were studied in order to determine the branch content dependence, the molecular weight dependence, and the temperature dependence of $\chi_{23}$ for the blends. Previously, Zhao (2001) had determined that for 50/50 composition HDPE/LLDPE blends that when the branch content of LLDPE was raised to (or above) ~50 branches per 1,000 backbone carbons that phase separation was induced. And $\chi_{23}$ were found to be insensitive to temperature. For the current work, two HDPE samples or different molecular weights were used in the blends. Using the same sample preparation methods, experimental procedures, and analysis techniques as Zhao used, it was found that a branch content dependence trend was observed for blends containing both low and high molecular weight HDPE. Similar to Zhao's results, $\chi_{23}$ does not show a strong temperature dependence. Since the $\chi_{23}$ values for the blends were much larger ($\sim 10^{-2}$) than those obtained by other methods (e.g. SANS, $\sim 10^{-4}$) and the associated error values for $\chi_{23}$ were fairly large, measures were taken to improve the accuracy of the results obtained by IGC.

It was noted that the term that is experimentally calculated for the calculation of $\chi$ values is the specific retention volume ($V_g^\circ$). Without making significant (costly and time consuming) modifications to the IGC equipment, the experimental variables whose

accuracy could be improved were the carrier gas flow rate ($F$) and the polymer mass ($w$). The accuracy of $F$ was improved upon using a new digital flow meter, which was fitted with a U-tube to prevent the diffusion of helium through the soap bubble. The accuracy of $w$ was improved by increasing the column length from 1 m to 3 m and 6 m. By doing so, the same absolute measurement errors are retained, but due to the increase of the column length more polymer was present, thereby reducing the overall effect of the measurement errors. Additionally, increasing the column length also improved the retention time ($t_n$) measurements since the same absolute retention errors were retained, but the $t_n$ increases with the polymer mass, thereby reducing the effect of the error.

Pure HDPE samples were analyzed using 1, 3, and 6 m columns. The results indicated that the measured polymer-solvent ($\chi_{12}$) values were dependent on the mass of the polymer analyzed. In order to determine if void spacing (i.e. column loading) had a significant effect on the measured values, pure HDPE samples were analyzed using different column loadings. It was noted that well packed columns produced reproducible results (typically within ~10%) regardless of whether or not 3 or 6 m columns were used. However, 6m columns were difficult to load without void spaces due to the shear length of the column. For columns known to have void spaces, the results were not reproducible. The calculated $\chi_{12}$ values are noted to be quite different from one another, ranging from 9 to 63% difference between temperatures of 170 to 210°C. However, at T = 230°C, the $\chi_{12}$ values are typically within about 2% of each other. This suggested that column packing was an important parameter.

The branch content dependence, HDPE molecular weight dependence, and the temperature dependence of $\chi$ for the HDPE/LLDPE blends were reinvestigated using

well-packed 3 m columns. These columns were chosen over 1 m columns in order to reduce the effect of the measurement errors. 6 m columns were not used since they were difficult to load without creating void spaces. Also, the analysis of the 6 m columns was time consuming. Therefore, they were undesirable for this work.

Typically, the low molecular weight HDPE/LLDPE blends followed a trend that as the branch content of LLDPE was increased the blends became more immiscible with the critical branch content occurring ~90 branches per 1,000 backbone carbons. When the branch content was 87.2 branches per 1,000 backbone carbons the blends were noted to be always immiscible, but for the other blends typically a minimum was reached at T = 230°C. However, the blends did not follow a clear temperature trend, indicating that the effect of temperature on the miscibility of the blends was secondary to that of the branch content.

For the higher molecular weight HDPE/LLDPE blends, a clearer branch content trend was observed with phase separation being induced when the branch content was raised to 87.2 branches per 1,000 backbone carbons regardless of the temperature. No clear temperature dependence was observed. Therefore, the effect of temperature was believed, once again, to be secondary.

Comparing the results for the low molecular weight HDPE/LLDPE blends with those for the higher molecular weight HDPE/LLDPE blends, no clear molecular weight dependence was observed. This was not unexpected since the absolute difference between the HDPEs with the LLDPE blend components was not significantly different in order to induce phase separation, as previously observed by Tanem and Stori (2001).

The calculated $\chi_{23}$ values using the 3 m columns and the associated error values are still noted to be large, indicating that further improvements should be made to improve the accuracy of the results. Using the 3 m columns appears to reduce the effect of the measurement errors associated with the 1 m columns, thereby producing more reproducible results. However, a continuous increase in the column length was not reasonable since it was observed for 6 m columns that the sample preparation becomes more difficult due to the length of the columns and void spaces can be introduced.

It was found that for a LLDPE column analyzed twice that the resulting $\chi_{13}$ values were reproducible typically within ~5%, with the differences being due to measurement errors. However, when a new sample was prepared (i.e. the polymer mass changed) the $\chi_{13}$ values were not in good agreement (typically 20-30% discrepancies). Thus, further improvements to the sample preparation are required to reduce this error since significant error will be introduced into $\chi_{23}$ if $\chi_{12}$, $\chi_{13}$, and $\chi_{1(23)}$ all have significantly large errors.

Also, it should be noted that for both the 1 m and 3 m HDPE/LLDPE blends, the graphs that were used to determine the $\chi_{23}$ values had slopes that frequently differed from unity. This was problematic since the theory indicates that the slopes of these graphs should be unity for solvent independency. Thus, it is possible that the solvent dependency has not been totally eliminated or that experimental errors caused significant deviations in the slopes. As a result, these errors are passed onto the calculated $\chi_{23}$ values.

Further work should focus on the IGC method of analysis in order to obtain more accurate results for the determination of $\chi_{23}$. Some variables that could be further improved upon are: more accurate measurement of $t_n$ values, possibly with the use of an automated sample injector; a more accurate polymer mass determination procedure, such

as the method suggested by Al-Saigh and Munk (1984); improved flowrate measurements, etc. If possible, the accuracy of each experimental variable should be precisely controlled.

In order to determine if the results that are being obtained using the existing method are accurate, it would be advantageous to study the same polymer samples using SANS. If agreement could be obtained from SANS results for the determination of $\chi_{23}$, it would help to validate the current results.

It would also be valuable to determine if this IGC method is applicable for other polymer blends consisting of polymers interacting with each other through both non-directional and directional interactions. It may be possible to study well-characterized blends so that results could easily be compared.

## 6.2 References


Al-Saigh, Z.Y., and Munk, P. (1984) Study of Polymer-Polymer Interaction Coefficients in Polymer Blends Using Inverse Gas Chromatography, *Macromolecules*, 17, 803-809.

Tanem, B.S. and Stori, A. (2001) Investigation of Phase Behaviour in the Melt in Blends of Single-site Based Linear Polyethylene and Ethylene-1-alkene Copolymers, *Polymer*, 42, 4309-4319.

Tanem, B.S., and Stori, A. (2001) Phase Separation in Melt Blends of Single-Site Linear and Branched Polyethylene, *Polymer*, 42, 5689-5694.

Zhao, L. (2001) PhD. Thesis, University of Alberta.

Zhao, L. and Choi, P. (2001) Determination of Solvent-Independent Polymer-Polymer Interaction Parameter by an Improved Inverse Gas Chromatographic Approach, *Polymer*, 42, 1075-1081.

# Appendix A

## Sample Calculations of Flory-Huggins Interaction Parameters

### A.1 Sample Calculations of $\chi_{12}$, $\chi_{13}$, and $\chi_{1(23)}$

Solvent – 1-Hexene

Polymers 2 – HDPE-2 at 170°C

Polymer 3 – LLPDE-1 at 170°C

For HDPE-2,

Mass of polymer in the column: $w = 0.161$ g

Flowrate of Carrier Gas: $F = 25.11$ mL/min

Inlet Pressure: $P_i = 287.7$ kPa

Outlet Pressure: $P_o = 92.7$ kPa

Retention time of Methane (marker): $t_m = 0.472$ min

Retention time of 1-Hexene: $t_R = 0.571$ min

Net Retention Time: $t_n = t_R - t_m = 0.098$ min

James Martin Correction Factor:

$$J = \frac{3}{2}\left[\frac{\left(\frac{P_i}{P_o}\right)^2 - 1}{\left(\frac{P_i}{P_o}\right)^3 - 1}\right] = 0.448$$

Specific Retention Volume for 1-Hexene:

$$V_g^\circ = \frac{273.15 t_n FJ}{wT} \qquad = 4.24 \text{ cm}^3/\text{g}$$

Specific Volume of Polyethylene at 170°C (Rudin et al., 1970):

$v = 1.282 + 9.0\times10^{-4}( 170 - 150) = 1.3 \text{ cm}^3/\text{g}$

Vapour Pressure of 1-Hexene calculated from the Antoine Equation (Reid, Prausnitz and Poling, 1987):

$$P_1^o = \exp\left( A - \frac{B}{T + C} \right) = 11.91 \text{ atm}$$

Second Virial Coefficient of 1-Hexene (Tsonopoulos, 1974):

$$\frac{B_{11} P_c}{RT_c} = f^o + \omega f^1$$

where:

$$f^0 = 0.1445 - \frac{0.330}{T_r} - \frac{0.1385}{T_r^2} - \frac{0.0121}{T_r^3} - \frac{0.000607}{T_r^8}$$

$$f^1 = 0.0637 + \frac{0.331}{T_r^2} - \frac{0.423}{T_r^3} - \frac{0.008}{T_r^8}$$

For 1-Hexene: $\alpha = 0.285$; $T_c = 504$ K; and $P_c = 31.7$ bar, therefore:

$f^0 = 0.429$; $f^1 = -0.153$; and $B_{11} = -0.625$

Liquid Density of 1-Hexene (Reid, Prausnitz, Poling, 1987):

$$\rho = A \times B^{-(1-T_r)^{2/7}}$$

For 1-Hexene; $A = 0.242$; $B = 0.27$

$\rho = 0.494$ g/mL

Molar Volume of 1-Hexene:

$$V_1 = \frac{M}{\rho} = 170.3 \text{ mL/mol}$$

where $M$ is the molecular weight of 1-Hexene.

The solvent-polymer interaction parameter is then calculated using Equation 44 as:

$$\chi_{12} = \frac{V_0}{V_1}\left( \ln \frac{273.15 R v_2}{V_g^0 V_1 P_1^0} - 1 + \frac{V_1}{M_2 v_2} - \frac{(B_{11} - V_1)}{RT} P_1^0 \right) = 0.103 \pm 0.022$$

The interaction parameters for the LLDPE and HDPE/LLDPE blend are both calculated using Equation 44 as well. For LLDPE-1 and 1-Hexene:

$\chi_{13} = 0.125 \pm 0.023$

For 50/50 blend of HDPE-2/LLDPE-1 and 1-Hexene:

$\chi_{1(23)} = 0.213 \pm 0.018$

The same procedure is followed for all the solvents that are used to characterize the polymers. Sample error calculations are presented in Appendix B.

## A.2 Sample Calculation of $\chi_{23}$

Once $\chi_{12}$, $\chi_{13}$, and $\chi_{1(23)}$ are known, the interaction parameter between polymer 2 and polymer 3 can be calculated from the intercept of the plot of:

$$\chi_{1(23)} = \phi_2 \chi_{12} + \phi_3 \chi_{13} - \phi_2 \phi_3 \chi_{23}$$

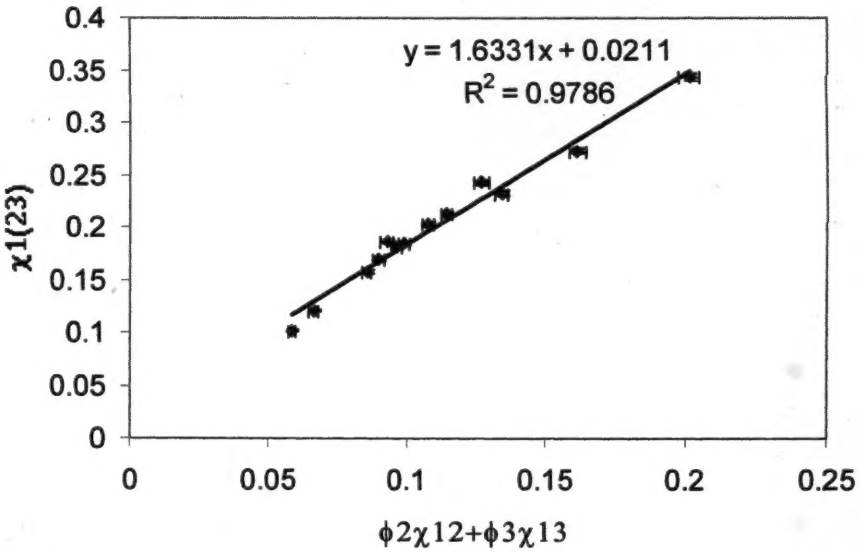


Therefore, with $\chi_{23} = \frac{-0.0211}{0.5 * 0.5} = -0.084 \pm 0.023$

Sample error calculations are presented in Appendix B.

# Appendix B

# Error Analysis of IGC Data

## B.1 Experimental Errors

The experimental variables that were taken into account for the error analysis were; the mass of the polymer in the column ($w$), the flowrate of the carrier gas ($F$), and the retention times of the solvent and marker ($t$). These three sources of error are believed to be the major sources of error in the calculation of the specific retention volume ($V_g^0$), as described in Chapter 5. These sources of error were also used so that the error analysis is consistent with Zhao's (2001).

The accuracy of the mass of the polymer in the column depends on the balance that is used for both the packing of the column and the ashing process. The accuracy of the balance is ±0.0001 g. For each sample that was ashed, three samples were ashed and each required three mass measurements. The average was taken as the loading of the polymer. In the loading of the column two mass measurements were made. Combining all these factors together, the absolute error for the mass of the polymer in the column was taken to be ±0.001 g. The flowrate of the carrier gas in Chapter 4 was measured using a bubble flow meter and is calculated from the average of three time measurements. The absolute error is taken to be ±0.2 mL/min due to diffusion of helium thru the bubble and inaccuracies in the time measurements. In Chapter 5 a different flow meter was used, which is calibrated to be accurate to 1.69% of the measured flowrate. The retention times of the solvents and marker were obtained from the average of three time measurements where the probe was manual injected while simultaneously engaging the time

measurement. The absolute error is taken to be ±0.01 min due to the human error in manual starting the time measurements and since the error is a combination of the error in both $t_p$ and $t_m$.

## B.2 Error Propagation

Assuming that the sources of error are due to $w$, $t_n$, and $F$ only; $\chi_{12}$ is defined as a function of $w$, $t_n$, and $F$:

$$\chi_{12} = f(w, F, t_n) \tag{B-1}$$

The deviation of $\chi_{12}$ is defined as:

$$\Delta\chi_{12} = \frac{\partial f}{\partial w}\Delta w + \frac{\partial f}{\partial F}\Delta F + \frac{\partial f}{\partial t_n}\Delta t_n \tag{B-2}$$

where $\Delta\chi_{12}$ is the deviation of $\chi_{12}$; $\Delta w, \Delta F,$ and $\Delta t_n$ are the deviations of $w$, $F$, and $t_n$. It should be noted that the inlet and outlet pressure errors were not taken into account for this analysis in order to be consistent with Zhao's (2001) analysis. All other parameters used in the calculation of $\chi_{12}$ were taken from the literature and errors where not accounted for.

The deviation of $\chi_{12}$ is then calculated by substituting equation 44 into equation B-2 resulting in,

$$\Delta\chi_{12} = \frac{V_0}{V_1}\left(\frac{1}{w}\Delta w + \frac{1}{F}\Delta F + \frac{1}{t_n}\Delta t_n\right) \tag{B-3}$$

Using equation B-3 the deviation of $\chi_{12}$ can be calculated. The deviation of $\chi_{13}$ and $\chi_{1(23)}$ are also calculated using the same equation.

The standard deviation can then be found using either:

$$S_\chi = \frac{V_0}{V_1}\sqrt{\left(\frac{\partial f}{\partial w}\Delta w\right)^2 + \left(\frac{\partial f}{\partial F}\Delta F\right)^2 + \left(\frac{\partial f}{\partial t_n}\Delta t_n\right)^2} \qquad \text{(B-4)}$$

or

$$S_\chi = \frac{V_0}{V_1}\sqrt{\left(\frac{1}{w}\Delta w\right)^2 + \left(\frac{1}{F}\Delta F\right)^2 + \left(\frac{1}{t_n}\Delta t_n\right)^2} \qquad \text{(B-5)}$$

The standard deviation of $\chi_{12}$ is determined using Equation B-5 (for the data presented in Appendix B) as:

For example, for the data presented in Appendix A, the error value is calculated as:

Mass of polymer in the column: $w = 0.161$ g

Flowrate of Carrier Gas: $F = 25.11$ mL/min

Net Retention Time: $t_n = t_R - t_m = 0.098$ min

$\Delta w = 0.001$ g

$\Delta t_n = 0.01$ minutes

$\Delta F = 0.2$ mL/min

$V_0 = 36.47$ mL/mol

$V_1 = 170.3$ mL/mol

$$S_{\chi 12} = \frac{V_0}{V_1}\sqrt{\left(\frac{1}{w}\Delta w\right)^2 + \left(\frac{1}{F}\Delta F\right)^2 + \left(\frac{1}{t_n}\Delta t_n\right)^2} = 0.022$$

Similarly the standard deviation for $\chi_{13}$ and $\chi_{1(23)}$ are calculated using Equation B-5 resulting in:

$S_{\chi 13} = 0.023$

$S_{\chi 1(23)} = 0.018$

### B.3 The Standard Deviation of $\chi_{23}$

The deviation of $\chi_{23}$ is caused by the deviation of both the x-axis and y-axis since it is calculated as the y-intercept of the plot of $\chi_{1(23)}$ versus $\phi_2\chi_{12} + \phi_3\chi_{13}$. The standard deviation can be estimated by the following:

$$S_{\chi_{23}} = \sqrt{\frac{\sum \frac{x^2}{\Delta x^2 + \Delta y^2}}{\sum \frac{1}{\Delta x^2 + \Delta y^2} \sum \frac{x^2}{\Delta x^2 + \Delta y^2} - \left(\sum \frac{x}{\Delta x^2 + \Delta y^2}\right)^2}} \qquad \text{(B-6)}$$

where $x$ represents $\phi_2\chi_{12} + \phi_3\chi_{13}$; $y$ is $\chi_{1(23)}$; $\Delta x$ is the standard deviation from the x-axis; and $\Delta y$ is the standard deviation from the y-axis. Therefore:

$\Delta x = 0.5^* S_{\chi 12} + 0.5^* S_{\chi 13} = 0.022$

$\Delta y = 0.018$

$S_{\chi 23} = 0.023$